Clinical Diagnostics For Immune Response Assessment Through Multiplexed Biosensor Immunoassays In At-Risk Populations

by

Cole Alexander Chapman

A dissertation submitted in partial fulfillment
of the requirements for the degree of
Doctor of Philosophy
(Chemistry)
in The University of Michigan
2021

Doctoral Committee:

Professor Ryan C. Bailey, Chair
Professor Robert Kennedy
Professor Denise Kirschner
Professor Brandon Ruotolo

Cole Alexander Chapman

coleac@umich.edu

ORCID iD: 0000-0001-6353-2328

DEDICATION

To my fiancé, Tori

ACKNOWLEDGEMENTS

Well, what an odd journey this has been. If you had asked me going into my first year at Wabash College for undergraduate where I expected this all to lead, it would not have been here. I never imagined an outcome where I would be doing the work that I have done or moving on to leave the Midwest to work at a biotech startup (thanks Mari for the assist!).

My pursuit of science began in earnest in college. While the whole Chemistry Department at Wabash College was always supportive, two individuals deserve distinct mention. The first was my faculty advisor, Lon Porter, was my guiding light, and saw a potential in me I didn't know I had. With summer work in his lab, nights playing board games in the basement, and conference trips, I found a welcoming community that helped shape the scientist I am today. The second was Richard Dallinger, my analytical professor. Truth be told, I didn't really know what analytical chemistry entailed until my junior year. Unbeknownst to me, he knew I would take this path before I did and had a list of schools and professors to look into before I had even considered graduate school. I owe much of my direction to these two, and I will be eternally grateful for them.

Since my time at the University of Michigan, I have many people to thank for a myriad of things. I would like to thank the members of my committee, Professor Denise Kirschner, Professor Robert Kennedy, and Professor Brandon Ruotolo for their support throughout this journey. I would also like to express my gratitude for funding and support

from the National Institute of Allergy and Infectious Diseases at the National Institutes of Health (AI141591), as well as Rackham for travel grants. I owe a big thank you to my advisor, Ryan Bailey. I wouldn't be doing the work I am today or have the career path I do without him making an insane wild card pick to take a sixth student my year. Thank you for being the crazy, off-the-cuff person you are. I never felt like I couldn't speak what was on my mind, whether project related or other. And while I have had some unique ups and downs in my graduate career, you were always supportive, and I know how rare that quality can be to find. Here's to science we've discussed, beers we've had, and trees we've felled in your backyard.

Next, shoutout goes to labmates, past and present. I want to thank the Old Guard, Dr. James Wade, Dr. Richard Graybill, and Dr. Yi Xu for early guidance and friendship. I received a lot of "character building" in my formative graduate school years and I am thankful to know you all. In particular of this crew, I want to thank Dr. Heather Robison, my mentor. I never knew someone that was a Type AA+, but you certainly proved me wrong. There are a lot of things I could say here, but in the end, I am incredibly thankful to have you as a friend first and foremost. Brainstorming sessions at Ashley's and late-night bar crawls kept my spirit alive while running our grueling sample analysis gauntlets. Thank you for helping me be the scientist and subsequently person I am today.

To my cohort since there are six of us; I can't believe that we are all going to make it out of here in one piece. It's not always been fun, but it has been an experience and I appreciate all of you. To Sara and Emily, thanks for making lab sassy and interesting and keeping me on my toes. To Shannon, thanks for being a curious human and for many oddball conversations through the years. To Colleen, thanks for being the realist in the

group and making sure I was staying out of trouble. And to John, for getting me into trouble, but normally the fun kind. Here's to scattering to the four winds so we don't work in the same lab again. To my other labmates; Dr. Mari, Gloria, Marina, Krista, Nico, Claire, and Nick. Mari, thank you for not wanting to move back to the states so I could have your potential job. Cheers. Nick and Claire, thank you for being you, and keep going. You both will do great. Gloria, you will in fact make it through all this, even if I'm not your deskmate. I appreciate you keeping me grounded, mainly by utterly confusing me with your sometimes spontaneous decisions. Marina, sorry you had to put up with a lot of bioinformatics talks at you and late nights because Josh and I don't know when to call it quits (keep him in line). Thank you for being you, and be sure to throw away that accursed cork at your earliest convenience. Nico, thank you for never turning down "one more" on our nights out. It's an important job, and someone has to do it. Krista, thank you for putting up with my chaotic mentoring style, the crazy projects, and all the conversations on how to deal with Ryan when he decides he knows what's best for the clinical projects (he's a pretty funny dude sometimes).

To my Ann Arbor friends, both fellow graduate students and others. I have appreciated the support throughout the years. A special thank you to my best friend and doppelganger, Joe. You know damn well I don't have the words to express how much you mean to me, but I'll try. The chances of finding someone who understands you so well is statistically abysmal, but you and I have always been those who beat the odds. My life would be much darker without you, and so it is with complete sincerity that I tell you I'm glad you are here to be a part of it.

To my family, who have certainly dealt with me for the longest and therefore I owe the most to. To Mom, who put up with my science babble and all of my years of being an annoying, loud-mouthed son. To Dad, thanks for all the practical knowledge and pushing me to keep going. To Liz, sorry you had to have me as a brother. That's a tough roll of the dice, but you have handled it gracefully. And finally, to my fiancé, Tori. Thank you for making some seriously horrible life decisions to get to this point. Through long distance, multiple states, and many hurdles, you are still here, and I'm excited for our future together. Thank you for being patient and understanding, and I look forward to where we will finally live in the same state and can start our life together in earnest.

TABLE OF CONTENTS

LIST OF TABLES

LIST OF FIGURES

FIGURE

LIST OF ABBREVIATIONS

4-CN	4-chloronapthol
AG	QuantiFERON antigen stimulation
ANA	Anti-nuclear antibody test
AUC	Area-under-the-curve
BAL	Bronchoalveolar lavage
BCG	Bacillus Calmette–Guérin vaccine
BSA	Bovine serum albumin
CAN	Candida stimulation
CCL2	C-C Motif Chemokine Ligand 2
CCL3	C-C Motif Chemokine Ligand 3
CCL4	C-C Motif Chemokine Ligand 4
CCL7	C-C Motif Chemokine Ligand 7
CCL8	C-C Motif Chemokine Ligand 8
CD3	anti-CD3 pan stimulation
CDC	Center for Disease Control

CE	CFP-10/ESAT-6 stimulation
CGA	Corrected gestational age
CMOS	Complementary metal oxide semiconductor
CSF	Cerebrospinal fluid
CT	Computerized tomography
Δpm	Net shift in resonance condition from microring resonators in picometers
DMSO	Dimethyl sulfoxide
DOL	Days of life
dsDNA	Double-stranded deoxyribonucleic acid
ELISA	Enzyme-linked immunosorbent assay
EONS	Early onset neonatal sepsis
GFAP	Glial fibrillary acidic protein
GM-CSF	Granulocyte-macrophage colony-stimulating factor
HCW	Healthcare worker
HIV	Human immunodeficiency virus
IAM-1	Intercellular adhesion molecule-1
IFN-γ	Interferon-gamma
IFN-λ1	Interferon-lambda 1

IgG	Immunoglobulin
IGRA	Interferon-gamma release assay
IL-10	Interleukin-10
IL-15	Interleukin-15
IL-16	Interleukin-16
IL-17	Interleukin-17
IL-18	Interleukin-18
IL-1β	Interleukin-1 beta
IL-2	Interleukin-2
IL-6	Interleukin-6
IL-7	Interleukin-7
IL-8	Interleukin-8
IP-10	Interferon gamma-induced protein 10
ISE	Ion-selective electrodes
LDA	Linear discriminant analysis
LOD	Limit of detection
LONS	Late onset neonatal sepsis
LOQ	Limit of quantitation

LTBI	Latent tuberculosis infection
MCP-1	Monocyte chemoattractant protein-1
MED	Negative media control stimulation
miRNA	microribonucleic acid
MIT	QuantiFERON mitogen stimulation
Mtb	Mycobacterium tuberculosis
MTB300	Peptide pool stimulation with 300 Mtb-derived T cell epitopes
MW	Mann-Whitney
MYO	Myoglobin stimulation
NEC	Necrotizing enterocolitis
NF-L	Neurofilament light chain
NICU	Neonatal intensive care unit
PBMC	Peripheral blood mononuclear cell
PBS	Phosphate buffered saline
PCR	Polymerase chain reaction
POC	Point-of-care
PPD	Purified protein derivative stimulation
QFT	QuantiFERON Test

RNA	Ribonucleic acid
ROC	Receiver operator characteristic
SA-HRP	Streptavidin-horseradish peroxidase
SARS	SARS-CoV-1 stimulation
SD	Standard deviation
SiMOA	Single molecule array
SS1	SARS-CoV-2 S1 spike protein stimulation
SS2	SARS-CoV-2 S2 spike protein stimulation
ssDNA	single-stranded deoxyribonucleic acid
TB	Tuberculosis
TET	Tetanus toxoid stimulation
TGF-α	Transforming growth factor alpha
TNF-α	Tumor necrosis factor alpha
tRNA	Transfer ribonucleic acid
TST	Tuberculin skin test
UCH-L1	Ubiquitin carboxy-terminal hydrolase L1
UTI	Urinary tract infection
VIMP	Variable importance

ABSTRACT

Immunoassays are a vital tool for clinical quantification of relevant biomarkers, which often lead to diagnostic utility. Plate-based enzyme-linked immunosorbent assays (ELISAs) are a gold-standard technique for quantitatively measuring a variety of biomarkers. However, sample consumption, time-to-result, laborious handling, biological matrix effects, and analyte plexity limitations hinder novel applications in disease diagnostics. While many diagnostic tests focus on a single analyte, multiplexed analyses can contribute a signature profile that can differentiate disease states. Commercialization of multiplexable technologies has led to their increase in clinical relevance. Therefore, analytical advancements, in the form of technology commercialization and multiplexing, are vital for productive clinical translation.

In my doctoral dissertation, I present the validation, development, and implementation of custom microring sensor-based multiplexed immunoassays for a variety of clinical challenges. Chapter 1 reviews current technologies where multiplexed analyses have been applied to clinical samples, focusing on examples used within clinical workflows. Current limitations of these technologies are examined, including sample type accessibility and multiplexity challenges.

Chapters 2 and 3 describe distinct clinical evaluations within latent tuberculosis infection (LTBI) diagnostics, an asymptomatic form of TB. Through multiplexed cytokine measurements in cell supernatant, I examined immunoprofiles of interest and was able

to make accurate predictions regarding risk of reactivation. This study evaluates a panel of thirteen cytokines across six stimulation conditions, including a peptide pool with 300 *Mtb*-derived T cell epitopes, utilizing normalization strategies to account for basal cytokine levels. Random Forest feature selection identified correlative cytokine signatures from normalized stimulation conditions. Receiver Operator Characteristic curves revealed predictive accuracies of greater than 80% for both LTBI+ and High Risk designations.

Chapter 3 uses this LTBI analysis workflow to incorporate the current clinical pipeline, wherein QuantiFERON testing (QFT) stimulated plasma samples for TB evaluation. Our results show predictive accuracy of 90% for detection of LTBI and >80% for risk of reactivation. I successfully designed a combinatorial technique that can be implemented into the clinical workflow to predict LTBI and risk of reactivation using patient QFT samples.

Chapter 4 describes a multiplexed panel for neonates, evaluating basal immune signatures at different gestational ages and the effects of chorioamnionitis. This analysis shows important changes in immature immune responses for unstimulated serum and indicates that there are distinctive profiles for healthy and chorio-exposed preterm infants. Statistical analyses revealed significance for CCL2, TNF-α, IL-1β, IL-6, IL-8, and IL-10. Biomarkers of interest were identified across 23-36 weeks of corrected gestational age. These findings indicate that exposure to chorioamnionitis has long-lasting immune consequences, which may alter their ability to respond to infections. Through this rapid (<1hr) immunoassay, relevant measurements can be made to directly affect treatment options and clinical outcomes.

Chapter 5 establishes a diverse panel for immunoassay implementation, with a total of 15 cytokines for SARS-CoV-2 related analyses. Following the workflow established in Chapter 2, stimulated conditions are utilized to understand how COVID infection produces and (dys)regulates host response. Statistical analyses were utilized to distinguish biomarkers of importance for COVID+ individuals, which include absolute and normalized levels of CCL3, GM-CSF, IFN-λ1, IL-1β, IL-2, and IL-7. Although currently sample limited, multiple cytokines show promise for continued evaluation and potential clinical utility.

Finally, Chapter 6 summarizes the current diagnostic space created, and the future implementations in longitudinal LTBI diagnostics, co-infections in neonatal subjects, and the potential for vaccine immunity evaluation in COVID.

CHAPTER 1

Multiplexed Immunoassays and Clinical Diagnostics: An Unmet Clinical Challenge and Need

Abstract

Immunoassays are a vital tool for clinical quantification of relevant biomarkers, which often lead to diagnostic utility. While many diagnostic tests focus on a single analyte, multiplexed analyses can contribute a signature profile that can differentiate disease states, as well as severity of disease. Multiplexed immunoassays are uncommon due to their complexity, prohibitive cost, and their often nonintuitive outputs. Commercialization of multiplexable technologies, including examples such as Quanterix, Luminex, and sensor technologies, has led to recent increases in clinical relevance. This chapter reviews current available technologies where multiplexed analyses have been applied to clinical samples, focusing on examples used within the clinical workflow. It also examines the current limitations of these technologies, including sample type accessibility, analysis complications, and multiplexity challenges. Finally, it discusses recent developments to implement biosensor-based technologies in a clinical setting.

An Introduction to Diagnostic Assays: Considerations and Challenges

Diagnostic assays are a foundational element of clinical evaluation, spanning importance in academic understanding of biological pathways[1] to determining disease severity[2], clinical outcomes, and treatment feasibility for individuals.[3] In particular, molecular diagnostics are a powerful tool to assist clinicians in investigating causes of infection and clinical outcomes by quantifying a specific antigen in a biological sample.[4] For these diagnostic assays to be useful, multiple considerations are necessary and the translational application must always be prioritized.

Assay considerations are as numerous as they are complex. The first step in assay development is determining a clinical problem to address, and that correlates to finding the proper biomarkers of interest. These can include ion concentrations[5], proteins[6], RNA[7], DNA[8], whole cells (host or foreign), and complexes, among others. The target analyte is the primary concern since all subsequent analytical assay metrics are directly related to this decision. For example, if your target of interest is DNA, there may be steps necessary to ensure there is no enzymatic loss of sample, or samples may need to be treated to convert dsDNA to ssDNA for detection. Once an analyte has been selected, the proper assay format is determined, whether that be sandwich immunoassay, PCR, ion-selective electrodes (ISEs), etc. These will all come with differences in sensitivity, selectivity, robustness, accessibility, and general usability.

Indirect to these analytical considerations are clinical aspects of the assay.[9] The sample type of interest can vary widely and drastically affect the assay formats and analytes possible. Samples can range from whole blood[10] to plasma and serum, saliva[11], sweat[12], nasal swabs[13], bronchoalveolar lavage (BAL)[14], urine[15], cerebrospinal fluid

(CSF)[16], and more. Complications from ionic strength, protein content, cross-reactive species, enzymatic degradation, expected analyte concentrations, and matrix effects on assay feasibility all need to be carefully evaluated to ensure that a reproducible and clinically translatable system is created. Finally, understanding what output metrics are required (time-to-result, portability, technical knowledge required, etc.) to perform this assay are vital to final use.

However, this workflow is generally done for one analyte of interest. For example, plate-based enzyme-linked immunosorbent assays (ELISAs) are a workhorse for clinical laboratories. ELISAs generally utilize specific antibodies for an analyte to create a sandwich complex that can enzymatically amplify the signal from a small amount of analyte into a detectable response. As each well in the plate is specific for one target, it takes time, reagents, and excess sample to look at other targets that could be important for a given application.[17] In addition, biological processes are inherently complex, and it is almost assured that one analyte will not accurately describe a disease, infection, or pathological system. Therefore, multiplexed analyses are moving to the forefront of clinical methodologies. To truly “multiplex”, the goal is to measure multiple analytes within the same sample volume simultaneously. This adds even more complexity to assay development, with cross-reactivity, distinct response readouts, possible number of analytes measured, and matrix (background) effects being the foremost issues.

These challenges have been met recently by technological advances in the clinical diagnostics space. Commercialized instrumentation, accessible assay formatting, and useful time-to-results have become commonplace and therefore clinically viable. Methods for single-molecule detection (Quanterix)[18], multiplexed PCR (Luminex)[19], and sensor-

based (Genalyte)[20,21] assays have all been developed and used in a clinically relevant setting. Of these commercialized systems, each takes a unique focus and approach to solving challenging analytical and clinical problems.

Quanterix

Quanterix is a commercialized platform based around the Single Molecule Array, or SiMOA, assay. The SiMOA assay utilizes functionalized beads, generally with antibodies, to capture targets of interest. A sandwich immunocomplex, much like in plate ELISAs, is created using secondary antibodies that generate added specificity and an enzymatic complex to create an amplified fluorescent readout. These beads are then loaded into femtoliter microwell arrays, where there is a high probability of only one bead per well. Upon enzymatic turnover, wells can be analyzed digitally, and the number of positive wells correlates to a molecular count and therefore concentration of analyte (Figure 1-1).[22] This system is incredibly sensitive, leading to near single molecule detection limits. However, in multiplexing, cross-reactivity can be a major issue, and this system can be expensive and technically laborious. Nonetheless, Quanterix has made itself applicable to clinical audiences in several applications.

One such instance focuses on cytokine levels in inflammatory responses. For this study Rosenthal et al utilized a 9-plex assay to investigate primarily interleukins and chemokines in cardiopulmonary bypass surgery. Dried blood spots from subjects who underwent cardiopulmonary bypass surgery were analyzed for IL-1β, IL-6, IL-8, IL-16, IL-18, MCP-1, CCL3, CCL4, and IAM-1.[23] Looking at samples post-surgery, significant cytokine level differences were identified for all 9 biomarkers. This study, while sample limited, shows the utility, both in multiplexing and temporal evaluations, for Quanterix

diagnostics. We also see more general protein markers being evaluated in a clinical space. Two brief examples are preliminary studies on traumatic brain injury biomarkers. Initially, Korley et al created a 4-plex panel to diagnose TBI from blood biomarkers. From a panel of GFAP, UCH-L1, NF-L, and tau, comparisons were analyzed between healthy and abnormal CT scans. Promisingly, discriminative ability from these markers individually and in combination were shown as AUC results, which resulted in 90% accuracy for the latter.[24] This used a custom designed multiplexed immunoassay, indicating the need and utility of novel panels for clinical analyses. Other researchers took this a step further, by utilizing this panel for a 504-subject cohort. McCrea et al hypothesized that this panel could reveal underlying pathophysiological mechanisms for concussions, further concluding that the ability to use combinatorial assays is clinically important.[25]

Luminex

Luminex is another bead-based commercialized technology that specializes in multiplexed analyses. While originally focused on protein analyses, Luminex has recently reoriented their clinical implementation towards semi-quantitative multiplexed PCR measurements. In this system, beads or microspheres are functionalized with a capture probe for a given pathogen genomic sequence. A sample mixture of beads, clinical sample, and complementary probe are incubated and if pathogen DNA/RNA is found, the capture and complementary probes are ligated together. From this combined sequence, universal primers can be utilized to amplify a fluorescent tag, and a two-laser instrumentation platform identifies both the bead for capture identification and the fluorescence readout (Figure 1-2).[26] These multiplexed measurements are mainly limited

by fluorescence background in terms of sensitivity and distinct bead combinations for captures but can reach meaningful multiplexity in clinical applications.

Luminex has made great strides in pathogen detection, particularly with their xTAG pathogen panels. Two prominent examples are for gastrointestinal and respiratory infections, which prove initial clinical use. Huang et al compared the Luminex platform to two other clinically viable multiplexed assays for gastrointestinal pathogens. While all showed sensitivities above 75%, Luminex showed the most promise for high throughput stool samples screening, with 24 samples run in 5 hours.[27] It is important to note the use of stool samples, since this is an incredibly complex matrix, and shows the possibilities available for xTAG systems. We also find studies focusing on respiratory pathogens, which are particularly important currently. Tang et al evaluated the FDA-approved 17-plex Luminex NxTAG Respiratory Pathogens Panel for sensitivity and specificity across 404 clinical samples. Assays results showed sensitivities and specificities of 80.0% to 100.0% and 98.9% to 100.0%, respectively. Of note, influenza A genotyping was correct 95.5% of the time, which is of particular utility in a clinical setting.[28] Another study by Chen et al shows similar results, and therefore clinical reproducibility.[29] Finally, customized multiplexed assays are also viable. Yin et al developed a novel multiplexed PCR TRIOL (Tuberculosis-Rifampicin-Isoniazid-Ofloxacin-Luminex) analysis using Luminex to measure first- and second-line anti-tuberculosis drug resistance. This assay reached an impressive 100% sensitivity and specificity for identifying Mtb.[30] The authors confirmed that this system was higher throughput and less labor intensive than PCR-sequencing assays, and that the flexibility of assay parameters could allow for inclusion of additional primers to identify uncommon mutations.

Genalyte Microring Resonators

Outside of bead-based diagnostics, sensor technologies have made substantial advances. Through CMOS batch fabrication and simple functionalization, sensors, and in particular silicon photonic sensors, have reach commercialized potential. One such system is produced by Genalyte, where high sensor density (128 sensors) that can be interrogated simultaneously within a small chip footprint has led to recent improvements in multiplexing capabilities.[31] These microring resonators can be functionalized in a variety of methods for different analytes of interest, including miRNA, phosphorylated proteins, DNA, and cytokines. In principle, the universal sensors are functionalized with a capture agent, normally ssDNA or antibodies. Samples are flown across the sensor surface using integrated fluidics, and as binding occurs on the surface, a change in the resonance condition on the sensors is recorded. Secondary and tertiary binding can lead to multiple customizable avenues for amplification and therefore quantitative outputs (Figure 1-3).[21] While not as sensitive as Quanterix, or as potentially multiplexable as Luminex (since a maximum of 32 distinct captures are possible per chip), the Genalyte platform is versatile and quantitative, with the ability to approach a number of assay formats in a reasonable time-to-result of less than 2 hours, with the added advantage of real-time monitoring of assay steps and results. The Genalyte system is currently being used for autoantibody diagnostics in clinical settings, and has a variety of other applications developed from the Bailey Lab.

The Bailey Lab has utilized the Genalyte platform for many multiplexed analyses that could produce clinical utility. Scheler et al used the 32-ring resonator system, measuring primary binding of Streptococcus pneumoniae tmRNA against 4 captures of

different bacterial species. Detection of as low as 53 fmol was achieved, with high specificity shown by monitoring off target rings. Additionally, this was done with primary binding, which is fast and reproducible.[32] This is one of the first publications to show that the real-time monitoring of the assay has many benefits, from troubleshooting, to binding profile fitting, to endpoint results. Wade et al showed the multiplexed utility of the Genalyte platform in a clinical direction, measuring phosphoproteins in both cell line lysate and tumor samples. The updated platform used 128 microrings, functionalized for 12 separate biomarkers. This study also used an ELISA sandwich assay format, which on the rings can be both monitored continuously and be used as an end-point analysis from enzymatic turnover. By measuring both basal levels for the glioblastoma cell lines, as well as expression responses from treatment in culture, they were able to create expression heat mapping, showing fold changes of phosphoproteins due to potential treatments.[33] They were also able to use this panel to distinguish between glioma tissue homogenates and isolated primary glioma stemlike cell samples. With the assay-to-result being under 2 hours, this could be a viable strategy to inform pathologists in making surgical decisions. Graybill et al showed the versatility of the biosensor platform by performing a multiplexed assay for miRNA profiling using label-free asymmetric PCR. Eight miRNAs were measured simultaneously from 20 glioblastoma samples, showing the clinical utility of this panel.[34] And while mainly focused on biomarker discovery, this paper highlights the utility of the platform, as well as the low samples inputs that can be utilized for analyses.

More recently, Robison et al moved the closest to clinical translation, using a 7-plex cytokine panel for analysis of stimulated cell supernatant for LTBI signatures. Tuberculosis (TB) is a pervasive and devastating infectious disease, which can manifest

as an asymptomatic infection known as latent tuberculosis (LTBI). Among this population, 5-10% are estimated to develop an active, transmissible, and potentially lethal TB infection, and so distinguishing LTBI and risk of reactivation from healthy individuals is vital for proper disease management. Measuring cytokine levels in isolated Peripheral Blood Mononuclear Cells (PBMC) samples from 50 subjects across 6 stimulation conditions, both absolute levels and basally controlled levels could be obtained and correlated to clinical information. PBMCs are leukocytes that should contain the immune systems current immunological profile for infection protection and immunity, and by investigating this cell population, direct results to host response challenges can be obtained. This works moved ever closer to clinical importance using bioinformatics and the Boruta method, wherein they identify cytokine and stimulation condition combinations of most importance to distinguish LTBI and risk of reactivation.[35]

To continue these advancements into clinical applications, Genalyte has implemented a new platform known as the Matchbox. This instrument utilizes injection-molded thermoplastic devices for disposable, plug-and-play fluidic handling and sensor placement. With increased precision in flow cell geometries across the chip, assays can be developed that use minimal samples volumes (50-350uL) in under an hour to result. This positions these disposable cartridges as a crucial step towards clinical implementation. Currently, Genalyte Matchbox systems are being used in hospitals to measure multiplexed autoimmune antibodies from whole blood in as little as 15 minutes from primary binding of antigen to specific capture species.[36] Furthermore, the universal sensor platform is amenable to custom multiplexed clinical diagnostics for precision medicine diagnostics.

These technologies are summarized in Table 1-1. In short, there are many considerations necessary for developing clinically usable assays and instrumentation. And while each technology has its unique strengths and weaknesses, ultimately the application of interest will drive the final decisions for necessary capabilities. For the purposes of this thesis, I will be focusing on the Genalyte microring technology for applications in clinical evaluations of disease and infection.

Development of Custom Immunoassays for Clinical Translation

The Genalyte platform is a chip-integrated silicon photonic microring resonator system which is used for sensitive and quantitative multiplexed immunoassay detection with analytical capabilities comparable or better than traditional enzyme-linked immunosorbent assays. The versatility of this refractive index-based platform is in the ability to functionalize rings with multiple capture agents to detect antigens in solution in a concentration-dependent manner. Each chip has 128 individually addressable refractive index sensors that are coupled to a linear waveguide. Under certain resonance conditions, defined by:

$$m\lambda = 2\pi r n_{eff}$$

where the resonant wavelength is dependent upon the microring radius (r), the effective refractive index at the surface of the ring (n_{eff}), and the input wavelength of light (λ). When the proper resonance conditions are met, a characteristic drop in transmission occurs. As the effective refractive index changes on the surface of the ring, based on changes in solvent, adsorption to the surface, binding events, etc., the transmission drop shifts in

wavelength. The corresponding wavelength shift is monitored over time to reveal surface interactions in a quantitative manner.

For the purposes of utilizing immunoassay amplification with this technology, the sensor arrays are functionalized with antibodies covalently tethered to the ring surface via aminosilane chemistry and amine linker chemistries. During the assay, target protein is flown across the sensor surface. For specificity and amplification, secondary antibody modified with biotin is flown to interact with protein bound to the surface. Streptavidin-Biotin interactions are used to tether a horseradish peroxidase (HRP) to the sandwiched protein, and HRP then turns 4-chloronapthol to 4-chloronapthon, an insoluble product, and quantification is accomplished by measuring the magnitude shift in the local refractive index. This amplification strategy allows for analyte quantification at or below pg/ml ranges in an almost identical format as traditional ELISAs, and is outlined on the microring platform in Figure 1-3. Thoughtful analytical validation is necessary for proper implementation, including optimization of saturating conditions, reagent concentrations, calibrations and metrics thereof, and matrix effects. This assay can be multiplexed for the robust detection of multiple protein targets within the same sample through careful cross-reactivity validation and continued multiplexed assay optimization.

The research performed herein focuses on my continual analytical validation, development, and implementation of cytokine multiplexed immunoassays for a variety of clinical needs. In Chapter 2, I continued the development of LTBI diagnostics within the lab, expanding the immunoassay panel, stimulation conditions, and sample cohort size for latent tuberculosis infection (LTBI). The current iteration of this study focuses on identifying normalized cytokine signature profiles within stimulated supernatant samples

and creating predictive model ROC curves for LTBI infection evaluation and risk of reactivation. The biosensor platform is vital to this high-plexity analysis since it would be incredibly laborious and time-consuming to attempt with traditional immunoassay formats across this many biomarkers. It is also important to note the analytical validation and development within this clinical study, as diagnostic metrics within this work are impossible without rigorous analytical evaluation in a multiplexed and matrix relevant fashion.

In Chapter 3 I extended my studies from Chapter 2 but focused on creating a truly clinical workflow for LTBI diagnostics. While supernatant analyses are vital for understanding the physiological mechanisms associated with TB latency and reactivation, clinical relevance is most efficient when utilizing the current clinical workflow. QuantiFERON Tests (QFT) are commonly used blood tests within clinics for TB diagnosis, which include 3-4 stimulation conditions depending on the kit available. Plasma samples are stimulated using protein cocktails pertinent to basal immune responses and TB specifically, and IFN-γ is measured using standard ELISA methods. The main hinderance within this workflow is the final step analyzes only IFN-γ production, and is therefore underpowered for LTBI diagnostics, as recent literature indicates this pathway could be IFN-γ independent.[37] We reevaluated the analytical metrics for our 13-plex assay in plasma conditions, which can be problematic for immunoassays at low dilution factors. Utilizing the same informatics workflow from Chapter 2, we show clinical efficacy with predictive accuracies of >85% for both LTBI and risk of reactivation with minimal cytokine profiles. The additional merits of this approach are in available sample matrices for analysis, clinical workflow feasibility, and potentially quick time-to-result of under an

hour. With proper training and equipment, a multiplexed assay similar to this could be used within clinics to replace the single-plex IFN-γ ELISA and create additional immunoprofiling data for evaluation.

In Chapter 4, I shift focus to utilizing these custom biosensor immunoassays for unstimulated, longitudinal immune response analyses within neonatal subpopulations. Preterm birth affects approximately 11% of all live births globally, and these earlier gestational times can be attributed to conditions such as diabetes, genetic predispositions, and infection. Among the most prominent issues is chorioamnionitis, an often-undiagnosed fetal membrane infection, which accounts for many preterm instances. Current understanding of neonatal immature immune response to chorioamnionitis is limited and diagnostic testing is difficult due to low sample volumes. The present study used a custom 7-plex immunoassay to measure cytokines in unstimulated neonatal waste serum samples. Mann-Whitney analyses compared cytokine levels for healthy and chorioamnionitis-positive preterm infants, and biomarkers of interest were identified across 23-36 weeks of gestational age. This assay demonstrates not only the ability to create custom assays for a given application, but also the feasibility of our endpoint analyses to be implemented in more traditional clinical metrics, such as non-parametric comparisons. With the fully assay lasting 38 minutes, this approach brings near real-time measurements to an underserved and vital clinical space where temporal dynamics could change potential clinical outcomes, disease progression, and treatments.

Finally, in Chapter 5 I focus on one of our most pressing world events, the COVID-19 pandemic. While most analytical focus has been in SARS-CoV-2 detection strategies, and pharmaceutical companies have been preparing viable vaccines, there continues to

be the issue of therapeutics designed to treat COVID infection, and subsequently understanding the pathophysiological underpinnings attributed to disease severity and immunity. However, overall understanding of this infection and its outcomes and long-term effects are limited. Therefore, we need to investigate diagnostic metrics to understand disease severity and the host-pathogen response, so that proper care can be met. While most infected individuals develop only mild disease, a subset of patients progress to develop severe COVID-19, which is associated with high morbidity and mortality. Currently, disease severity has been linked to dysregulated and excessive immunity in COVID-19 and the early pathophysiologic drivers of this immune dysregulation has yet to be further defined. Unfortunately, though early identification of patients with COVID-19 likely to develop critical illness is of enormous importance, reliable biomarkers to identify these patients are lacking.

Chapter 5 is similar to what I accomplished in Chapter 2, but using a 15-plex cytokine panel on our microring resonator platform to analyze stimulated PBMC serum samples from COVID patients to define immunological parameters of disease severity and longitudinal immunity. These cytokines provide a broad immunoprofile, consisting of chemokines, pro- and anti-inflammatory cytokines, as well as immune growth factors, all with potential significance to COVID-19. From stimulation conditions for SARS-CoV-2 spike protein subunits and off-target responses, we interrogated PMBC cytokine levels using precision medicine approaches. Mann-Whitney analyses were utilized to distinguish biomarkers of importance for COVID+ individuals, which at this time include absolute and normalized levels of CCL3, GM-CSF, IFN-λ1, IL-1β, IL-2, and IL-7. And while we are sample limited in this preliminary phase, initial significances are promising

for continued evaluation. By implementing a known workflow that we have evaluated previously, we can investigate important biomarkers for infection response, disease progression, severity, and recovery.

Through each chapter, the central goal has been to create interdisciplinary solutions to clinically relevant problems. Stemming from analytical validation, calibration, and multiplexing, through completion of sample analysis and bioinformatics evaluation, we have developed robust and efficient customized immunoassay methods to identify biomarkers of interest, investigate disease severity, and implement clinical strategies for real world applications.

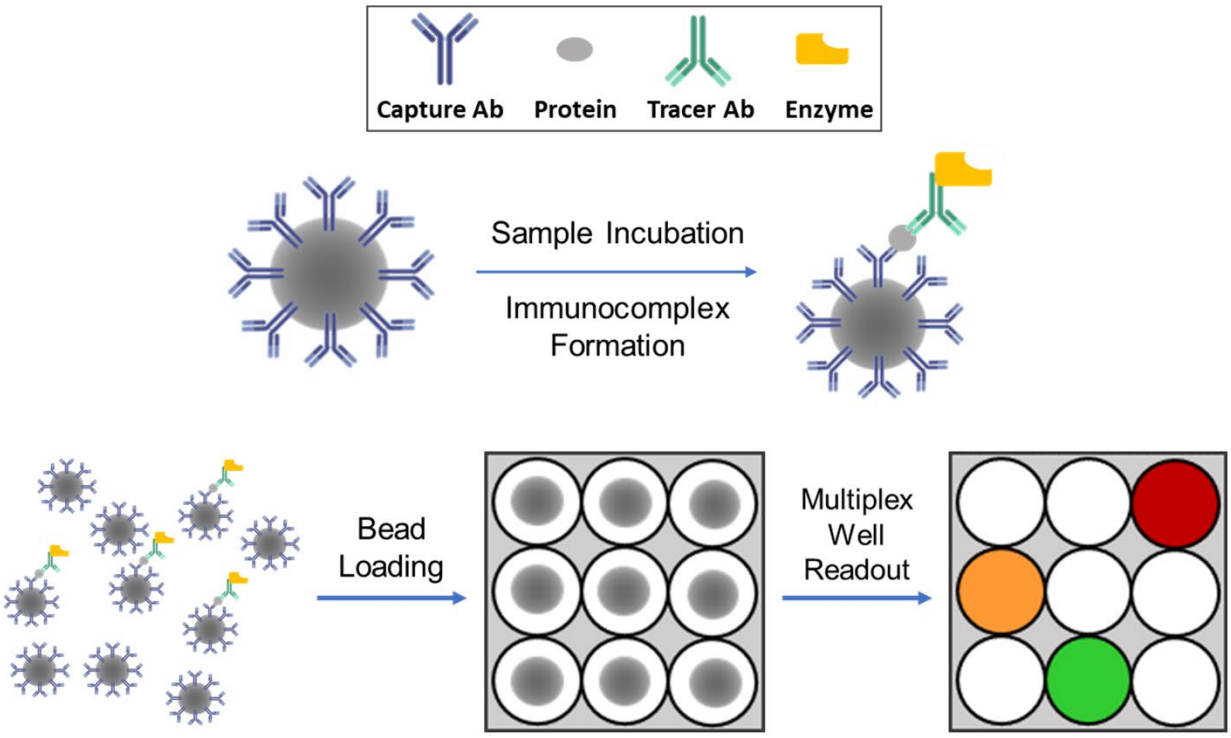

Figure 1-1. Example workflow of the Quanterix SiMOA platform. Beads functionalized with an antibody of interest are incubated with a mixture of sample and detection antibodies. These beads are loaded into femtoliter microwells where fluorescence turnover can occur and each well can be digitally read. In the case of multiplexing, multiple fluorophores would be implemented.

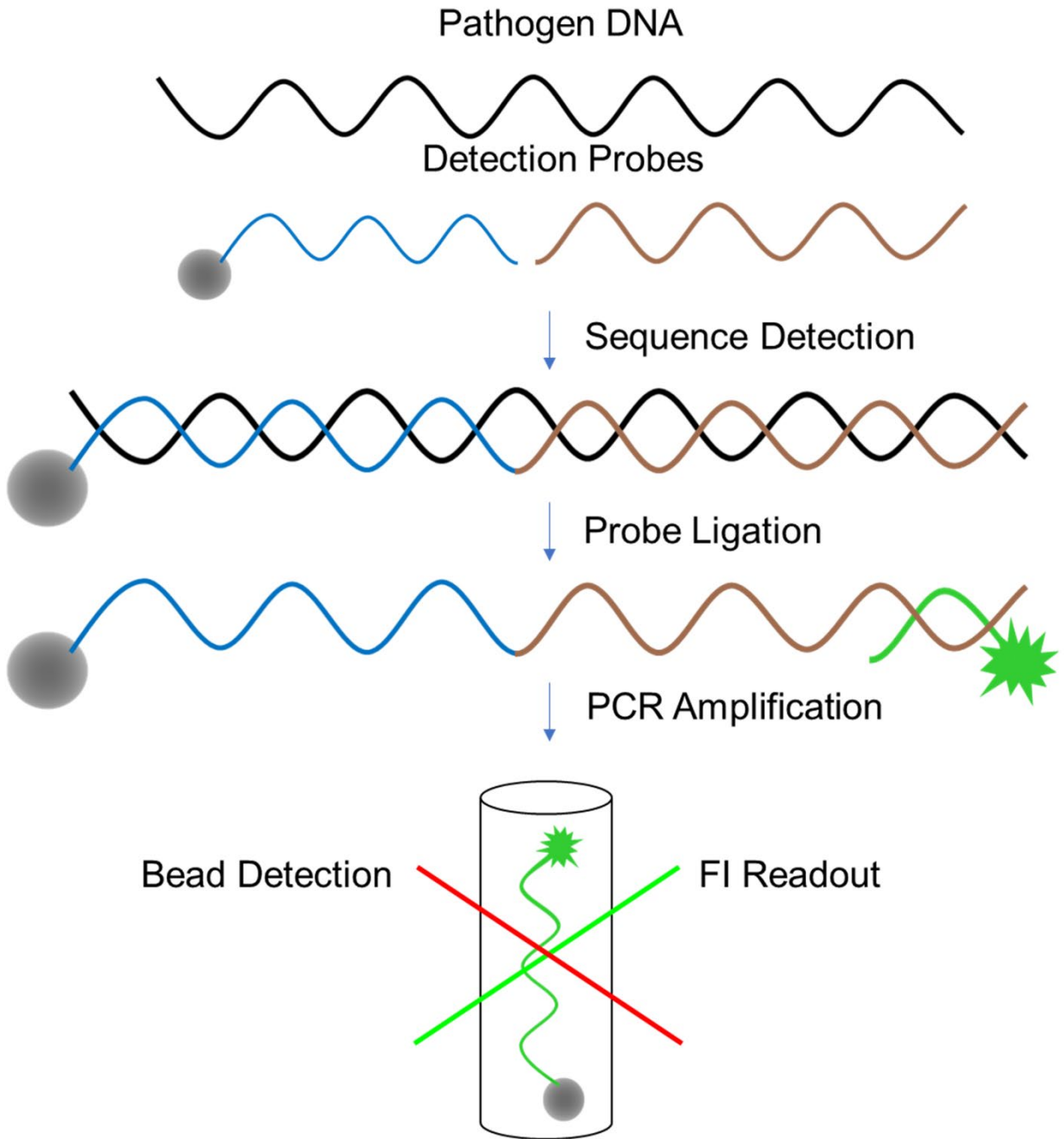

Figure 1-2. Example workflow for Luminex PCR Analysis. Bead coupled capture sequences and detection sequences are incubated with the sample of interest. If a pathogenic sequence is detected, the capture and detection sequences ligate. Subsequent universal PCR primers can be used to turnover fluorescent product. In a multiplexed format, beads would be dyed such that each dye corresponded to a capture sequence, and the two-laser system would read out bead ID and fluorescent count.

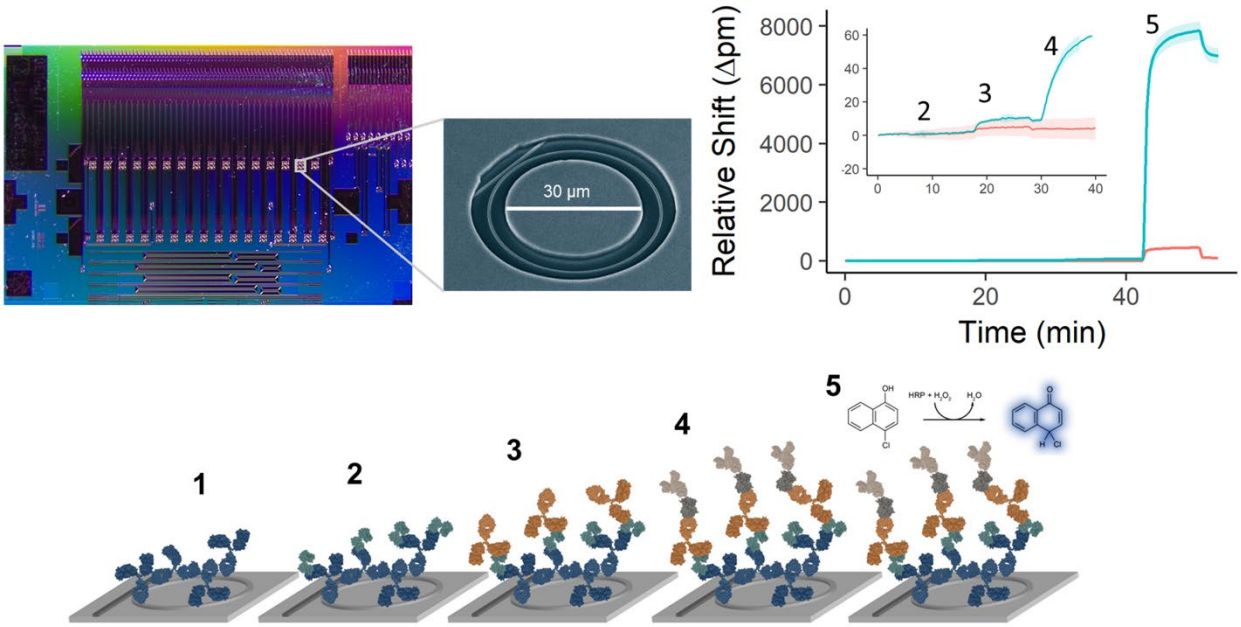

Figure 1-3. Example of the Genalyte mircoring resonator sensors and ELISA assay. All readout occurs on the 4mmx6mm chip, containing 128 microrings for evaluation. Rings are functionalized with relevant capture antibodies (1) before use. Automated fluidic assays consist of sample (2), secondary biotinylated antibodies (3), Streptavidin-Horseradish Peroxidase (SA-HRP) (4), and 4-CN turnover (5), which will sequentially lead to changes in local refractive index due to mass deposited on the ring surface. In a multiplexed assay, clusters of 4 rings are spotted with identical captures, and a cocktail of all pertinent secondary antibodies is used to produce antigen-specific results from the spatially arrayed sensors.

Table 1-1. A summary of important metrics for clinical utility across Quanterix, Luminex, and Genalyte systems.

	Quanterix	Luminex	Genalyte
Sample Volume (uL)	10-50	50-200	50-350
Analyte Plexity	4 (commercially)	50 (commercially)	16 per channel
Sensitivity	Single molecule	pg-ng/mL	pg-ng/mL
Limitations	Technical knowledge needed, plexity	Reproducibility issues, cross-reactivity	Sensor biofouling, maximum plexity of 32 targets

References

1. Topalian, S. L., Taube, J. M., Anders, R. A. & Pardoll, D. M. Mechanism-driven biomarkers to guide immune checkpoint blockade in cancer therapy. *Nature Reviews Cancer* **16**, 275–287 (2016).
2. Lawn, S. D., Kerkhoff, A. D., Vogt, M. & Wood, R. HIV-associated tuberculosis: relationship between disease severity and the sensitivity of new sputum-based and urine-based diagnostic assays. *BMC Med* **11**, 231 (2013).
3. Kim, Y. W. *et al.* Evaluation of Xpert® MTB/RIF assay: diagnosis and treatment outcomes in rifampicin-resistant tuberculosis. *The International Journal of Tuberculosis and Lung Disease* **19**, 1216–1221 (2015).
4. Afshari, A., Schrenzel, J., Ieven, M. & Harbarth, S. Bench-to-bedside review: Rapid molecular diagnostics for bloodstream infection - a new frontier? *Crit Care* **16**, 222 (2012).
5. Scott, L. E. & Orvig, C. Medicinal Inorganic Chemistry Approaches to Passivation and Removal of Aberrant Metal Ions in Disease. *Chem. Rev.* **109**, 4885–4910 (2009).
6. Anderson, N. L. The Clinical Plasma Proteome: A Survey of Clinical Assays for Proteins in Plasma and Serum. *Clinical Chemistry* **56**, 177–185 (2010).
7. Byron, S. A., Van Keuren-Jensen, K. R., Engelthaler, D. M., Carpten, J. D. & Craig, D. W. Translating RNA sequencing into clinical diagnostics: opportunities and challenges. *Nature Reviews Genetics* **17**, 257–271 (2016).

8. Bratman, S. V., Newman, A. M., Alizadeh, A. A. & Diehn, M. Potential clinical utility of ultrasensitive circulating tumor DNA detection with CAPP-Seq. *Expert Review of Molecular Diagnostics* **15**, 715–719 (2015).

9. Masson, J.-F. Surface Plasmon Resonance Clinical Biosensors for Medical Diagnostics. *ACS Sens.* **2**, 16–30 (2017).

10. Danila, D. C. *et al.* Analytic and Clinical Validation of a Prostate Cancer–Enhanced Messenger RNA Detection Assay in Whole Blood as a Prognostic Biomarker for Survival. *European Urology* **65**, 1191–1197 (2014).

11. Malamud, D. Saliva as a Diagnostic Fluid. *Dental Clinics* **55**, 159–178 (2011).

12. Zhang, Y. *et al.* Passive sweat collection and colorimetric analysis of biomarkers relevant to kidney disorders using a soft microfluidic system. *Lab on a Chip* **19**, 1545–1555 (2019).

13. Dangerfield, B., Chung, A., Webb, B. & Seville, M. T. Predictive Value of Methicillin-Resistant Staphylococcus aureus (MRSA) Nasal Swab PCR Assay for MRSA Pneumonia. *Antimicrobial Agents and Chemotherapy* **58**, 859–864 (2014).

14. Paonessa, J. R. *et al.* Rapid Detection of Methicillin-Resistant Staphylococcus aureus in BAL: A Pilot Randomized Controlled Trial. *Chest* **155**, 999–1007 (2019).

15. Zhao, F. *et al.* A urine-based DNA methylation assay, ProCUrE, to identify clinically significant prostate cancer. *Clin Epigenet* **10**, 147 (2018).

16. Vos, S. J. B. *et al.* Variability of CSF Alzheimer's Disease Biomarkers: Implications for Clinical Practice. *PLOS ONE* **9**, e100784 (2014).

17. Aydin, S. A short history, principles, and types of ELISA, and our laboratory experience with peptide/protein analyses using ELISA. *Peptides* **72**, 4–15 (2015).

18. Wu, C., Maley, A. M. & Walt, D. R. Single-molecule measurements in microwells for clinical applications. *Critical Reviews in Clinical Laboratory Sciences* **57**, 270–290 (2020).

19. Reslova, N., Michna, V., Kasny, M., Mikel, P. & Kralik, P. xMAP Technology: Applications in Detection of Pathogens. *Front. Microbiol.* **8**, (2017).

20. Washburn, A. L. & Bailey, R. C. Photonics-on-a-chip: recent advances in integrated waveguides as enabling detection elements for real-world, lab-on-a-chip biosensing applications. *Analyst* **136**, 227–236 (2010).

21. Robison, H. M. & Bailey, R. C. A Guide to Quantitative Biomarker Assay Development using Whispering Gallery Mode Biosensors. *Current Protocols in Chemical Biology* **9**, 158–173 (2017).

22. Chunyk, A. G. *et al.* A Multi-site In-depth Evaluation of the Quanterix Simoa from a User's Perspective. *AAPS J* **20**, 10 (2017).

23. Rosenthal, L.-M. *et al.* A Prospective Clinical Trial Measuring the Effects of Cardiopulmonary Bypass Under Mild Hypothermia on the Inflammatory Response and Regulation of Cold-Shock Protein RNA-Binding Motif 3. *Therapeutic Hypothermia and Temperature Management* **10**, 60–70 (2019).

24. Korley, F. K. *et al.* Performance Evaluation of a Multiplex Assay for Simultaneous Detection of Four Clinically Relevant Traumatic Brain Injury Biomarkers. *Journal of Neurotrauma* **36**, 182–187 (2018).

25. McCrea, M. *et al.* Association of Blood Biomarkers With Acute Sport-Related Concussion in Collegiate Athletes: Findings From the NCAA and Department of Defense CARE Consortium. *JAMA Netw Open* **3**, e1919771 (2020).

26. McArdle, A. *et al.* Developing clinically relevant biomarkers in inflammatory arthritis: A multiplatform approach for serum candidate protein discovery. *PROTEOMICS – Clinical Applications* **10**, 691–698 (2016).

27. Huang, R. S. P. *et al.* Performance of the Verigene® enteric pathogens test, Biofire FilmArray™ gastrointestinal panel and Luminex xTAG® gastrointestinal pathogen panel for detection of common enteric pathogens. *Diagnostic Microbiology and Infectious Disease* **86**, 336–339 (2016).

28. Tang, Y.-W. *et al.* Clinical Evaluation of the Luminex NxTAG Respiratory Pathogen Panel. *Journal of Clinical Microbiology* **54**, 1912–1914 (2016).

29. Chen, J. H. K. *et al.* Clinical Evaluation of the New High-Throughput Luminex NxTAG Respiratory Pathogen Panel Assay for Multiplex Respiratory Pathogen Detection. *Journal of Clinical Microbiology* **54**, 1820–1825 (2016).

30. Yin, F. *et al.* Development and in-use evaluation of a novel Luminex MicroPlex microsphere-based (TRIOL) assay for simultaneous identification of Mycobacterium tuberculosis and detection of first-line and second-line anti-tuberculous drug resistance in China. *Journal of Clinical Pathology* **70**, 342–349 (2017).

31. Washburn, A. L., Shia, W. W., Lenkeit, K. A., Lee, S.-H. & Bailey, R. C. Multiplexed cancer biomarker detection using chip-integrated silicon photonic sensor arrays. *Analyst* **141**, 5358–5365 (2016).

32. Scheler, O. *et al.* Label-free, multiplexed detection of bacterial tmRNA using silicon photonic microring resonators. *Biosensors and Bioelectronics* **36**, 56–61 (2012).

33. Wade, J. H. *et al.* Rapid, Multiplexed Phosphoprotein Profiling Using Silicon Photonic Sensor Arrays. *ACS Cent. Sci.* **1**, 374–382 (2015).

34. Graybill, R. M., Cardenosa-Rubio, M. C., Yang, H., Johnson, M. D. & Bailey, R. C. Multiplexed microRNA expression profiling by combined asymmetric PCR and label-free detection using silicon photonic sensor arrays. *Anal. Methods* **10**, 1618–1623 (2018).

35. Robison, H. M. *et al.* Precision immunoprofiling to reveal diagnostic signatures for latent tuberculosis infection and reactivation risk stratification. *Integrative Biology* **11**, 16–25 (2019).

36. Mudumba, S., *et al*. Photonic ring resonance is a versatile platform for performing multiplex immunoassays in real time. *Journal of Immunological Methods* **448**, 34–43 (2017).

37. Lu, L. L. *et al.* IFN-γ-independent immune markers of Mycobacterium tuberculosis exposure. *Nature Medicine* **25**, 977–987 (2019).

CHAPTER 2

Latent Tuberculosis Infection Classification and Risk Assessment through a Multiplexed Cytokine Biosensor Assay with Random Forest Reduced Feature Selection

Acknowledgements

This chapter has been adapted from the research article “Risk Assessment of Latent Tuberculosis Infection through a Multiplexed Cytokine Biosensor Assay and Machine Learning Feature Selection” (Robison, H. M.*, Chapman, C. A.* *et al. Scientific Reports* (2021) – In Submission). Dr. Heather Robison conceived the project, and my contributions include multiplexed assay validation, sample analysis, bioinformatics interpretation, and writing. I would like to acknowledge Dr. Patricio Escalante, Dr. Elitza Theel, and Courtney Erskine for clinical assistance, cell stimulations, and general guidance. I also acknowledge Haowen Zhou and Dr. Ruoqing Zhu for their Random Forest analysis expertise. This work was supported by the National Institute of Allergy and Infectious Diseases at the National Institutes of Health (AI141591). Part of this project was also supported by Grant Number UL1 TR000135 from the National Center for Advancing Translational Sciences (NCATS).

Abstract

Latent tuberculosis infection (LTBI) is a quiescent and asymptomatic infection in which the immune system cannot fully eradicate the tuberculosis (TB) pathogen. Existing diagnostics for TB are strongly indicative of prior and active infection but hold limited predictive value for LTBI progression or reactivation risk. We previously utilized multiplexed immunoassays to profile cytokines from peripheral blood mononuclear cells stimulated with TB-derived and non-specific antigens to identify signatures for LTBI status and reactivation risk. As an extension of this work, this study evaluates a panel of thirteen cytokines across six stimulation conditions, including a peptide pool with 300 *Mtb*-derived T cell epitopes (MTB300). Random Forest feature selection and data reduction methods identified correlative cytokine signatures from normalized stimulation conditions. Receiver Operator Characteristic curves revealed predictive accuracies of greater than 80% for both LTBI+ and High Risk designations. This approach provides rich biomarker signatures for a disease framework of enormous global need.

Introduction

Tuberculosis (TB) is a pervasive and devastating infectious disease that led to 1.5 million deaths in 2018.[1] Beyond the acute morbidity of the disease, it also can manifest as an asymptomatic infection known as latent tuberculosis (LTBI), which greatly complicates disease management. Approximately 1.7 billion people are estimated to have this quiescent infection state.[1-3] Among this population, 5-10% are estimated to develop an active, transmissible, and potentially lethal TB infection.[4-6] LTBI is treatable with prolonged antibiotic regimens, but potential drug-related toxicities and treatment non-adherence issues obviate the need to identify patients most likely to benefit from these therapies. To properly diagnose individuals with LTBI, and more specifically those with high reactivation potential, improved diagnostic tools are needed. While current assays for TB, including the Tuberculin Skin Test (TST) and Interferon-Gamma Release Assays (IGRAs), reveal previous exposure to TB, they offer limited benefit for LTBI diagnosis and reactivation risk stratification.[7] There is a growing consensus that this latent infection and the conditions that foster reactivation include complex changes in the immunological landscape that may be independent of the pathogen itself.[8-14] Therefore, multiparameter strategies that probe immune (dys)regulation in response to TB-specific and non-specific antigen challenge may provide new diagnostic insights into not only the status of LTBI infection, but also the risk of reactivation.

Previously, our groups described an approach to multiplexed cytokine profiling of supernatants from stimulated peripheral blood mononuclear cells (PBMCs) using arrays of silicon photonic microring resonators.[15] This workflow involved five different TB-specific and non-specific stimulation conditions, and the quantification of seven cytokines. Using

a precision normalization approach to correct for individual patient heterogeneity and a bioinformatic feature selection approach, we identified multi-biomarker signatures that preliminarily correlated with LTBI status and elevated reactivation potential. This study suggested relevant biomarkers beyond interferon-gamma (IFN-γ), which is the cytokine detected in IGRAs, and also highlighted the importance of precision normalization using non-TB-related antigen challenges as a way of accounting for differences in basal immune response. However, this was only a first proof-of-concept study towards the development of a new LTBI detection paradigm as it focused on a limited number of cytokines and a relatively small population of research subjects.

Building upon this previous study, we have now expanded to a larger panel of cytokines (13) as suggested by experimental studies in immunity to TB, again detected using silicon photonic microring sensor arrays, and enrolled a larger research cohort (75 subjects). We also have added a new antigen condition with the MTB300 reagent, which is a comprehensive “megapool” of *M. tuberculosis* (Mtb) peptides that captures a large fraction of the *Mtb*-specific T cells.[16] Cytokine concentrations were determined for each stimulation condition and normalized by pairwise subtraction of levels from other stimulation conditions. The resulting normalized cytokine levels were then subjected to Random Forest feature selection to identify biomarker signatures correlating with LTBI+ status and High Risk of reactivation (the entire workflow is illustrated in Figure 2-1). Statistically-driven thresholding was then applied to identify the most relevant biomarkers having the highest predictive accuracy for these clinical designations. Receiver-Operator Characteristic (ROC) curves were generated for both full and reduced data sets with Area-Under-the-Curve (AUC) analyses revealing predictive accuracies exceeding 80%

for reduced biomarker signatures. These studies suggest that multiplexed analyses and precision cytokine normalization can generate highly predictive signatures for LTBI status and reactivation potential that may find utility in clinical management of patients with LTBI through a personalized medicine approach.

Methods

Reagents and buffers

Reagents, including Dulbecco's phosphate buffered saline (PBS), bovine serum albumin (BSA), (3-Aminopropyl)triethoxysilane, glycerol, bis(sulfosuccinimidyl)suberate, starting block blocking buffer, Pierce high sensitivity streptavidin-HRP (SA-HRP), 4-chloronaphthol (4-CN), and Drycoat assay stabilizer were purchased from commercial vendors as listed in Table 2-1. Vendors and catalog numbers for antibodies against all cytokines and the mouse IgG isotype control are summarized in Table 2-2. Running buffer for all assays was 0.5% BSA in 1X PBS, pH 7.4.

Cell Culture and Antigen Stimulations

Cell culture and antigen stimulation methods have been described previously.[15] Briefly, PBMCs were separated by from whole blood by Ficoll separation and the pellets frozen with 10% DMSO in liquid nitrogen. Thawed PBMC pellets (viability ≥85%) were stimulated for 40–48 h with either TB-relevant or off-target antigens. Supernatants from stimulated PBMCs were stored at −80°C and shipped on dry ice for cytokine measurements using the 13-plex antigen immunoassay on the microring resonators. Samples were thawed and vortexed prior to loading into a 96-well plate for microring assays. Each sample was analyzed undiluted and after a 10-fold dilution in running buffer.

Clinical Category Determination

This study was approved by the Mayo Clinic Institutional Review Board and Olmsted County Public Health Services. All study participants signed an informed written consent and were enrolled in Rochester, MN between July 2017 and December 2018. Study subjects included unexposed individuals and subjects with various risk for TB infection, including untreated LTBI patients and patients with having had LTBI therapy and thus at low risk of reactivation. Risk factors for TB infection, TB progression, and/or TB reactivation were extracted through a validated questionnaire and review of medical records as previously described.[15,17] LTBI diagnoses were made per the Center for Disease Control and Prevention (CDC) criteria and based on TB risk factors, and by prior TST and QuantiFERON®-TB Gold In-Tube (QFT) results.[18] A modified multifactorial predictive modeling platform (i.e. 'Online TST/IGRA interpreter'), adjusted by LTBI treatment effect, was also applied to estimate the cumulative risk of TB reactivation in all subjects as previously described.[19,20] Table 2-3 details all clinically relevant cohort information.

Multiplexed immunoassay instrumentation and assay design

Microring immunoassays were performed on the Maverick Matchbox system (Genalyte, Inc., San Diego, CA) as previously described.[21] This platform utilizes injection-molded microfluidic devices to introduce fully automated flow for all assay steps across functionalized sensor arrays. These devices are disposable, to ensure no contamination between assays.[22,23] Microring arrays were batch functionalized via spotting to yield a 13-plex array of capture antibodies covalently immobilized on sensor substrates. After flowing the sample across the chip, a cocktail containing all the tracer antibodies was

flowed across the array followed by signal enhancement reagents. Antibody capture and tracer concentrations used are listed in Table 2-4. Shifts in resonance wavelength from the signal enhancement step are directly correlated to the concentration of target analytes in solution. Immunoassays were performed with a consistent 30μl/min flow rate for all steps. There was an initial rinse of 5 minutes with the running buffer to ensure equilibration of the chip prior to sample analysis. The assay included steps as follows: 1) running buffer (2min); 2) sample (7min); 3) running buffer rinse (2min); 4) biotinylated tracer antibodies (7min); 5) running buffer rinse (2min); 6) SA-HRP (7min); 7) running buffer rinse (2min); 8) 4-CN (7min); 9) running buffer rinse (2min). The total assay time was 38 minutes. Figure 2-2 shows a real-time trace of resonance wavelength shifts during a representative multiplexed immunoassay.

Calibrations and Sample Analyses

Immunoassays were simultaneously calibrated for all antigens in a multiplexed format. Serial dilutions from a saturating antigen concentration for each multiplexed immunoassay yielded eight-point calibrations relating relative resonance shifts to standard concentrations. To quantify relative shifts, the signal during the buffer rinse before the assay enhancement step (t=29min) was subtracted from the final assay rinse step (t=38min). Net resonance wavelength shifts (Δpm) were plotted as a function of standard concentration and fit to a four-parameter logistic function as described previously[21] via the following equation:

$$\Delta pm = A_2 + \frac{(A_1 - A_2)}{1+\left(\frac{[antigen]}{[antigen]_{0.5}}\right)^p} \quad [1]$$

where A_1 is the lower resonance shift bound, A_2 is the upper resonance shift bound, $[antigen]_{0.5}$ is the concentration yielding 50% of maximum signal, and p is the power parameter affecting the slope at $[antigen]_{0.5}$. Limits of detection (LOD) and quantification (LOQ) were defined as the blank signal plus 3 times and 10 times the standard deviation of the blank, respectively. Each calibration was performed in triplicate for each sample dilution (Figure 2-3) as measured with 4 sensors per technical replicate.

Samples were analyzed undiluted (1X) and diluted (0.1X) into running buffer. Cytokine concentrations within supernatant samples were determined from corresponding serum calibrations (10% and 1% serum, respectively, matching the serum content in supernatant samples). Final concentrations were measured using the most appropriate dilution/calibration as determined by how close the value came to the midpoint of the calibration. Precision normalization was achieved by separately subtracting the control or off-target cytokine concentration from that measured at the other stimulation conditions.

Random Forest and ROC Curve Analyses

Random Forest methods[24] were utilized to determine the biomarker features associated with both LTBI+ and High Risk clinical designations. Random Forest is an ensemble classification algorithm that can detect nonlinear effects of covariate features. Moreover, it provides a ranking of importance of each covariate, while the importance is identified by their effect on classification of either LTBI or risk of reactivation. Using these randomized decision tree outputs, a ROC curve can be established that indicates the predictive accuracy the variables hold for a given classification.

Feature importance analysis was done for all variables available (143 total), and ROC curves were produced. Utilizing the important features from those analyses, a secondary Random Forest algorithm was produced for further enhancement of predictive accuracy by removing unimportant or noisy features. This was done identically for both LTBI+ and High Risk clinical designations. Mann-Whitney plots were utilized to evaluate each important variable in the signature. All informatics and plotting were performed using R coding language.[25,26]

Results

Study subjects

We sequentially enrolled a total of 75 subjects, including 32 subjects with diagnosis of LTBI by QFT and/or TST results and 5 immunosuppressed patients for various medical conditions (Table 2-3). All HIV-tested subjects were non-reactive by ELISA (45 out of 75). The majority of study participants were health care workers (73%) with various risks of TB exposure, and 23 unexposed subjects with negative QFT and a predicted annual risk of zero. There were no significant age differences across the study clinical designations.

Full vs Reduced Random Forest Feature Selection

The initial Random Forest analysis was performed using all possible normalized features from the full dataset (13 cytokines x 11 normalized, pairwise conditions), identifying 143 features viable for the LTBI+ clinical designation. Based on all possible features, a ROC curve for LTBI+ was produced, yielding an AUC of 0.767 (76.7% predictive value). From this full feature analysis, a reduced random forest validation containing all the important features from the full analysis was created using the statistical

variance of each feature and establishing a threshold based on predictive accuracy improvement. Therefore, the 19 identified features after data reduction, which span a variety of cytokines and normalized conditions, can be considered as the most relevant to the ROC curve's predictive power. A ROC curve constructed using only these reduced features yielded an AUC of 0.874. Mann-Whitney analyses of the statistical significance of variables included in the reduced analysis are detailed in Table 2-5.

Importance of MTB300 Stimulation Condition

To assess the added benefit of the MTB300 stimulation condition, which specifically targets a large fraction of *Mtb*-specific CD4+ and CD8+ T cell populations, separate Random Forest feature selection and data reduction algorithms were performed for LTBI+ in the absence of any normalized conditions that included the MTB300 stimulation. A quantitative comparison between the previous reduced feature set for LTBI and the further reduced analysis without MTB300 shows a loss of 5.3% in prediction accuracy (AUC changed from 0.874 to 0.821), indicating a valuable role for MTB300 in improving LTBI diagnostic utility.

Stratification of Subjects Based upon High Risk of Reactivation

Reduced Random Forest analysis was performed using the entire normalized dataset as input for the High Risk of reactivation clinical designation. Though this subpopulation is smaller than the LTBI+ pool, it is still large enough for robust feature identification. The full data set analysis for High Risk used all 143 features with a resulting AUC of 0.715. Upon performing the statistical feature reduction, 14 features were identified as most relevant, and these reduced features yielded a predictive accuracy of

0.855. Mann-Whitney analyses of the statistical significance of these reduced biomarkers is detailed in Table 2-6.

Discussion

LTBI is a persistent and quiescent infection that has proven difficult to identify accurately using conventional diagnostic methods. The added stratification of progression and/or reactivation potential has further been a diagnostic challenge that limits the ability to robustly identify patients most likely to benefit the most from antibiotic treatment. Utilizing our 13-target multiplexed cytokine panel and powerful bioinformatic approaches, we have identified multi-biomarker signatures that show strong correlations to clinical designations of LTBI+ and High Risk of reactivation with an approach that only uses input biomarker levels to achieve these diagnoses.

Based upon our previous study, we found that precision normalization revealed a richer biomarker signature compared to feature selection using non-normalized cytokine levels within stimulated PBMC supernatants. We attributed this to elimination of patient-to-patient heterogeneities in basal immune responses, which were corrected by subtracting non-TB control levels. Therefore, we utilized normalized cytokine levels obtained by subtracting control and off-target antigen stimulation conditions from other supernatant solutions. Using these normalized values as input, iterative feature selection methods were applied as described to identify biomarkers that first correlated with the LTBI+ designation, as determined via extensive clinical chart review. Using all 143 possible features from the full dataset (Figure 2-4A), a ROC curve was generated and found to have an AUC of 0.767, or a 76.7% predictive accuracy (Figure 2-4C). Realizing that some features might have more overall significance than others, a statistical data

reduction routine was performed, identifying 19 features that most strongly correlated with LTBI+ (Figure 2-4B). Biomarkers in the reduced set included IL-2, IFN-γ, IP-10, CCL8, CCL2, IL-6, and CCL3 under varying normalized stimulation conditions. The ROC/AUC analysis using just the reduced feature showed a predictive accuracy of 87.4%, which was a 10.7% improvement over the full feature set (Figure 2-4C). We hypothesize that some of the features in the full data set feature reduction, while weakly correlated with LTBI+, contained higher levels of biological variance that reduce the overall predictive potential across the diverse LTBI+ cohort. Application of this thresholding approach to data reduction focused the biomarker signature on those features most relevant, thereby increasing the predictive accuracy of the ROC curve and diagnostic efficacy. For future studies, this realization is also important as it will allow for the development of more focused and simplified cytokine panels that do not require non-essential biomarkers.

Beyond the inclusion of more cytokines in this updated panel, we also included the MTB300 stimulation condition, so as to probe the relative value of this stimulation condition in more accurately diagnosing LTBI. MTB300 is a mixture of 300 Mtb-derived T cell epitopes that specifically targets a large fraction of *Mtb*-specific CD4+ and CD8+ T cells.[16,27] Both Purified Protein Derivative (PPD) and CFP-10/ESAT-6 (CE) have traditionally been used in TST and QFT testing, respectively. While these stimulations can elucidate an immune response that is indicative of tuberculosis exposure, they are potentially insufficient to differentiate LTBI or reactivation risk. In addition, the majority of the human response to peptide antigens from *Mtb* is not contained in the peptide mixtures of IGRAs.[16] In this context, the use of the MTB300 “megapool” of peptides in our immune profiling method may theoretically confer a better sensitivity over IGRA methods by

targeting a larger fraction of the *Mtb*-specific T cells. Importantly, MTB300 contains 300 primarily MHC class II restricted T cell epitopes from 90 different antigens in Mtb. While these epitopes are derived from Mtb many of these epitopes are also conserved in the *M. bovis* bacillus Calmette-Guérin (BCG) and also non-tuberculous mycobacteria. To verify that the new stimulation condition adds value to our multiplexed cytokine profiling approach, we performed identical feature selection and data reduction methods omitting all normalized features that contained the MTB condition. Focusing just on the reduced feature sets for LTBI+ for comparison (Figure 2-5), we found that AUCs fell by 5.3% upon the removal of the MTB condition, indicating the importance of MTB300 for improved diagnostic accuracy.

Similarly to the LTBI+ designation, we also performed identical feature selection of both the full normalized feature set and after data reduction for the High Risk clinical designation (Figure 2-6). Again, the reduced data set yields an improved predictive value (85.5% reduced vs 71.5% full). Additionally, we find a similar number of relevant biomarker features for High Risk and LTBI+ designations, with IFN-γ, IP-10, IL-2, IL-6, CCL3, and CCL8 appearing in both designations. These targets are important in T cell recruitment, granuloma formation, and inflammatory regulation,[28-32] and so the overlapping relevance for these biomarkers is not unsurprising.[9,10,33] Interestingly, we also find some markers that are unique between the designations. Specifically, the chemotactic marker CCL2, which is induced by tissue injury or infection,[34] was identified as relevant for LTBI+, but not for High Risk. Conversely, the cytokines TNF-α, IL-17, and IL-15 were found to be uniquely relevant for the High Risk designation.[35-38] Given that LTBI reactivation is thought to occur due to global changes to host immune regulation, it

is intriguing that cytokines not typically associated with the acute TB infection response to have diagnostic utility in reactivation risk stratification. As a corollary, patients on anti-TNF-α therapies are known to have higher risk of reactivation, which suggests the potential for diagnostic monitoring of multiple immune regulatory factors when surveilling for reactivation risk.

Overall, we found that this multiplexed, precision normalization approach to diagnosing LTBI and stratifying high reactivation potential resulted in multi-biomarker signatures with AUCs in excess of 0.80 for reduced feature sets. This study highlights the critical value in moving beyond single biomarker-based methods, such as IGRAs that just analyze for IFN-γ. Furthermore, we found that MTB300 provides a measurable improvement in the predictive accuracy of the LTBI+ diagnostic signature.

Our study does have some potential limitations. Specifically, there is no diagnostic gold standard for LTBI, and available diagnostic tests are imperfect. However, our study subjects were carefully selected to minimize heterogeneity in the study groups and to align with current clinical diagnostic standards.[18] In addition, most of our study cohort included non-HIV immunocompetent individuals, which could limit the applicability of our study findings to immunosuppressed subjects and people with HIV infection. Another potential limitation is the use of the 'Online TST/IGRA interpreter,' which has not been prospectively validated. However, we decided to use this predictive tool for research purposes in absence of any other unbiased clinical tool that theoretically quantifies cumulative risk of TB reactivation in LTBI using TST and/or IGRA results plus evaluation of an individual's most relevant epidemiologic and clinical characteristics.[20] Moreover, the annual risk of infection estimated by the 'Online TST/IGRA interpreter' is based on long-

term longitudinal data of TB reactivation.[39] Lastly, nine study subjects participated twice several months after their initial study participation; however, we decided to include their study data since some of them had changes their follow-up QFT results, and thus their LTBI diagnostic designation. These immune profiling changes probably represent the dynamic nature of LTBI in some of these subjects, which we wanted to also capture during this study.

Conclusion

Using this expanded 13-plex cytokine immunoassay biosensor panel, we have demonstrated the ability to better identify complex biomarker signatures for LTBI diagnosis and to elucidate targets of interest for reactivation risk assessment. Our bioinformatics approach using Random Forest feature selection has shown excellent utility in determining important biomarkers and normalized conditions vital for clinical discrimination between subjects. Furthermore, the feature reduction leads to an improved predictive accuracy and the potential to optimize the multiplexed panel to its most essential components for simplified assay development. We found multiple markers that are essential for both LTBI and reactivation risk, including IFN-γ, IP-10, IL-2, IL-6, CCL3, and CCL8, which represents a broader immunological profile than single target assays. Conversely, distinctive targets such as CCL2 reveal subjects at higher risk of reactivation from the greater LTBI+ cohort. We also revealed the value of the peptide pool MTB300 for future stimulated cell-based analyses through data reduction methods. Predictive accuracies for both designations were above 80%, which indicates the potential for improved patient monitoring and clinical care. This biosensor technique, combined with

robust bioinformatics, supports this unique strategy for biomarker-only signatures yielding reliable evidence-based clinical decisions for LTBI and the reactivation risk.

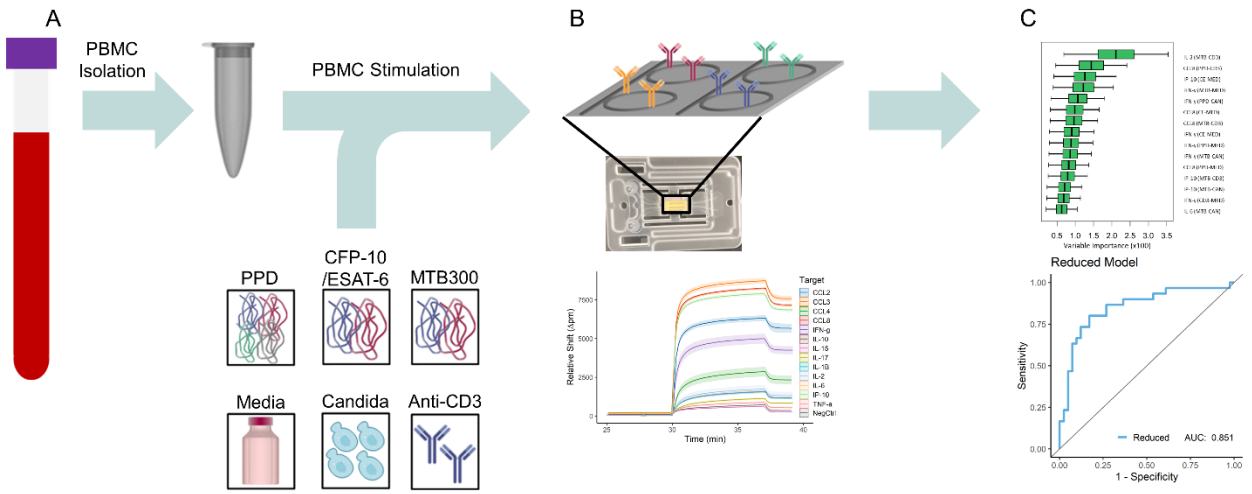

Figure 2-1. Workflow for LTBI supernatant sample analysis. A) Subject PBMCs are stimulated under multiple on- and off-target conditions. B) Samples are analyzed using the Genalyte Matchbox system, which uses plug-and-play chip and device interfaces to measure cytokine concentrations quickly and reproducibly in a multiplexed assay format. The resonance shift output is recorded and converted to concentrations based on individual cytokine calibrations in the sample matrix. C) Random Forest bioinformatics determine what clinical features are important for categorical distinctions and predictive accuracy, with statistical data reduction methods employed to identify biomarker signatures most highly correlated with given clinical determinants.

Table 2-1. Reagents for buffers, chip functionalization and storage, and immunoassay steps.

Reagent	Source	Catalog Number
Dulbecco's phosphate buffered saline	Millipore Sigma	D5573
Bovine serum albumin	Millipore Sigma	A2153
(3-Aminopropyl)triethoxysilane	Millipore Sigma	440140
Glycerol	Thermo Fisher Scientific	BP229
bis(sulfosuccinimidyl)suberate	Thermo Fisher Scientific	A39266
starting block blocking buffer	Thermo Fisher Scientific	37538
Pierce high sensitivity streptavidin-HRP	Thermo Fisher Scientific	21130
4-chloronaphthol	Thermo Fisher Scientific	34012
Drycoat assay stabilizer	Virusys Corporation	AG066

Table 2-2. Antibodies and recombinant standard proteins used in the multiplexed immunoassay.

Target	Role	Source	Catalog Number
CCL2	Capture Antigen Tracer	Thermo Fisher Thermo Fisher Thermo Fisher	14-7099 14-8398 13-7096
CCL3	Capture Antigen Tracer	R&D Systems R&D Systems R&D Systems	MAB670-100 270-LD-010 MAB270-100
CCL4	Capture Antigen Tracer	R&D Systems R&D Systems R&D Systems	CUSTOI702-AZY021708A 271-BME-010 CUSTOI702-IGH021710A
CCL8	Capture Antigen Tracer	R&D Systems R&D Systems R&D Systems	MAB281-100 281-CP-010 BAF281
IFN-γ	Capture Antigen Tracer	Mabtech Thermo Fisher Mabtech	3420-3-250 BMS303 3420-6-250
IL-1β	Capture Antigen Tracer	Thermo Fisher Thermo Fisher Thermo Fisher	14-7018-85 RIL1BI 13-7016-85
IL-2	Capture Antigen Tracer	BD Biosciences Thermo Fisher BD Biosciences	555051 14-8029 555040
IL-6	Capture Antigen Tracer	Thermo Fisher Thermo Fisher Thermo Fisher	16-7069 14-8069 13-7068
IL-10	Capture Antigen Tracer	Thermo Fisher Thermo Fisher Thermo Fisher	16-7108 14-8109-80 13-7109
IL-15	Capture Antigen Tracer	R&D Systems R&D Systems R&D Systems	MAB647 247-ILB-005 BAM247
IL-17	Capture Antigen Tracer	Mabtech Mabtech Mabtech	3520-3-250 3520-10 3520-6-250
IP-10	Capture Antigen Tracer	BD Biosciences BD Biosciences BD Biosciences	555046 551130 555048
TNF-α	Capture Antigen Tracer	Biolegend Biolegend Biolegend	502802 570102 502904

Table 2-3. Clinical characteristics for the study cohort.

Group	All	TST+*	QFT+**	LTBI+***	High Risk+
N (%)	75 (100)	37 (49.3)	32 (42.7)	32 (42.7)	24 (32)
Male, N (%)	24 (32)	16 (43.2)	13 (40.6)	14 (43.8)	11 (45.8)
Female, N (%)	51 (68)	21 (56.8)	19 (59.4)	18 (56.2)	13 (54.2)
HCW, N (%)	55 (73.3)	37 (100)	26 (81.3)	27 (84.4)	18 (75)
Age (mean years ± SD)	53.2 ± 17.5	49.6 ± 18.4	46.3 ± 17.0	48.6 ± 19.1	45.7 ± 18.6
Predicted Risk (mean ± SD)	2.7 ± 7.3	2.9 ± 3.0	4.8 ± 10.6	3.0 ± 2.5	6.3 ± 11.9

(*) Cohort includes 4 subjects with unavailable TST results.

(**) Cohort includes 2 subjects with indeterminate QFT results.

(***) LTBI clinical designation was based on current diagnostic guidelines with positive QFT and/or TST results.[18]

Abbreviations – N (number), HCW (health care worker), SD (standard deviation), TST (Tuberculin Skin Test), QFT (QuantiFERON Gold TB In-Tube™ test). Cumulative predicted risk of TB reactivation was based on a modified multifactorial modeling platform (i.e. 'Online TST/IGRA interpreter') applied to all subjects as previously described.[19,20] All clinical variables are aggregated by positive tests or indications. Study subjects included 5 patients with non-HIV immunosuppressed conditions (one on methotrexate for rheumatoid arthritis, one on sirolumus for lymphangioleiomyomatosis, one with history of chemotherapy and stem-cell transplantation for angioimmunoblastic lymphoma, one on 50 mg daily of prednisone for bullous pemphigoid, and one on hydroxychloroquine and low-dose prednisone for lichenoid mucositis). The total sample set is 75 samples, encompassing 65 unique subjects and 10 additional time points separated by 5-11 months in testing, representing unique samples.

Table 2-4. Antibody concentrations used for capture and tracer pairs. Captures were spotted in 1xPBS, 5% glycerol. All tracers were diluted in running buffer. Streptavidin-Horseradish Peroxidase (SA-HRP) was diluted to 4µg/mL for all experiments.

Target	Capture (mg/mL)	Tracer (µg/mL)
CCL2	0.25	2
CCL3	0.25	1
CCL4	0.25	2
CCL8	0.25	2
IFN-γ	0.25	2
IL-1β	0.25	2
IL-2	0.25	2
IL-6	0.25	2
IL-10	0.25	2
IL-15	0.25	2
IL-17	0.25	2
IP-10	0.25	2
TNF-α	0.25	2

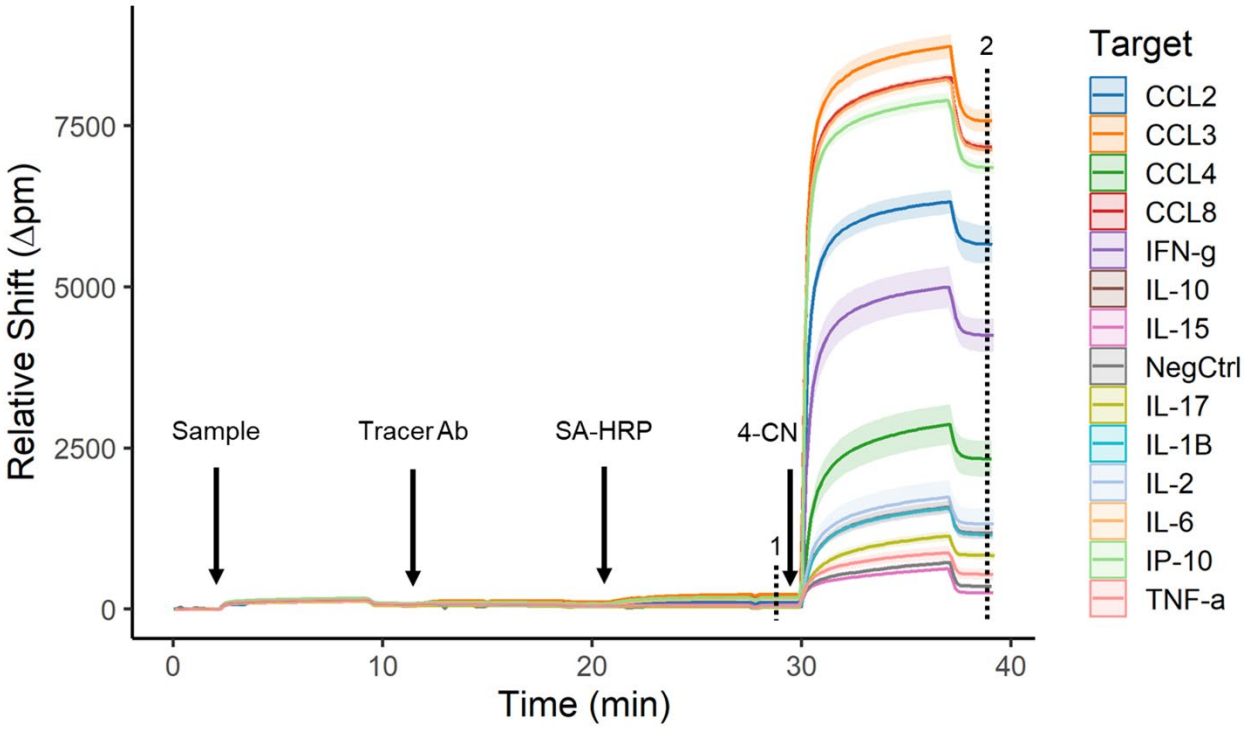

Figure 2-2. Real-time resonance wavelength shifts for a representative multiplexed immunoassay. Two-minute buffer rinses occur between each reagent step. Shaded areas represent the standard deviation across four sensors per target in a single assay. Net shifts are calculated as the difference in signal between the end of the assay (2) and the running buffer rinse signal before amplification (1).

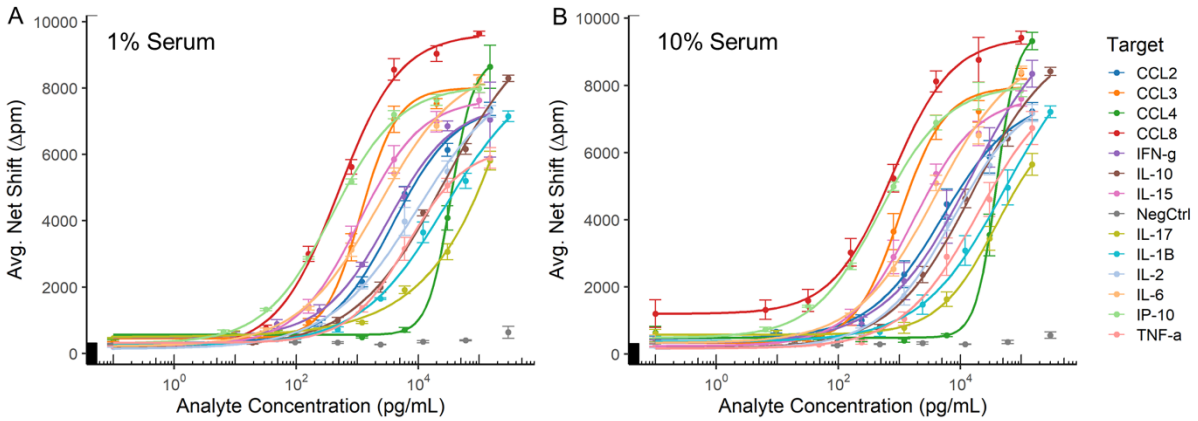

Target		CCL2	CCL3	CCL4	CCL8	IFN-γ	IL-10	IL-15	IL-17	IL-1β	IL-2	IL-6	IP-10	TNF-α
LOD (pg/mL)	1% Serum	9.0	0.8*	3394	6.7	0.01*	55.7	1.5	27.1	9.6	5.4	3.3	0.3	0.3*
	10% Serum	105.6	87.1	19543	288.1	206.6	427.9	99.7	4452	897.5	128.4	142	9.5	326.7

Figure 2-3. Simultaneous multiplexed calibrations on the Genalyte Matchbox platform for A) 1% serum samples and B) 10% serum samples. Error bars represent standard deviation and are from n=3 calibrations, n=4 rings per target. LODs were calculated for each target in each matrix dilution as the blank signal plus three times the standard deviation of the blank. *Values were calculated from the asymptotic minimum of the fit, due to the LOD calculation falling below the fit parameters.

Table 2-5. Mann-Whitney tests for significant features from the reduced random forest analysis of the LTBI clinical category.

Condition	Target	P Value
PPD-CD3	CCL2	0.007
CE-CD3	CCL3	0.2
PPD-CD3	CCL8	0.001
PPD-MED	CCL8	0.005
MTB-CD3	CCL8	0.001
CE-MED	CCL8	0.005
MTB-MED	IFN-γ	0.0002
PPD-CAN	IFN-γ	0.5
PPD-MED	IFN-γ	0.0001
CE-MED	IFN-γ	0.01
MTB-CAN	IFN-γ	0.03
CD3-MED	IFN-γ	0.08
MTB-CD3	IL-2	0.0004
MTB-CAN	IL-6	0.07
CE-MED	IP-10	0.0004
MTB-CD3	IP-10	0.002
MTB-CAN	IP-10	0.003
PPD-CAN	IP-10	0.8
MTB-MED	IP-10	0.01

Table 2-6. Mann-Whitney tests for significant features from the reduced random forest analysis of the High Risk clinical category.

Condition	Target	P Value
MTB-CAN	CCL3	0.03
PPD-CD3	CCL8	0.02
CE-MED	CCL8	0.1
MTB-MED	IFN-γ	0.0002
CE-MED	IFN-γ	0.04
CE-MED	IL-15	0.2
PPD-CD3	IL-17	0.1
MTB-CD3	IL-2	0.0003
MTB-MED	IL-6	0.2
CE-MED	IP-10	0.0006
MTB-CD3	IP-10	0.003
MTB-MED	IP-10	0.01
PPD-CAN	IP-10	0.4
PPD-MED	TNF-α	0.6

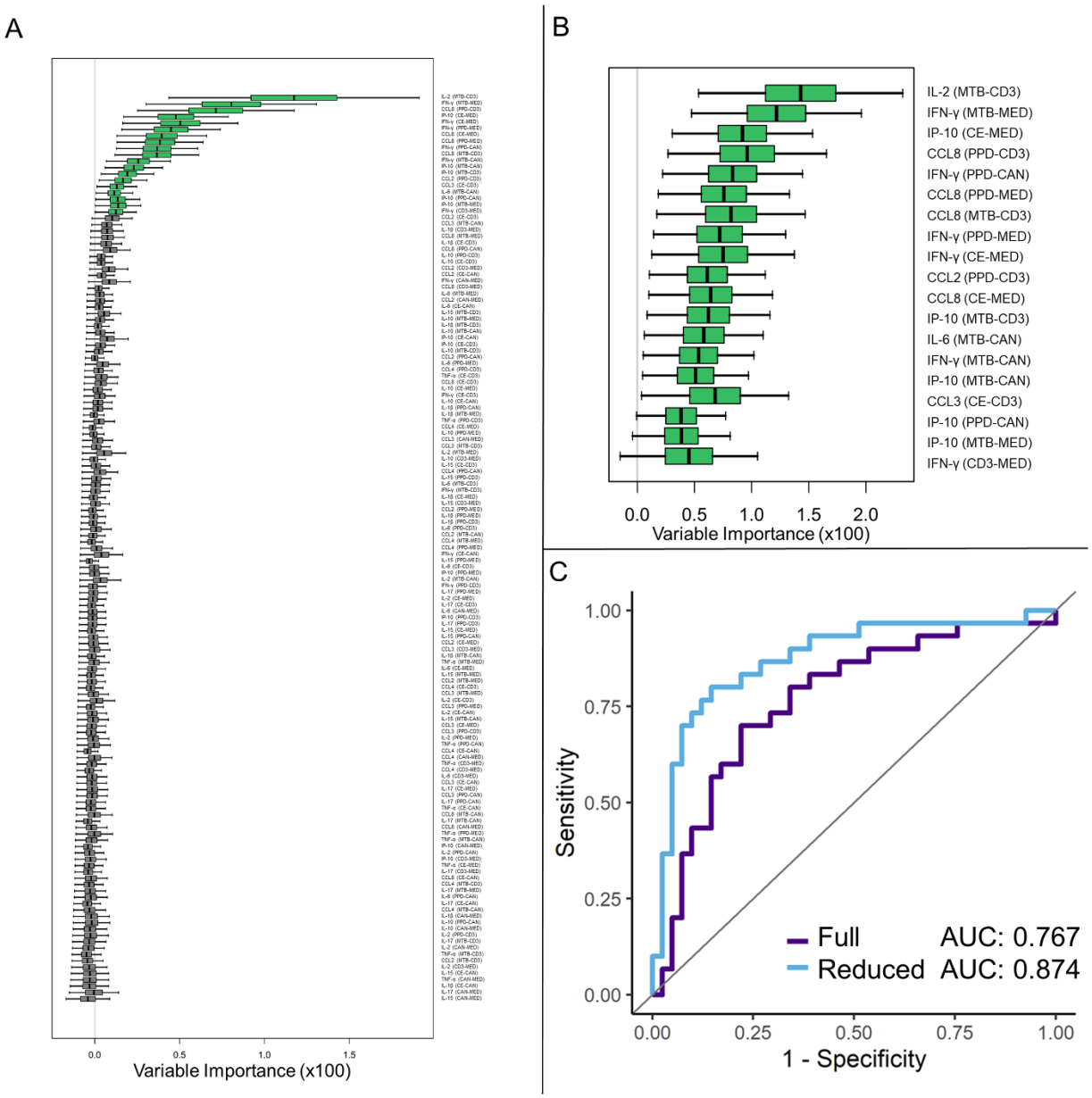

Figure 2-4. Comparison of A) full random forest feature and B) the threshold-based reduced random forest feature analysis for the LTBI+ clinical category. Features for the reduced analysis are determined by Variable Importance (VIMP) metrics. C) ROC Curves for full and reduced analysis represent the predictive power of each method, with AUC values corresponding to the percent predictive accuracy. Notably, the reduced biomarker set offers improved predictive accuracy. Abbreviations – MED (cell media), CAN (Candida), CD3 (anti-CD3), PPD (purified protein derivative), CE (CFP-10/ESAT-6), MTB (MTB300). Normalized conditions are denoted as Condition 1 minus Condition 2 (i.e. PPD-MED is the PPD condition minus the negative control cell media condition).

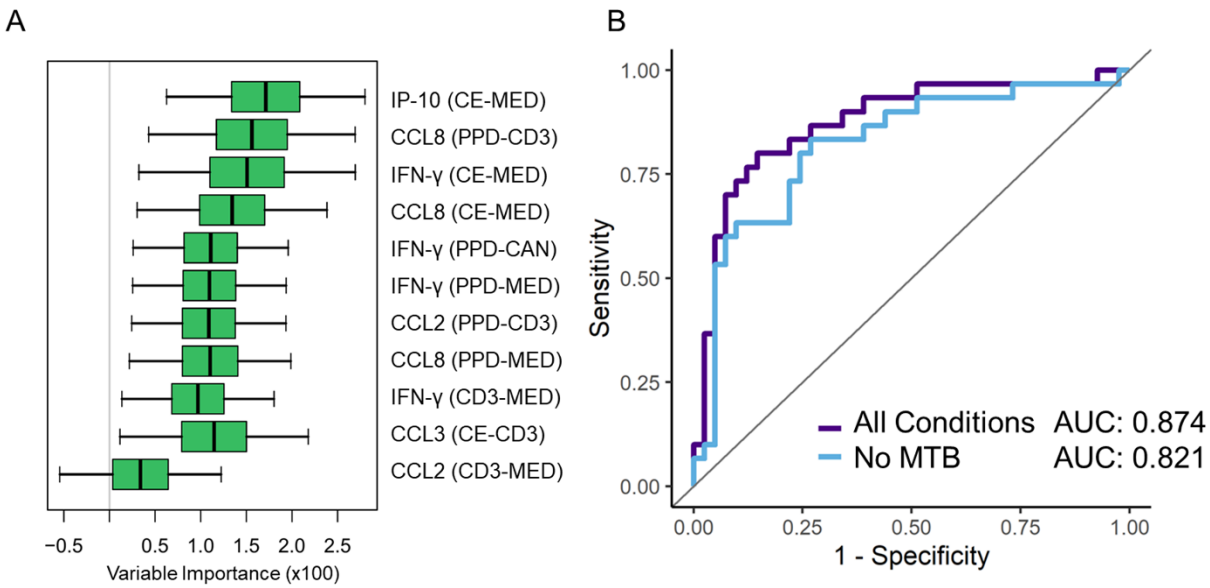

Figure 2-5. A) Reduced random forest feature analysis for the LTBI+ clinical designation when the MTB stimulation is removed. B) ROC curve comparison of LTBI+ reduced random forest with and without MTB stimulation condition. This indicates an improved predictive accuracy through the inclusion of the MTB stimulation condition.

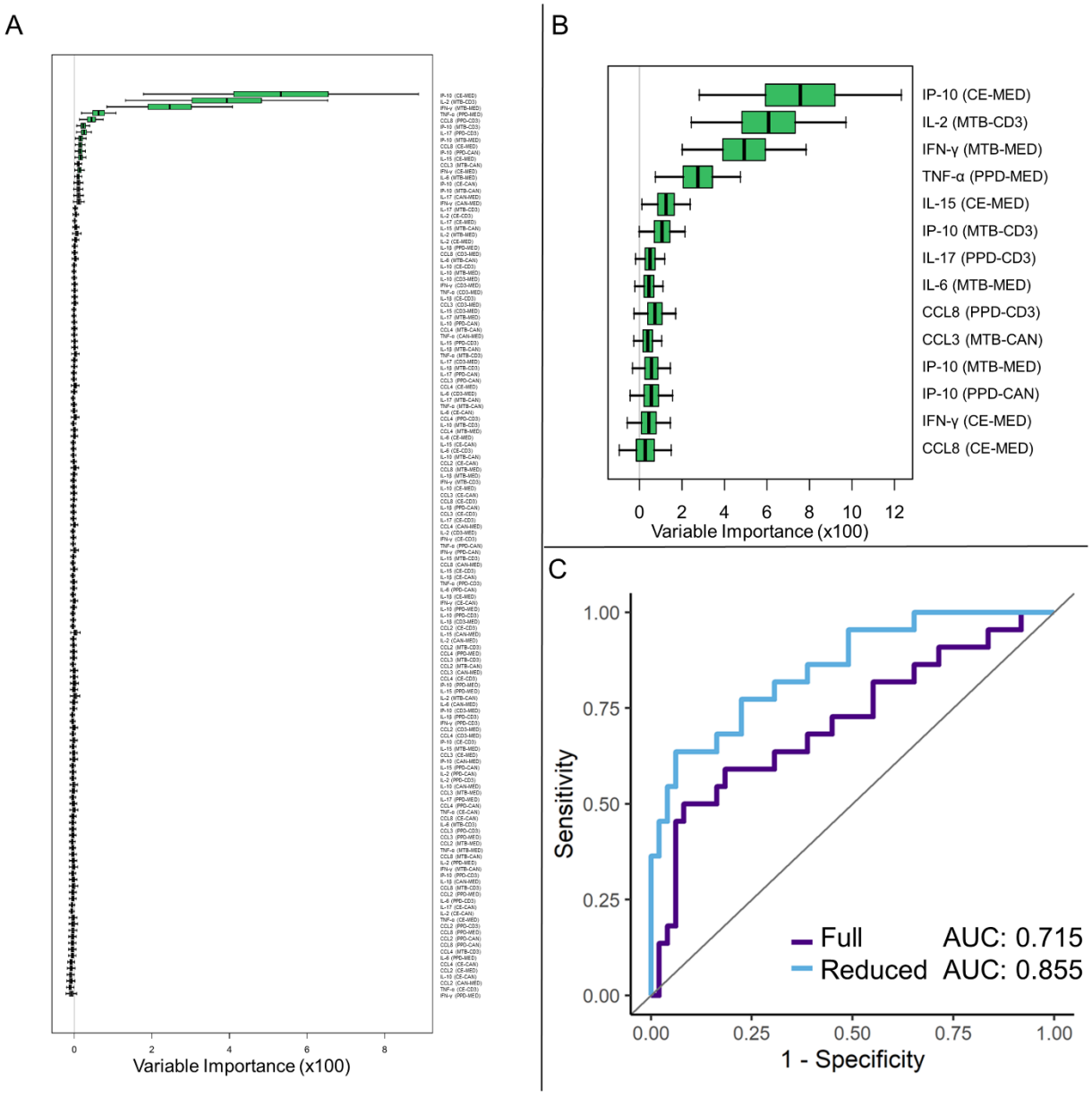

Figure 2-6. Comparison of A) full random forest feature and B) the threshold-based reduced random forest feature analysis for the High Risk clinical designation. C) ROC Curves for full and reduced analysis show an increase in predictive accuracy for the reduced feature set.

References

1. WHO | Global tuberculosis report 2019.
2. Ernst, J. D. The immunological life cycle of tuberculosis. *Nat. Rev. Immunol.* **12**, 581–591 (2012).
3. Houben, R. M. G. J. & Dodd, P. J. The Global Burden of Latent Tuberculosis Infection: A Re-estimation Using Mathematical Modelling. *PLOS Medicine* **13**, e1002152 (2016).
4. Esmail, H., Barry, C. E., Young, D. B. & Wilkinson, R. J. The ongoing challenge of latent tuberculosis. *Philos. Trans. R. Soc. Lond., B, Biol. Sci.* **369**, 20130437 (2014).
5. Salgame, P., Geadas, C., Collins, L., Jones-López, E. & Ellner, J. J. Latent tuberculosis infection--Revisiting and revising concepts. *Tuberculosis (Edinb)* **95**, 373–384 (2015).
6. Mack, U. *et al.* LTBI: latent tuberculosis infection or lasting immune responses to M. tuberculosis? A TBNET consensus statement. *Eur. Respir. J.* **33**, 956–973 (2009).
7. Rangaka, M. X. *et al.* Predictive value of interferon-γ release assays for incident active tuberculosis: a systematic review and meta-analysis. *The Lancet Infectious Diseases* **12**, 45–55 (2012).
8. Lu, L. L. *et al.* IFN-γ-independent immune markers of Mycobacterium tuberculosis exposure. *Nature Medicine* **25**, 977–987 (2019).

9. Porter, B. W. & Venkatappa, T. K. Uncloaking an ancient adversary: Can pathogen biomarker elicitors play a role in confirming extrapulmonary TB and latent TB infection? *Tuberculosis* **113**, 30–37 (2018).
10. Essone, P. N. *et al.* M . tuberculosis infection and antigen specific cytokine response in healthcare workers frequently exposed to tuberculosis. *Scientific Reports* **9**, 1–13 (2019).
11. Kim, S. Y. *et al.* The Responses of Multiple Cytokines Following Incubation of Whole Blood from TB Patients, Latently Infected Individuals and Controls with the TB Antigens ESAT-6, CFP-10 and TB7.7. *Scandinavian Journal of Immunology* **76**, 580–586 (2012).
12. Kellar, K. L. *et al.* Multiple Cytokines Are Released When Blood from Patients with Tuberculosis Is Stimulated with Mycobacterium tuberculosis Antigens. *PLOS ONE* **6**, e26545 (2011).
13. Chegou, N. N., Black, G. F., Kidd, M., van Helden, P. D. & Walzl, G. Host markers in Quantiferon supernatants differentiate active TB from latent TB infection: preliminary report. *BMC Pulmonary Medicine* **9**, 21 (2009).
14. Wang, X. *et al.* Diagnostic performance of multiplex cytokine and chemokine assay for tuberculosis. *Tuberculosis (Edinb)* **92**, 513–520 (2012).
15. Robison, H. M. *et al.* Precision immunoprofiling to reveal diagnostic signatures for latent tuberculosis infection and reactivation risk stratification. *Int Bio (Cam)* **11**, 16–25 (2019).

16. Arlehamn, C. S. L. *et al.* A Quantitative Analysis of Complexity of Human Pathogen-Specific CD4 T Cell Responses in Healthy M. tuberculosis Infected South Africans. *PLOS Pathogens* **12**, e1005760 (2016).
17. El Sahly, H. M. *et al.* Epidemiologic Differences between United States— and Foreign-Born Tuberculosis Patients in Houston, Texas. *The Journal of Infectious Diseases* **183**, 461–468 (2001).
18. Lewinsohn, D. M. *et al.* Official American Thoracic Society/Infectious Diseases Society of America/Centers for Disease Control and Prevention Clinical Practice Guidelines: Diagnosis of Tuberculosis in Adults and Children. *Clin Infect Dis* **64**, 111–115 (2017).
19. Escalante, P. *et al.* Combinatorial Immunoprofiling in Latent Tuberculosis Infection. Toward Better Risk Stratification. *Am. J. Respir. Crit. Care Med.* **192**, 605–617 (2015).
20. Menzies, D., Gardiner, G., Farhat, M., Greenaway, C. & Pai, M. Thinking in three dimensions: a web-based algorithm to aid the interpretation of tuberculin skin test results. *Int J Tuberc Lung Dis* **12**, 498–505 (2008).
21. Robison, H. M. & Bailey, R. C. A Guide to Quantitative Biomarker Assay Development using Whispering Gallery Mode Biosensors. *Current Protocols in Chemical Biology* **9**, 158–173 (2017).
22. Mudumba, S. *et al.* Photonic ring resonance is a versatile platform for performing multiplex immunoassays in real time. *Journal of Immunological Methods* **448**, 34–43 (2017).

23. Miyara, M. *et al.* Detection in whole blood of autoantibodies for the diagnosis of connective tissue diseases in near patient testing condition. *PLoS One* **13**, (2018).
24. Breiman, L. Random Forests. *Machine Learning* **45**, 5–32 (2001).
25. R Core Team. R: A language and environment for statistical computing. (2013).
26. Ishwaran, H., Kogalur, U. B. Package 'randomForestSRC'. (2020).
27. Yang, J. D. *et al.* Mycobacterium tuberculosis-specific CD4+ and CD8+ T cells differ in their capacity to recognize infected macrophages. *PLOS Pathogens* **14**, e1007060 (2018).
28. Ruhwald, M., Bjerregaard-Andersen, M., Rabna, P., Eugen-Olsen, J. & Ravn, P. IP-10, MCP-1, MCP-2, MCP-3, and IL-1RA hold promise as biomarkers for infection with M. tuberculosis in a whole blood based T-cell assay. *BMC Research Notes* **2**, 19 (2009).
29. Martinez, A. N., Mehra, S. & Kaushal, D. Role of Interleukin 6 in Innate Immunity to Mycobacterium tuberculosis Infection. *J Infect Dis* **207**, 1253–1261 (2013).
30. Singh, B., Chitra, J. & Selvaraj, P. CCL2, CCL3 and CCL4 gene polymorphisms in pulmonary tuberculosis patients of South India. *International Journal of Immunogenetics* **41**, 98–104 (2014).
31. Tang, N. L.-S. *et al.* Genetic association between a chemokine gene CXCL-10 (IP-10, interferon gamma inducible protein 10) and susceptibility to tuberculosis. *Clin. Chim. Acta* **406**, 98–102 (2009).

32. Millington, K. A. *et al.* Dynamic Relationship between IFN-γ and IL-2 Profile of Mycobacterium tuberculosis-Specific T Cells and Antigen Load. *The Journal of Immunology* **178**, 5217–5226 (2007).

33. Ahmed, M. *et al.* Immune correlates of tuberculosis disease and risk translate across species. *Science Translational Medicine* **12**, (2020).

34. Hasan, Z. *et al.* CCL2 Responses to Mycobacterium tuberculosis Are Associated with Disease Severity in Tuberculosis. *PLOS ONE* **4**, e8459 (2009).

35. Harari, A. *et al.* Dominant TNF-α+ Mycobacterium tuberculosis-specific CD4+ T cell responses discriminate between latent infection and active disease. *Nat. Med.* **17**, 372–376 (2011).

36. Okamoto Yoshida, Y. *et al.* Essential role of IL-17A in the formation of a mycobacterial infection-induced granuloma in the lung. *J. Immunol.* **184**, 4414–4422 (2010).

37. Khader, S. A. *et al.* IL-23 and IL-17 in the establishment of protective pulmonary CD4+ T cell responses after vaccination and during Mycobacterium tuberculosis challenge. *Nat. Immunol.* **8**, 369–377 (2007).

38. Umemura, M., Nishimura, H., Hirose, K., Matsuguchi, T. & Yoshikai, Y. Overexpression of IL-15 In Vivo Enhances Protection Against Mycobacterium bovis Bacillus Calmette-Guérin Infection Via Augmentation of NK and T Cytotoxic 1 Responses. *The Journal of Immunology* **167**, 946–956 (2001).

39. Styblo, K. The relationship between the risk of tuberculosis infection and the risk of developing infectious tuberculosis. *Bull. Int. Union Tuberc.* **60**, 117-19 (1985).

CHAPTER 3

Improved Multiplexed Cytokine Diagnostics for Latent Tuberculosis Signatures in QuantiFERON Plasma through Bioinformatics

Acknowledgements

I would like to acknowledge Dr. Heather Robison for her work in establishing this project. I also acknowledge Dr. Patricio Escalante, Dr. Elitza Theel, and Courtney Erskine for clinical guidance, and Haowen Zhou and Dr. Ruoqing Zhu for their Random Forest analysis expertise. This work was supported by the National Institute of Allergy and Infectious Diseases at the National Institutes of Health (AI141591). Part of this project was also supported by Grant Number UL1 TR000135 from the National Center for Advancing Translational Sciences (NCATS).

Abstract

Latent tuberculosis infection (LTBI) is an asymptomatic infection that manifests when mycobacterium tuberculosis pathogen is not cleared by the host immune system. Current blood-based diagnostics are specific to detecting active tuberculosis infection, but blood-based detection of LTBI is lacking. To improve the clinical outcome of LTBI positive patients, we have developed a 13-plex cytokine panel immunoassay utilizing a microring resonator platform and a random forest bioinformatics approach to predict patient LTBI status and the risk of reactivation from latent to active TB. Previous work used stimulated cell supernatant for analysis; herein, we show this to be successful using stimulated QFT plasma direct from the LTBI clinical workflow. Our results show predictive accuracy of 90% for detection of LTBI and >80% for risk of reactivation. We successfully designed a combinatorial technique that can be implemented into the LTBI clinical workflow to predict LTBI and risk of reactivation using patient QFT samples.

Introduction

Tuberculosis (TB) continues to be one of the most fatal diseases in the world, totaling 1.5 million deaths in 2018.[1] Areas with high population densities, low sanitation infrastructure, and sparse healthcare services incur the most TB burden. The main complicating factors are both biological and clinical in nature. Upon infection, the host immune response will attempt to clear the TB bacteria, but under most circumstances, only succeeds in sequestering the bacteria in granulomas, primarily in the lungs. This latent infection (LTBI) accounts for 80% of all infections worldwide, totaling an expected 1 billion individuals.[2,3] Of this population, 10% are expected to reactivate to the transmissible, and often fatal, infectious form. Therefore, one way to eradicate TB is to treat any active cases and also determine which individuals will reactivate and treat them preventatively.

To reach this ambitious goal, diagnostics of high performance are needed. Current testing for active TB includes the Tuberculin Skin Test (TST) and the QuantiFERON-Gold Test (QFT). The TST is a simple test that takes a purified protein derivative and injects it under the skin, which elicits an immune response if an individual has been in contact with the bacteria. However, the metrics for this test include the height and size of the resulting welt, and is severely limited in precision, as even individuals that have been tested previously can develop an immune response.[4,5] The QFT is a blood-based diagnostic, which takes plasma and stimulates monocytes under multiple conditions for subsequent assay analysis for interferon-gamma.[6] While this QFT is highly accurate for TB, it along with the TST, have almost no predictive accuracy for LTBI.[7] Therefore, diagnostics are

needed that can work within the current clinical pipeline to elucidate the asymptomatic disease state, as well as understand the potential for reactivation.

Multiplexed assays are an area of intense interest in clinical diagnostics. While research has often focused on single biomarkers for any given disease, it has become clear that the complex biological processes at play in the immune system give rise to diverse signature profiles.[8-13] This is especially true for LTBI, as recent research has also shown that outside of TB, there are subpopulations of LTBI that are IFN-γ independent, indicating that current clinical testing would never identify such individuals.[14] Many multiplexed methods are based on enzyme-linked immunosorbent assays (ELISAs), which utilize antibody captures to pulldown targets of interest and through amplification create an endpoint concentration readout. Plate-based ELISAs are labor intensive and limited in plexity and suffer from reduced dynamic ranges and troubling background signals from more complicated sample matrices. Therefore, alternative methodologies and technologies utilizing capture agents, much like ELISA, have found some success. A promising field of possible point-of-care methods are biosensors. These platforms utilize spectroscopic techniques to interrogate sensor surfaces, limited largely by biological, rather than technical, restraints. Multiplexed microring resonators have been shown to be an incredibly powerful technique for diagnostic applications in multiple disease states.[15-17] Our lab utilizes the commercialized Genalyte platform to continue to push the application space necessary for truly useful clinical needs, and the technology is currently deployed in multiple hospitals for ANA testing[18], proving their POC viability.

Previous research in our lab has focused on proving the utility of our multiplexed assay platform in stimulated cell supernatants, as well as the ability for personalized

subject responses, through informatics approaches, to lead to signature discovery.[19] Furthermore, we have demonstrated recently that we can create profiles that are not only biologically driven, utilizing diverse immune markers directly related to TB infection, but also lead to predictive accuracies through ROC curves that indicate the potential for clinical value. However, these studies utilized peripheral blood mononuclear cells (PMBCs) that were cultured and stimulated, which is technically laborious and time consuming.

To create a more rapid profiling technique, we present the potential for our 13-plex cytokine assay to interrogate markers including and beyond IFN-γ using QFT plasma. The assay was performed in under an hour and through the same random forest informatics workflow, has established signatures for both LTBI and those at high risk for TB reactivation. Through this implementation, we show the viability of our platform to be used in the current clinical pipeline to elucidate LTBI and subpopulations thereof.

Methods

Clinical Designations and QFT Sample Collection

This study was approved by the Mayo Clinic Institutional Review Board and Olmsted County Public Health Services. All study participants signed an informed written consent and were enrolled in Rochester, MN. Risk factors for TB infection, TB progression, and/or TB reactivation were obtained through a questionnaire and review of medical records as previously described.[20-22] LTBI diagnoses were made per the Center for Disease Control and Prevention (CDC) criteria and based on TB risk factors, and by prior TST and QuantiFERON®-TB Gold In-Tube (QFT) results.[22] A modified multifactorial

predictive modeling platform (i.e. 'Online TST/IGRA interpreter'), adjusted by LTBI treatment effect, was applied to estimate the cumulative risk of TB reactivation in all subjects as previously described.[23,24] Blood samples were collected for immediate exposure to QFT stimulations as per clinical guidelines. Stimulated plasma was frozen and stored at -80 C to be thawed when necessary for multiplexed cytokine analyses.

Assay Reagents

Dulbecco's phosphate buffered saline (PBS), bovine serum albumin (BSA), (3-Aminopropyl)triethoxysilane, glycerol, bis(sulfosuccinimidyl)suberate, starting block blocking buffer, Pierce high sensitivity streptavidin-HRP (SA-HRP), 4-chloronaphthol (4-CN), and Drycoat assay stabilizer were purchased from commercial vendors as listed in Table 3-2. Vendors and catalog numbers for antibodies for all cytokines and the mouse IgG isotype control are detailed in Table 3-3. Running buffer for all assays was 0.5% BSA in 1X PBS, pH 7.4.

Multiplexed immunoassay instrumentation and assay design

Microring immunoassays were performed on the Maverick Matchbox system (Genalyte, Inc., San Diego, CA) as previously described.[16] This platform utilizes injection-molded microfluidic devices to introduce fully automated flow for all assay steps across functionalized sensor arrays. These devices are disposable, to ensure no contamination between assays.[17,18] Microring arrays were batch functionalized via spotting to yield a 13-plex array of capture antibodies covalently immobilized on sensor substrates. After flowing the sample across the chip, a mixture of all the tracer antibodies was flowed across the array followed by amplification reagents. Antibody capture and tracer

concentrations are listed in Table 3-4. Immunoassays were performed with a consistent 30µl/min flow rate for all steps. There was an initial rinse of 5 minutes with the running buffer to ensure equilibration of the chip prior to sample analysis. The assay included steps as follows: 1) running buffer (2min); 2) sample (7min); 3) running buffer rinse (2min); 4) biotinylated tracer antibodies (7min); 5) running buffer rinse (2min); 6) SA-HRP (7min); 7) running buffer rinse (2min); 8) 4-CN (7min); 9) running buffer rinse (2min). The total assay time was 38 minutes.

Calibrations and Sample Analyses

Immunoassays were simultaneously calibrated in a multiplexed format. Serial dilutions from a saturating analyte concentration for each immunoassay yielded eight-point calibrations relating standard concentrations to relative resonance shifts. To quantify relative shifts, the signal during the buffer rinse before the assay amplification step (t=29min) was subtracted from the final assay rinse step (t=38min). Net resonance wavelength shifts (∆pm) were plotted as a function of standard concentration and fit to a logistic function as described previously.[21] Limits of detection (LOD) and quantification (LOQ) were defined as the blank signal plus 3 times and 10 times the standard deviation of the blank, respectively. Each calibration was performed in triplicate for each sample dilution (Figure 3-1) as measured with 4 sensors per technical ring replicate.

Samples were analyzed at 2 dilutions (2X and 10X) into running buffer. Cytokine concentrations determined from corresponding plasma calibrations (50% and 10% plasma, respectively). Final concentrations were measured using the most appropriate dilution/calibration as determined by proximity to the inflection point of the calibration. Precision normalization was achieved through subtracting media (MED) and pan-

stimulation (MIT) cytokine concentrations from the TB-specific stimulation (AG), as well as looking at overall immunocompetency (MIT-NIL).

Random Forest and ROC Curve Analyses

Random Forest methods[25] were used to determine the biomarker features associated with both LTBI+ and High Risk clinical designations as described previously. Briefly, Random Forest is an ensemble classification algorithm that can detect nonlinear effects of covariate features. It creates a ranking of importance for each variable, while the importance is identified by their effect on classification of either clinical designation. Utilizing these randomized decision tree results, a ROC curve can be formed that evaluates the predictive accuracy the covariates hold for a given classification.

Feature importance analysis was done for all variables available (39 total), and ROC curves were created. Utilizing the important features from these analyses, a secondary Random Forest algorithm was produced for further enhancement of predictive accuracy by removing unimportant features, as described previously. This was done identically for both LTBI+ and High Risk clinical designations. Mann-Whitney plots were utilized to evaluate each important variable in the signature. All informatics and plotting were performed using R coding language.[26,27]

Results/Discussion

Assay Development and Matrix Evaluations

Our goal was to investigate what cytokines are stimulated from isolated PBMCs using our 13-plex cytokine immunoassay panel.[28] 10% and 50% plasma dilutions were chosen for our analysis, to both minimize sample needed and to cover suggested

literature ranges for the range of cytokines in our multiplexed panel. Figure 3-1 details the calibrations under these conditions, as well as the calculated LODs and LOQs for each target. While some targets, such as CCL4, produce worse limits of detection in the more complicated matrix, biomarkers such as IP-10 see almost no change from our serum analyses previously published. Utilizing the inflection points of each calibration, the most appropriate dilution factor for each sample run was chosen, and the dilution factor applied. Therefore, we could not only quickly analyze these 13 targets using 210uL of plasma, but also account for sample concentrations that skewed towards either asymptotic calibration ranges. These selected concentrations were used for further bioinformatic analysis.

Plasma Stimulations and Normalization

Analyses were performed on two clinical designations of interest (LTBI and High Risk of reactivation) to understand the immunological signatures relevant to each class. Three stimulation conditions were utilized from the QFT, including a negative control (NIL), positive control (MIT), and the CFP-10/ESAT-6 peptide mixture for antigen stimulation (AG). These conditions were used to create normalized values specific to each subject; AG-NIL, MIT-NIL, and AG-MIT. These conditions account for the potential maximum range of immune responses (MIT-NIL) as well as changes in immune response with respect to an individual's basal immune levels. Normalized immune responses were categorized into either LTBI+ or LTBI- for the LTBI category, or as High Risk+ or High Risk- for the High Risk category. These clinical distinctions were evaluated through random forest and subsequent predictive accuracy evaluations from AUCs.

Random Forest Analyses

The random forest analyses for the subject cohort utilized the 3 normalized conditions across the 13-plex panel, yielding 39 possible features. Using all 39 cohort features (Figure 3-2), a ROC curve was established for the LTBI clinical designation, producing an AUC of 0.86. A reduced random forest analysis was then performed, as described previously. In brief, the goal of this feature reduction is to remove any unimportant condition/biomarker combinations to minimize biological noise from our analyses. It also tends to remove false negatives from our prediction, which also parallels our informatics analyses in cell supernatant. This reduced set revealed 9 of 39 as important features, and a marginally increased AUC of 0.896 (Figure 3-3). Biomarkers of interest include chemokines such as CCL4[29] and CCL8[30], early response interleukins, such as IL-2[31] and IL-17[32,33], and directly interferon-induced markers like IP-10.[34] All three stimulations conditions are present in the reduced analysis, indicating that they all contribute to the overall clinical profile. Mann Whitney analyses of all relevant features are conglomerated in Table 3-5. Through this analysis, we produced a nearly 90% predictive accuracy for LTBI, using 25% of our total feature pool. This highlights not only the importance of multiplexed assays for clinical use, but also the potential to make an impactful contribution to clinical classifications through minimal modifications to the current workflow.

It is imperative that we also understand an individual's risk to reactivate. If that risk is high, antibiotic regiments would most likely be recommended, while low risk would likely indicate that longitudinal monitoring is more viable. Therefore, we looked at a subpopulation of the LTBI category that were deemed clinically high risk. Identical analyses from the LTBI clinical designation were applied to this High Risk category. The

resultant full analysis (Figure 3-4) produced a ROC curve with an AUC of 0.76. The reduced analysis included 8 features and AUC of 0.827 (Figure 3-5). The biomarkers of interest overlap those of LTBI, utilizing CCL4, CCL8, IP-10, and IL-2 for the reduced analysis, which cover monocyte and leukocyte attraction, inflammation induced cell recruitment, and microbial infection response.[29-31,34] Mann Whitney analyses of all relevant features are in Table 3-6. While this analysis produces a lower predictive accuracy for risk, it is still successful in distinguishing this category from the general cohort population.

When the QuantiFERON Test specifically focuses on IFN-γ, it is surprising that we did not find it present in and of our reduced analyses. IFN-γ is a strong predictor of active TB, as IFN-γ is one of the drivers of inducing or clearing granuloma formation.[2] However, recent literature details specific instances where LTBI equilibrium is IFN-γ independent, with all other immunological elements within comparable ranges. Interestingly, when analyzing the full random forest results, we see that all normalized combinations of IFN-γ are deemed unimportant (Figures 3-2 and 3-4). There are multiple factors which could account for this quintessential TB biomarker not attributing to our LTBI clinical significance. Biologically, one explanation could be that the dynamic equilibrium that is yielding the latent infection state and the propensity for it to shift towards tuberculosis proliferation either doesn't rely on IFN-γ levels, or that other peripheral immune pathways contribute more to this dynamic shift.[35] Another could be that there are distinct differences in blood diagnostics and localized sample types, such as Bronchoalveolar Lavage (BAL), as localized conditions of latency may not directly correlate to a blood-based test. An additional explanation could be attributed to the clinical designations themselves, where

LTBI is not only determined by the QFT IFN-γ results, and therefore heterogeneous populations in both clinical categories lead to an insignificant contribution.

This finding also highlights drastic differences in the QFT IFN-γ and multiplexed platform assays. The current protocol uses 3 standards and a blank, ranging from 0-4 IU/mL (0-200pg/mL) for IFN-γ. Values are determined from 0-8 IU/mL in diluted samples (between 1:100 and 1:1000 dilutions), and above 10 IU/mL are marked as >10.[7] Therefore, the dynamic range to measure IFN-γ is small and not necessarily indicative of actual biomarker levels. The multiplexed platform has both viable performance in much higher plasma content, as well as an increased dynamic range which could elucidate more distinct population differences. It could also show that for LTBI and High Risk, these populations are similar. Furthermore, the IFN-γ analysis could be done solely with our multiplexed panel, further reducing the analysis workflow.

This work has some clear limitations. The sample cohort is preliminary, with only 45 subjects. This is insufficient to create robust predictive models for either LTBI or risk of reactivation. It can only suggest that this workflow could be used in clinical application with more rigorous testing. We also find that some assays suffer in plasma, mainly in terms of limits of detection and dynamic ranges. These variable metrics could obfuscate markers of interest that show minimal, but distinct changes in transient levels.

Conclusions

We have demonstrated the viability for multiplexed plasma diagnostics to be implemented withing the current clinical pipeline to distinguish LTBI and the risk of potential reactivation using random forest analyses. From our initial cohort, was have

achieved predictive accuracies approaching 90% for LTBI, using only 5 biomarkers. These cytokines show that extensive profiling is necessary to identify this highly complicated immune system and pathogen equilibrium. We can also achieve appreciable accuracies of more than 80% for high risk of reactivation using an overlapping pool of biomarkers. This is a vital population to identify if there is hope to fully eradicate tuberculosis. We have also identified that IFN-γ as a lone biomarker is insufficient to stratify these clinical populations, and therefore fuller diagnostics are essential in resolving these cohorts. From this study, we believe there is an accomplishable clinical workflow to be instituted, such that LTBI and reactivation can be readily determined at a point-of-care quickly and accurately.

Further work could include using this assay as a one analysis protocol to determine active TB, LTBI, and High Risk without clinical pipeline complications. Since QFT analyses are routine in most hospitals, supplementation of the IFN-γ ELISA with our multiplexed biosensor panel could be accomplished. Currently, there are Genalyte instruments that are deployed in core facilities focusing on ANA testing.[18] However, functionalized chips would be easy to supply for analyses. Simple combined mixtures of standards and tracer antibodies could be made available to create a minimal preparation analysis. Combined with the low sample volume input demonstrated, and the use of our current patient cohort as a training set, distinctions could be made rapidly in a point of care setting. While additional work is needed to expand sample numbers to ensure reproducibility across n+1 subject analyses, this current work show a high degree of promise in tackling a clinically challenging population, and to influence clinical outcomes for at-risk LTBI subjects.

Table 3-1. Clinical characteristics for the plasma sample cohort.

Group	All	TST+	QFT+	LTBI+	High Risk
N (%)	45 (100)	24 (53)	16 (36)	28 (62)	14 (31)
Male, N (%)	15 (33)	9 (20)	8 (18)	10 (22)	7 (16)
Female, N (%)	30 (67)	15 (33)	8 (18)	18 (40)	7 (16)
HCW, N (%)	32 (71)	24 (53)	14 (31)	24 (53)	10 (22)
Age (Mean years ± SD)	53 ± 18	51 ± 18	44 ± 18	49 ± 17	45 ± 20
Predicted Risk (mean + SD)	3.1 ± 9.0	2.6 ± 2.2	2.8 ± 2.4	4.9 ± 11.1	8.3 ± 14.8

Abbreviations – N (number), HCW (health care worker), SD (standard deviation), TST (Tuberculin Skin Test), QFT (QuantiFERON Gold TB In-Tube™ test). Cumulative predicted risk of TB reactivation was based on a modified multifactorial modeling platform (i.e. 'Online TST/IGRA interpreter') applied to all subjects as previously described.[23,24] All clinical variables are aggregated by positive tests or indications.

Table 3-2. Reagents for buffers, chip functionalization and storage, and immunoassay steps.

Reagent	Source	Catalog Number
Dulbecco's phosphate buffered saline	Millipore Sigma	D5573
Bovine serum albumin	Millipore Sigma	A2153
(3-Aminopropyl)triethoxysilane	Millipore Sigma	440140
Glycerol	Thermo Fisher Scientific	BP229
bis(sulfosuccinimidyl)suberate	Thermo Fisher Scientific	A39266
starting block blocking buffer	Thermo Fisher Scientific	37538
Pierce high sensitivity streptavidin-HRP	Thermo Fisher Scientific	21130
4-chloronaphthol	Thermo Fisher Scientific	34012
Drycoat assay stabilizer	Virusys Corporation	AG066

Table 3-3. Antibodies and recombinant standard proteins used in the multiplexed immunoassay.

Target	Role	Source	Catalog Number
CCL2	Capture Antigen Tracer	Thermo Fisher Thermo Fisher Thermo Fisher	14-7099 14-8398 13-7096
CCL3	Capture Antigen Tracer	R&D Systems R&D Systems R&D Systems	MAB670-100 270-LD-010 MAB270-100
CCL4	Capture Antigen Tracer	R&D Systems R&D Systems R&D Systems	CUSTOI702-AZY021708A 271-BME-010 CUSTOI702-IGH021710A
CCL8	Capture Antigen Tracer	R&D Systems R&D Systems R&D Systems	MAB281-100 281-CP-010 BAF281
IFN-γ	Capture Antigen Tracer	Mabtech Thermo Fisher Mabtech	3420-3-250 BMS303 3420-6-250
IL-1β	Capture Antigen Tracer	Thermo Fisher Thermo Fisher Thermo Fisher	14-7018-85 RIL1BI 13-7016-85
IL-2	Capture Antigen Tracer	BD Biosciences Thermo Fisher BD Biosciences	555051 14-8029 555040
IL-6	Capture Antigen Tracer	Thermo Fisher Thermo Fisher Thermo Fisher	16-7069 14-8069 13-7068
IL-10	Capture Antigen Tracer	Thermo Fisher Thermo Fisher Thermo Fisher	16-7108 14-8109-80 13-7109
IL-15	Capture Antigen Tracer	R&D Systems R&D Systems R&D Systems	MAB647 247-ILB-005 BAM247
IL-17	Capture Antigen Tracer	Mabtech Mabtech Mabtech	3520-3-250 3520-10 3520-6-250
IP-10	Capture Antigen Tracer	BD Biosciences BD Biosciences BD Biosciences	555046 551130 555048
TNF-α	Capture Antigen Tracer	Biolegend Biolegend Biolegend	502802 570102 502904

Table 3-4. Antibody concentrations used for capture and tracer pairs. Captures were spotted in 1xPBS, 5% glycerol. All tracers were diluted in running buffer. Streptavidin-Horseradish Peroxidase (SA-HRP) was diluted to 4µg/mL for all experiments.

Target	Capture (mg/mL)	Tracer (µg/mL)
CCL2	0.25	2
CCL3	0.25	1
CCL4	0.25	2
CCL8	0.25	2
IFN-γ	0.25	2
IL-1β	0.25	2
IL-2	0.25	2
IL-6	0.25	2
IL-10	0.25	2
IL-15	0.25	2
IL-17	0.25	2
IP-10	0.25	2
TNF-α	0.25	2

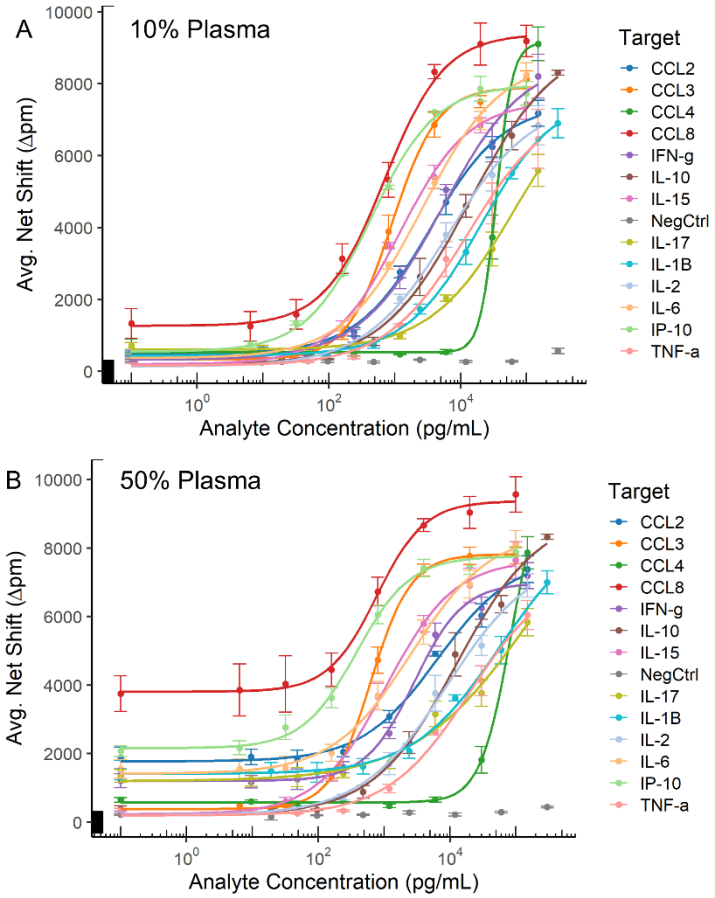

Target	LOD (pg/mL)	
	10% Plasma	50% Plasma
CCL2	41.6	841
CCL3	65.2	9.6
CCL4	18308	12427
CCL8	123.8	329.6
IFN-γ	71.4	461.8
IL-10	196.2	175.6
IL-15	47.6	15
IL-17	880.3	1057
IL-1β	323.4	3162
IL-2	56.2	71.8
IL-6	62.4	206.5
IP-10	2.9	33.3
TNF-α	136.8	315.8

Figure 3-1. Multiplexed plasma calibrations for A) 10% plasma samples and B) 50% plasma samples. Error bars represent standard deviation from n=3 calibrations, n=4 ring replicates per target. LODs were calculated for each target in each matrix dilution as the blank signal plus three times the standard deviation of the blank.

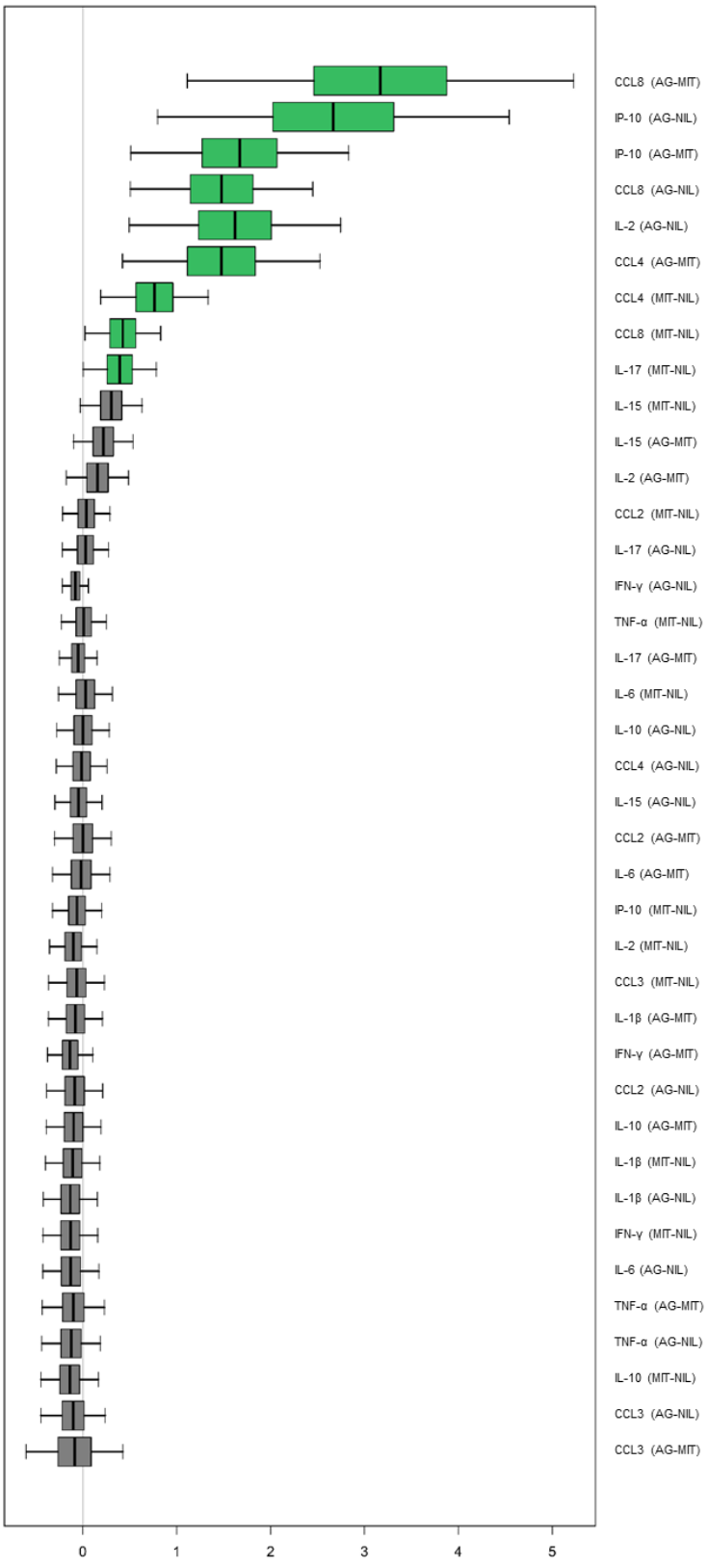

Figure 3-2. Full Random Forest analysis of variables for LTBI+ designation.

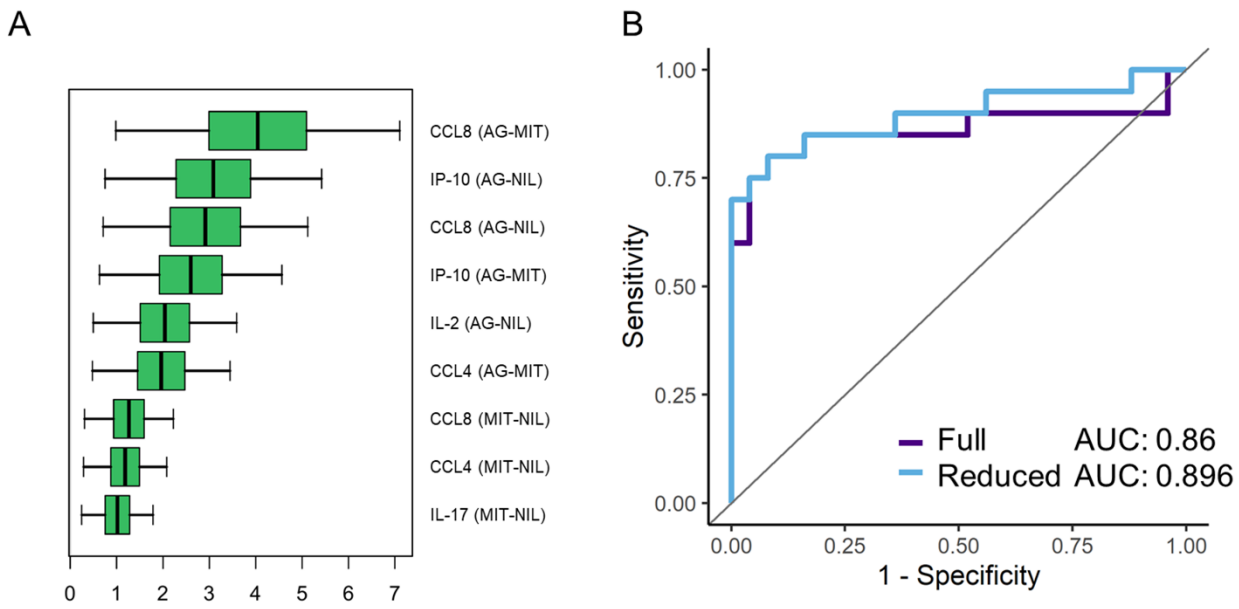

Figure 3-3. A) Reduced Random Forest features for the LTBI clinical designation. Features were determined by Variable Importance (VIMP) metrics. B) ROC Curves for full and reduced analyses. AUCs indicate the predictive accuracy of each curve.

Table 3-5. Mann-Whitney tests for significant features from the reduced random forest analysis of the LTBI clinical category.

Condition	Target	P Value
AG-MIT	CCL4	0.0009
MIT-NIL	CCL4	0.006
AG-MIT	CCL8	6e-05
AG-NIL	CCL8	0.006
MIT-NIL	CCL8	0.03
MIT-NIL	IL-17	0.3
AG-NIL	IL-2	0.0008
AG-MIT	IP-10	0.004
AG-NIL	IP-10	0.009

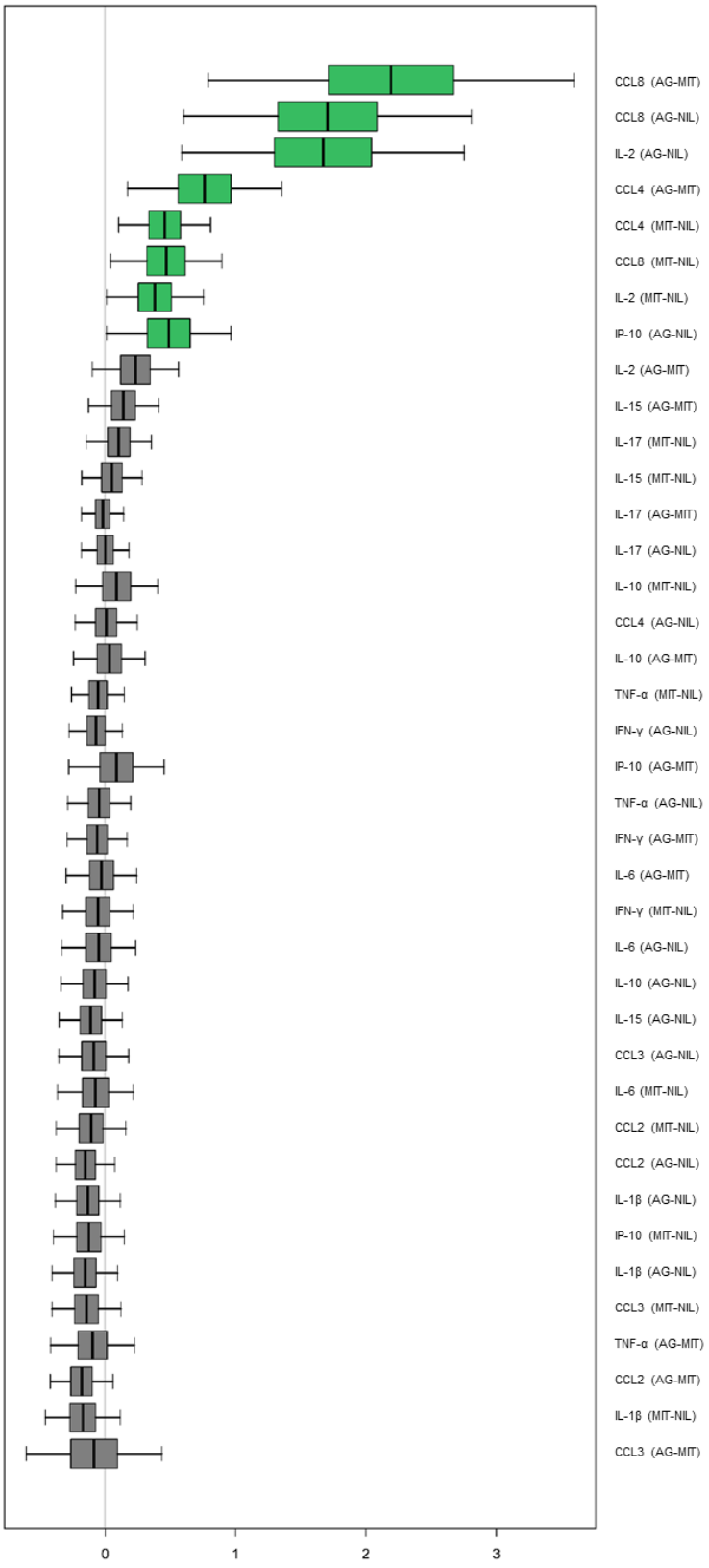

Figure 3-4. Full Random Forest analysis of variables for High Risk designation.

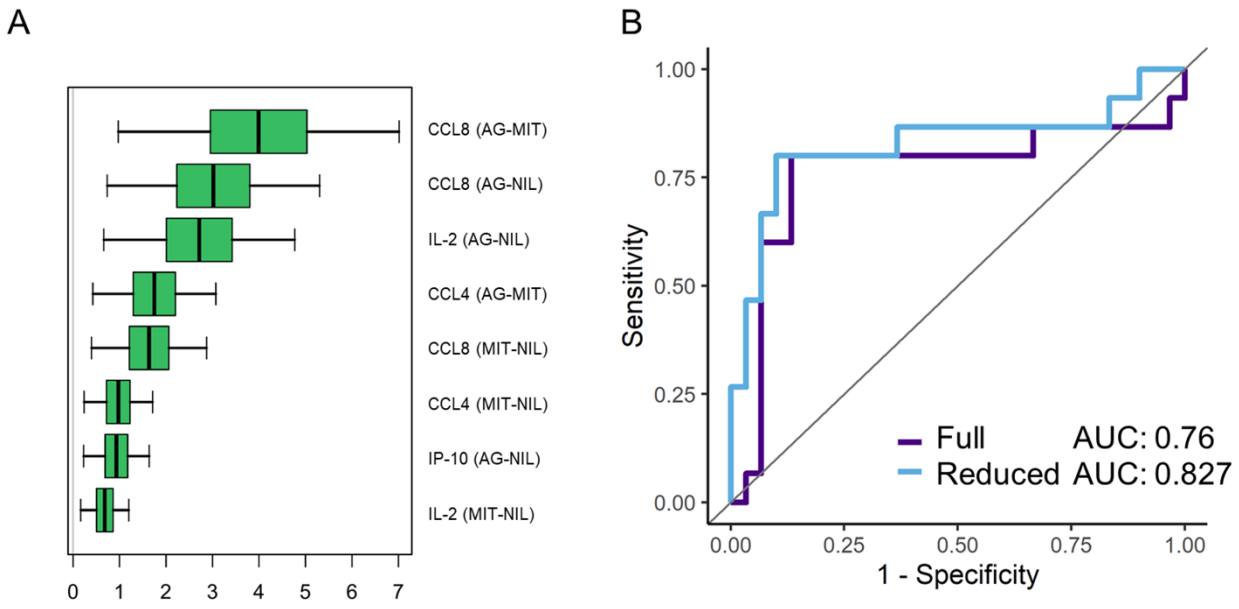

Figure 3-5. A) Reduced Random Forest features for the High Risk clinical designation. Features were determined by Variable Importance (VIMP) metrics. B) ROC Curves for full and reduced analyses. AUCs indicate the predictive accuracy of each curve.

Table 3-6. Mann-Whitney tests for significant features from the reduced random forest analysis of the High Risk clinical category.

Condition	Target	P Value
AG-MIT	CCL4	0.003
MIT-NIL	CCL4	0.01
AG-MIT	CCL8	0.0007
AG-NIL	CCL8	0.001
MIT-NIL	CCL8	0.09
AG-NIL	IL-2	0.0003
MIT-NIL	IL-2	0.06
AG-NIL	IP-10	0.09

References

1. WHO | Global tuberculosis report 2019.
2. Ernst, J. D. The Immunological Life Cycle of Tuberculosis. *Nat. Rev. Immunol.* **12**, 581–591 (2012).
3. Houben, R. M. G. J. & Dodd, P. J. The Global Burden of Latent Tuberculosis Infection: A Re-Estimation Using Mathematical Modelling. *PLOS Medicine* **13**, e1002152 (2016).
4. Esmail, H., Barry, C. E., Young, D. B. & Wilkinson, R. J. The Ongoing Challenge of Latent Tuberculosis. *Philos. Trans. R. Soc. Lond., B, Biol. Sci.* **369**, 20130437 (2014).
5. Salgame, P., Geadas, C., Collins, L., Jones-López, E., Ellner & J. J. Latent Tuberculosis Infection--Revisiting and Revising Concepts. *Tuberculosis (Edinb)* **95**, 373–384 (2015).
6. Mack, U., *et al.* LTBI: Latent Tuberculosis Infection or Lasting Immune Responses to M. Tuberculosis? A TBNET Consensus Statement. *Eur. Respir. J.* **33**, 956–973 (2009).
7. Rangaka, M. X., *et al.* Predictive Value of Interferon-γ Release Assays for Incident Active Tuberculosis: A Systematic Review and Meta-Analysis. *The Lancet Infectious Diseases* **12**, 45–55 (2012).
8. Porter, B. W. & Venkatappa, T. K. Uncloaking an Ancient Adversary: Can Pathogen Biomarker Elicitors Play a Role in Confirming Extrapulmonary TB and Latent TB Infection? *Tuberculosis* **113**, 30–37 (2018).

9. Essone, P. N., *et al.* M . Tuberculosis Infection and Antigen Specific Cytokine Response in Healthcare Workers Frequently Exposed to Tuberculosis. *Scientific Reports* **9**, 1–13 (2019).

10. Kim, S. Y., *et al.* The Responses of Multiple Cytokines Following Incubation of Whole Blood from TB Patients, Latently Infected Individuals and Controls with the TB Antigens ESAT-6, CFP-10 and TB7.7. *Scandinavian Journal of Immunology* **76**, 580–586 (2012).

11. Kellar, K. L., *et al.* Multiple Cytokines Are Released When Blood from Patients with Tuberculosis Is Stimulated with Mycobacterium Tuberculosis Antigens. *PLOS ONE* **6**, e26545 (2011).

12. Chegou, N. N., Heyckendorf, J., Walzl, G., Lange, C. & Ruhwald, M. Beyond the IFN-γ Horizon: Biomarkers for Immunodiagnosis of Infection with Mycobacterium Tuberculosis. *European Respiratory Journal* **43**, 1472–1486 (2014).

13. Wang, X., Jiang, J., Cao, Z., Yang, B., Zhang, J. & Cheng, X. Diagnostic Performance of Multiplex Cytokine and Chemokine Assay for Tuberculosis. *Tuberculosis (Edinb)* **92**, 513–520 (2012).

14. Lu, L. L., *et al.* IFN-γ-Independent Immune Markers of Mycobacterium Tuberculosis Exposure. *Nature Medicine* **25**, 977–987 (2019).

15. Robison, H. M., *et al.* Precision Immunoprofiling to Reveal Diagnostic Signatures for Latent Tuberculosis Infection and Reactivation Risk Stratification. *Int Bio (Cam)* **11**, 16–25 (2019).

16. Robison, H. M. & Bailey, R. C. A Guide to Quantitative Biomarker Assay Development Using Whispering Gallery Mode Biosensors. *Current Protocols in Chemical Biology* **9**, 158–173 (2017).

17. Mudumba, S., *et al.* Photonic Ring Resonance Is a Versatile Platform for Performing Multiplex Immunoassays in Real Time. *Journal of Immunological Methods* **448**, 34–43 (2017).

18. Miyara, M., *et al.* Detection in Whole Blood of Autoantibodies for the Diagnosis of Connective Tissue Diseases in near Patient Testing Condition. *PLoS One* **13**, 8 (2018).

19. Robison, H. M., *et al.* Risk Assessment of Latent Tuberculosis Infection through a Multipl-exed Cytokine Biosensor Assay and Machine Learning Feature Selection. *Scientific Reports* (2021) – In Submission.

20. Lindestam Arlehamn C.S., *et al.* A Quantitative Analysis of Complexity of Human Pathogen-Specific CD4 T Cell Responses in Healthy M. tuberculosis Infected South Africans. *PLoS Pathog* **12**, e1005760 (2016).

21. El Sahly H.M., Adams G.J., Soini H., Teeter L., Musser J.M. & Graviss E.A. Epidemiologic differences between United States- and foreign-born tuberculosis patients in Houston, Texas. *J Infect Dis.* **183**, 461-468 (2001).

22. Lewinsohn, D. M., *et al.* Official American Thoracic Society/Infectious Diseases Society of America/Centers for Disease Control and Prevention Clinical Practice Guidelines: Diagnosis of Tuberculosis in Adults and Children. *Clinical Infectious Diseases* e1-e33 (2017).

23. Escalante P., *et al.* Combinatorial immunoprofiling in latent tuberculosis infection. Toward better risk stratification. *Am J Respir Crit Care Med* **192**, 605–617 (2015).

24. Menzies, D., Gardiner, G., Farhat, M, Greenaway, C. & Pai, M. Thinking in Three Dimensions: A Web-Based Algorithm to Aid the Interpretation of Tuberculin Skin Test Results. *The International Journal of Tuberculosis and Lung Disease*. **8**, 498-505 (2008).

25. Breiman, Leo. Random Forests. *Machine Learning* **45**, 5-32 (2001).

26. Team, R Core. R: A language and environment for statistical computing. (2013)

27. Ishwaran, H. & Kogalur, U.B. Package 'randomForestSRC'. (2020)

28. Yang, J. D., *et al.* Mycobacterium Tuberculosis-Specific CD4+ and CD8+ T Cells Differ in Their Capacity to Recognize Infected Macrophages. *PLOS Pathogens* **14**, e1007060 (2018).

29. Singh, B., Chitra, J. & Selvaraj, P. CCL2, CCL3 and CCL4 Gene Polymorphisms in Pulmonary Tuberculosis Patients of South India. *International Journal of Immunogenetics* **41**, 98–104 (2014).

30. Ruhwald, M., Bjerregaard-Andersen, M., Rabna, P., Eugen-Olsen, J. & Ravn, P. IP-10, MCP-1, MCP-2, MCP-3, and IL-1RA Hold Promise as Biomarkers for Infection with M. Tuberculosis in a Whole Blood Based T-Cell Assay. *BMC Research Notes* **2**, 19 (2009).

31. Millington, K. A., *et al.* Dynamic Relationship between IFN-γ and IL-2 Profile of Mycobacterium Tuberculosis-Specific T Cells and Antigen Load. *The Journal of Immunology* **178**, 5217–5226 (2007).

32. Okamoto Yoshida, Y., *et al.* Essential Role of IL-17A in the Formation of a Mycobacterial Infection-Induced Granuloma in the Lung. *J. Immunol.* **184**, 4414–4422 (2010).

33. Khader, S. A., *et al.* IL-23 and IL-17 in the Establishment of Protective Pulmonary CD4+ T Cell Responses after Vaccination and during Mycobacterium Tuberculosis Challenge. *Nat. Immunol.* **8**, 369–377 (2007).

34. Tang, N. L.-S., *et al.* Genetic Association between a Chemokine Gene CXCL-10 (IP-10, Interferon Gamma Inducible Protein 10) and Susceptibility to Tuberculosis. *Clin. Chim. Acta* **406**, 98–102 (2009).

35. Ahmed, M., *et al.* Immune Correlates of Tuberculosis Disease and Risk Translate across Species. *Science Translational Medicine* **12**, 528 (2020).

CHAPTER 4

Evaluation of Preterm Neonatal Immature Immune Responses to Chorioamnionitis Using Multiplexed Cytokine Diagnostics

Acknowledgements

This chapter has been adapted from the research article “Chorioamnionitis Decreases Cytokine and Chemokine Expression in Preterm Neonates Up to 36 Weeks Postmenstrual Age” (Chapman, C. A.*, Stepanovich, G. *et al. Pediatric Research* (2021) – In Submission). My contributions include multiplexed assay validation, sample analysis, data analysis, and writing. I would like to acknowledge the contributions of Dr. Gretchen Stepanovich and Dr. Jennifer Bermick from the University of Michigan Neonatology for clinical guidance, sample collection, and extensive collaboration. I would also like to acknowledge Krista Meserve for her help in assay validation, sample processing, and data analysis.

Abstract

Preterm birth affects approximately 11% of live births globally. Preterm infants are at increased risk of sepsis, thought to be related to prematurity of the immune system and specifically, a decreased pro-inflammatory cytokine response compared to term infants when a secondary infectious is encountered. Furthermore, exposure to intrauterine infection of the fetal membranes, termed chorioamnionitis, results in an initial pro-inflammatory cytokine response, though it appears to alter the development of the immune system. It is unknown how long chorioamnionitis-induced dampened immune responses persist. The present study used a 7-plex immunoassay panel to measure cytokines in 49 subjects across 330 unstimulated neonatal waste serum samples. Mann-Whitney analyses compared cytokine levels between healthy and chorioamnionitis-exposed preterm infants at corrected gestational age intervals. Statistical analysis revealed significance for six out of seven cytokines in the multiplexed assay: CCL2, TNF-α, IL-1β, IL-6, IL-8, and IL-10. Biomarkers of interest were identified across 23-36 weeks of corrected gestational age. Qualitative results demonstrated immunosuppression in infants exposed to maternal chorioamnionitis. These findings indicate that exposure to chorioamnionitis has long-lasting immune consequences for preterm neonates, which may alter their ability to respond to infections.

Introduction

Preterm birth, defined as delivery that occurs prior to 37 weeks' gestation, complicates approximately 11% of births globally.[1] Neonates born prior to 32 weeks of completed gestation are considered very preterm and are at risk for numerous morbidities, including sepsis. Up to 5% of very preterm neonates develop culture positive sepsis during their initial NICU stay compared to 0.1% of term neonates.[2] This infection risk is often attributed to immaturity of the preterm immune system, particularly the innate immune system. Preterm neonates are known to have decreased pro-inflammatory cytokine responses when compared to term neonates, although this is context dependent. For example, umbilical cord blood monocytes from preterm neonates express less IL-1β, IL-6, and TNF-α when stimulated with either lipopolysaccharide (LPS) or *Staphylococcus epidermidis*, but express equivalent levels of these cytokines when stimulated with group B streptococcus.[3-5] These decreased cytokine responses are thought to contribute to a preterm neonate's heightened susceptibility to infection because appropriate cytokine responses are necessary to guide the clearance of microorganisms.[6]

There are multiple causes of preterm delivery, but intrauterine infection is the most common.[1,7] Chorioamnionitis is characterized by inflammation and infection of the chorion, amnion and placenta[8], and is present in up to 70% of preterm deliveries.[9-11] Chorioamnionitis leads to an initial fetal pro-inflammatory response, including increased expression of the pro-inflammatory cytokines IL-1β, IL-6, IL-8, and TNF-α in the plasma.[12] This fetal inflammatory response alters the developing immune system, resulting in decreased pro-inflammatory cytokine expression when umbilical cord blood monocytes from chorioamnionitis-exposed neonates undergo a secondary challenge with either LPS

or *Staphylococcus epidermidis*.[13,14] Chorioamnionitis exposure is known to increase the risk of developing both early and late onset neonatal sepsis, and this is thought to be at least partially due to these dampened monocyte responses.[15,16] It is currently unclear how long this chorioamnionitis-induced immune hypo-responsiveness persists, which could impact susceptibility to infection outside of the immediate neonatal period and may have long-term immune phenotype implications for the development of chronic disease.

In order to better understand how inflammatory mediators change over time in chorioamnionitis-exposed and unexposed preterm neonates, we performed longitudinal cytokine and chemokine profiling. To be useful in a clinical setting such as the NICU, we need fast multiplexed testing strategies that rely on small sample volumes. We have previously developed silicon photonic microring resonator bioassays for implementation in clinical evaluations.[17-19] With 128 sensors that can be simultaneously interrogated on a commercialized platform, we can measure multiple targets of interest quickly, with minimal sample volumes. For this study, we developed a 7-plex cytokine and chemokine assay to measure concentrations of CCL2, CCL3, IL-1β, IL-6, IL-8, IL-10, and TNF-α in neonatal serum samples. Using less than 200 μL of residual serum from clinically indicated routine blood tests, this assay produced time-to-result measurements in 38 minutes. Using this platform, we compared cytokine and chemokine levels at pre-defined corrected gestational age intervals to determine how long chorioamnionitis-induced dampened pro-inflammatory cytokine and chemokine expression persisted in preterm neonates.

Methods

Patient Recruitment and Blood Collection

After institutional IRB approval and informed parental consent was obtained, residual serum was collected from clinically indicated lab draws in 18 chorioamnionitis-exposed and 29 unexposed preterm neonates born at ≤32 weeks gestational age from birth through NICU discharge. Sample collection occurred from April, 2019 through March, 2020**.** Histopathologic examination of the placenta was used to diagnose chorioamnionitis.[14,20] Samples were collected from 47 patients from birth through 36 weeks postmenstrual age or discharge, whichever occurred first. The blood volume collected with each sample varied, as the serum available for testing was what remained after all clinically ordered testing was performed. As 200 µL was required for performance of the cytokine assay, samples were pooled if collected within three days of one another and the subject had no significant change in clinical status. A total of 330 residual serum samples were collected. Samples were excluded if the subject had a suspected or confirmed infection and was being treated with antibiotics at the time of sample collection (sepsis, urinary tract infection, pneumonia, necrotizing enterocolitis, or spontaneous intestinal perforation), excluding 75 samples from analysis. A total of 255 serum samples were included in the final analysis. Samples were frozen and stored in a -80° C freezer prior to use. A summary of clinical information is included in Table 4-1

Reagents and Buffers

Dulbecco's phosphate buffered saline (PBS, catalog # D5573), bovine serum albumin (BSA, catalog # A2153), and (3-Aminopropyl)triethoxysilane (catalog # 440140) were purchased from Millipore Sigma (3050 Spruce Street, St. Louis, MO 63103). Glycerol (catalog # BP229), bis(sulfosuccinimidyl)suberate (catalog # A39266), starting block blocking buffer (catalog # 37538), Pierce high sensitivity streptavidin-HRP (SA-

HRP, catalog # 21130), and 4-chloronaphthol (4-CN, catalog # 34012) were purchased from Thermo Fisher Scientific (168 Third Avenue, Waltham, MA USA 02451). Drycoat assay stabilizer (catalog # AG066) was obtained from Virusys Coproration (PO Box 56, Taneytown, MD 21787). Vendors and catalog numbers for antibodies for all multiplexed assay components are summarized in Table 4-2. Running buffer for all assays was 0.5% BSA in 1X PBS, pH 7.4.

Multiplexed Immunoassays

Microring resonator immunoassays were validated and performed on the Maverick M1 and Matchbox systems (Genalyte, Inc., San Diego, CA), respectively, as previously described.[17-19] The Maverick systems use multiple microfluidic system designs, with the M1 focusing on reusable cartridge devices and the Matchbox using injection-molded plug-and-play devices.[19] These both introduce automated flow for all assay steps for validation, calibration, and sample analysis on the multiplexed sensor arrays. Microring chips were functionalized through spotting to create a 7-plex cytokine and chemokine capture array, with duplicate sensor clusters per channel. After introducing the sample to the chip surface, a mixture of all tracer antibodies was flowed across the chip, followed by streptavidin-tagged enzymes for signal amplification. Assays were performed at a 30µl/min flow rate for all steps. There was an initial rinse of 5 minutes with the running buffer to ensure equilibration of the chip prior to sample analysis. The assay included steps as follows: 1) running buffer (2min); 2) sample (7min); 3) running buffer rinse (2min); 4) biotinylated tracer antibodies (7min); 5) running buffer rinse (2min); 6) SA-HRP (7min); 7) running buffer rinse (2min); 8) 4-CN (7min); 9) running buffer rinse (2min). The total assay time was 38 minutes (Figure 4-1).

The 7-plex immunoassay was simultaneously calibrated for all analytes in a multiplexed format, as described previously.[17] Serial dilutions from a mixed saturating analyte sample for all multiplexed targets created eight-point calibrations correlating relative sensor shifts to standard concentrations. To quantify relative shifts, the signal during the buffer rinse before the assay enhancement step (t=29min) was subtracted from the final assay rinse step (t=38min).

Net resonance wavelength shifts (Δpm) were plotted as a function of standard concentration and fit to a four-parameter logistic function (Figure 4-2 and 4-3) as described previously.[17] Limits of detection (LOD) and quantification (LOQ) were defined as the blank signal plus 3 times and 10 times the standard deviation of the blank, respectively (Table 4-3). Each calibration was performed at least in triplicate for each sample dilution as measured with 8 sensors per technical replicate.

Sample Evaluation

All samples contained at least 200µl of residual serum. Neonatal residual serum samples were analyzed at two dilutions (0.5X and 0.1X) in running buffer. Cytokine and chemokine concentrations were determined by using the corresponding serum calibrations (50% serum and 10% serum, respectively matching the serum content of the residual serum samples). Final concentrations were determined using the most appropriate dilution/calibration by comparing the closeness of the relative shift to the inflection point in the calibration dynamic range.

Data Analysis

All analyses and plotting were done using R coding language. Mann-Whitney tests were done for all modified gestational age bins, comparing chorioamnionitis-exposed and unexposed subpopulations. $p<0.05$ was considered statistically significant. Statistically significant populations were evaluated for cytokine and chemokine level relative differences.

Results/Discussion

Neonatal infections are a cause of significant morbidity and mortality in preterm neonates during their stay in the NICU.[2] Factors that increase a preterm neonate's susceptibility to infection and shape their ability to mount an effective immune response have not yet been fully elucidated. It is known that preterm neonates exposed to chorioamnionitis have an increased risk of developing early-onset sepsis (blood stream infection that occurs within the first 72 hours of life).[13,16,21] It is unclear if this infection risk is due to a common pathogen causing both conditions or alterations in the neonatal immune response following chorioamnionitis exposure, or both. Multiple studies have shown that exposure to chorioamnionitis impacts the neonatal immune system by altering gene transcription and innate immune responses.[12-14] These altered immune responses include dampened pro-inflammatory cytokine expression when a second pathogen is encountered.[13,14] Appropriate pro-inflammatory cytokine expression is necessary for the clearance of microorganisms, so these chorioamnionitis-induced changes to neonatal immune responses are thought to be at least partially responsible for this increased risk of infection. However, it is unclear how long chorioamnionitis-induced dampened cytokine expression persists, as studies are conflicting about whether chorioamnionitis

exposure protects against or increases the risk for developing late onset sepsis (blood stream infection that presents after 72 hours of life).[16,22-24]

To assess the persistence of chorioamnionitis-induced dampened pro-inflammatory cytokine expression in preterm neonates, we performed longitudinal cytokine and chemokine profiling in very preterm neonates from birth to NICU discharge. We chose a panel of cytokines and chemokines known to be significant contributors to neonatal immune responses. Neonates primarily rely upon the innate immune system early in life to protect against infections due to limited antigen exposure *in utero* and major deficiencies in adaptive immune responses.[25,26] Innate immune cells, including monocytes, macrophages, and neutrophils, require signaling from cellular messengers such as cytokines and chemokines in order to mount a coordinated response to an infectious pathogen.[27] CCL2 and CCL3 are chemokines that recruits monocytes, macrophages, and neutrophils to local sites of infection and are necessary for prominent signaling pathways in the neonatal immune system.[28] IL-8 shows similar chemotactic affinity for neutrophils and stimulates bacterial phagocytosis.[29] IL-6, IL-1β, and TNF-α are pro-inflammatory cytokines important to the acute phase response necessary to assist in the clearance of microorganisms.[30-32] IL-10 is an immunoregulatory cytokine important for immune homeostasis that also suppresses autoinflammation.[30,33] We believe this panel of cytokines and chemokines provides a broad overview of neonatal innate immune reactivity.

We found that preterm neonates exposed to chorioamnionitis had decreased expression of most of the cytokines and chemokines measured at some point during their NICU stay compared to unexposed preterm neonates (Figure 4-4). The exception to this

was CCL3, which was equivalent between chorioamnionitis-exposed and unexposed preterm neonates. Interestingly, the differences observed in cytokine and chemokine expression seemed to be temporally distinct. IL-1β and TNF-α were only decreased in the extremely preterm chorioamnionitis-exposed neonates (23-28 weeks and 23-25 weeks postmenstrual age respectively), with equivalent expression at later postmenstrual ages. Conversely, IL-10 was only decreased in chorioamnionitis-exposed preterm neonates at later postmenstrual ages (35-36 weeks postmenstrual age). CCL2, IL-6, and IL-8 were decreased in chorioamnionitis-exposed preterm neonates across most gestational age bins. The most striking result from this study was that chorioamnionitis-exposed preterm neonates demonstrated decreased expression of CCL2, IL-6, and IL-8 until 34-36 weeks postmenstrual age. The persistence of chorioamnionitis-induced dampened cytokine and chemokine expression throughout a preterm neonate's NICU stay provides insight into immune-related complications experienced by chorioamnionitis-exposed neonates, including late onset sepsis, persistent wheezing, and asthma.[23,24,34] These findings suggest that exposure to early life inflammation has long-lasting consequences for preterm neonates that increases their risk for immune-related diseases well beyond the neonatal period.

Our 7-plex cytokine microring resonator assay was robustly validated for all targets simultaneously to ensure reproducible results across all samples analyzed. Each assay was 38 minutes to result, creating a quick method for analyzing important clinical samples. Using this multiplexed immunoassay, we were able to collect large amounts of immunological data quickly and with very little starting sample volume. This technology

can provide clinically relevant information quickly for the most vulnerable patients, which has to potential to markedly impact bedside patient care.

While the Mann-Whitney analyses are the most statistically robust results, our analysis can continue on an individual level by tracking cytokines for a subject over time to help interpret treatment outcomes and results. We plotted longitudinal levels by subject and compared them to clinical treatment information available. For subjects with the longest longitudinal samples, we were able to correlate drops in cytokine levels with treatments associated with co-infections that had been removed for the MW analysis. Figure 4-5 is one such example, where we were able to identify spikes and subsequent drops in cytokine levels at each major treatment (A-C). Other instances of this correlation include that of late onset neonatal sepsis (Figure 4-6) and necrotizing enterocolitis (Figure 4-7). While not statistically robust, these correlates indicate the clinical importance of rapid and robust testing. With our 38-minute assay, clinically relevant information could be available to evaluate treatment options and change outcomes.

This study has several limitations. All samples were collected from clinically indicated laboratory tests, so the timing of sample collection varied between patients and was not standardized. There were differences between the exposure groups, and chorioamnionitis-exposed subjects were more likely to be born earlier, be African American and be born by vaginal delivery than unexposed subjects. It is unclear if these differences impacted cytokine and chemokine expression, but degree of prematurity and mode of delivery have been shown to impact immune responses in prior studies.[3,4,35] Samples were excluded from subjects who had a suspected or confirmed infection and were receiving antibiotics at the time of sample collection. However, samples were

included from these patients later during their NICU course once the infection was treated. It is unclear if the suspected or confirmed infections influenced future cytokine and chemokine expression. Consistent with previous reports, chorioamnionitis-exposed preterm neonates in this study had an increased incidence of early onset sepsis.[13,16,21] It is unclear what impact this had on subsequent cytokine or chemokine responses and if the presence of early onset sepsis further compounded dampened cytokine and chemokine expression. The numbers in this study are not large enough to directly address this, but future studies containing more subjects would be of benefit.

Conclusions

We identified that very preterm neonates exposed to chorioamnionitis had decreased expression of the cytokines and chemokines CCL2, IL-1β, IL-6, IL-8, IL-10, and TNF-α at some point during their NICU stay compared to unexposed very preterm neonates. The differences in IL-1β and TNF-α only appeared at very early postmenstrual ages while the difference in IL-10 presented much later. There was relatively consistent decreased expression of CCL2, IL-6 and IL-8 in very preterm chorioamnionitis-exposed neonates from birth to 34-36 weeks postmenstrual age. The persistent dampened immune responses seen in chorioamnionitis-exposed very preterm neonates may explain their increased risk for immune-mediated complications outside of the immediate neonatal period, including late onset sepsis, persistent wheezing, and asthma. Finally, the multiplexed immunoassay used in this study provides rapid immunologically relevant results with small sample volumes, which has the potential to improve the care of preterm infants in real time.

Table 4-1. Study group characteristics. *p<0.05. Quantitative variables were compared using the student's t-test and categorical variables were compared using the Chi-square test.

	Chorioamnionitis-exposed Preterm Neonates (n=18)	Unexposed Preterm Neonates (n=29)	p-value
Birth gestational age in weeks (mean ± SD)	27 ± 2.86	29.86 ± 2.86	0.025*
Birth weight in grams (mean ± SD)	954 ± 507	1167 ± 612	0.23
Male sex	7 (39%)	17 (59%)	0.19
Ethnicity			
- **Caucasian**	12 (66%)	24 (83%)	0.18
- **African American**	3 (17%)	0	0.023*
- **Other**	3 (17%)	5 (17%)	0.96
C-section	11 (61%)	28 (97%)	0.002*
Antenatal steroids at least 12 hours prior to delivery	16 (89%)	19 (66%)	0.07
Multiple gestation	8 (44%)	20 (69%)	0.1
1 minute Apgar score (mean ± SD)	4 ± 2	5 ± 2	0.67
5 minute Apgar score (mean ± SD)	7 ± 2	7 ± 2	0.36
Early onset sepsis (blood culture positive within 72 hours of birth)	4 (22%)	1 (3%)	0.042*
Late onset sepsis (blood culture positive after 72 hours of life)	3 (17%)	6 (21%)	0.73
Ventilator associated pneumonia	1 (6%)	2 (7%)	0.85
Urinary tract infection	2 (11%)	6 (21%)	0.4
Necrotizing enterocolitis (Bell's stage II or greater)	2 (11%)	5 (17%)	0.57
Spontaneous intestinal perforation	2 (11%)	1 (3%)	0.3

Table 4-2. Antibodies and recombinant standard proteins, along with tracer antibody concentrations, used in the multiplexed immunoassay.

Target	Role	Source	Catalog Number	Tracer Concentrations (µg/mL)
CCL2	Capture Antigen Tracer	Thermo Fisher Thermo Fisher Thermo Fisher	14-7099 14-8398 13-7096	2
CCL3	Capture Antigen Tracer	R&D Systems R&D Systems R&D Systems	MAB670-100 270-LD-010 MAB270-100	1
IL-1β	Capture Antigen Tracer	Thermo Fisher Thermo Fisher Thermo Fisher	14-7018-85 RIL1BI 13-7016-85	2
IL-6	Capture Antigen Tracer	Thermo Fisher Thermo Fisher Thermo Fisher	16-7069 14-8069 13-7068	2
IL-8	Capture Antigen Tracer	BD Biosciences BD Biosciences BD Biosciences	554716 554609 554718	2
IL-10	Capture Antigen Tracer	Thermo Fisher Thermo Fisher Thermo Fisher	16-7108 14-8109-80 13-7109	2
TNF-α	Capture Antigen Tracer	Biolegend Biolegend Biolegend	502802 570102 502904	2

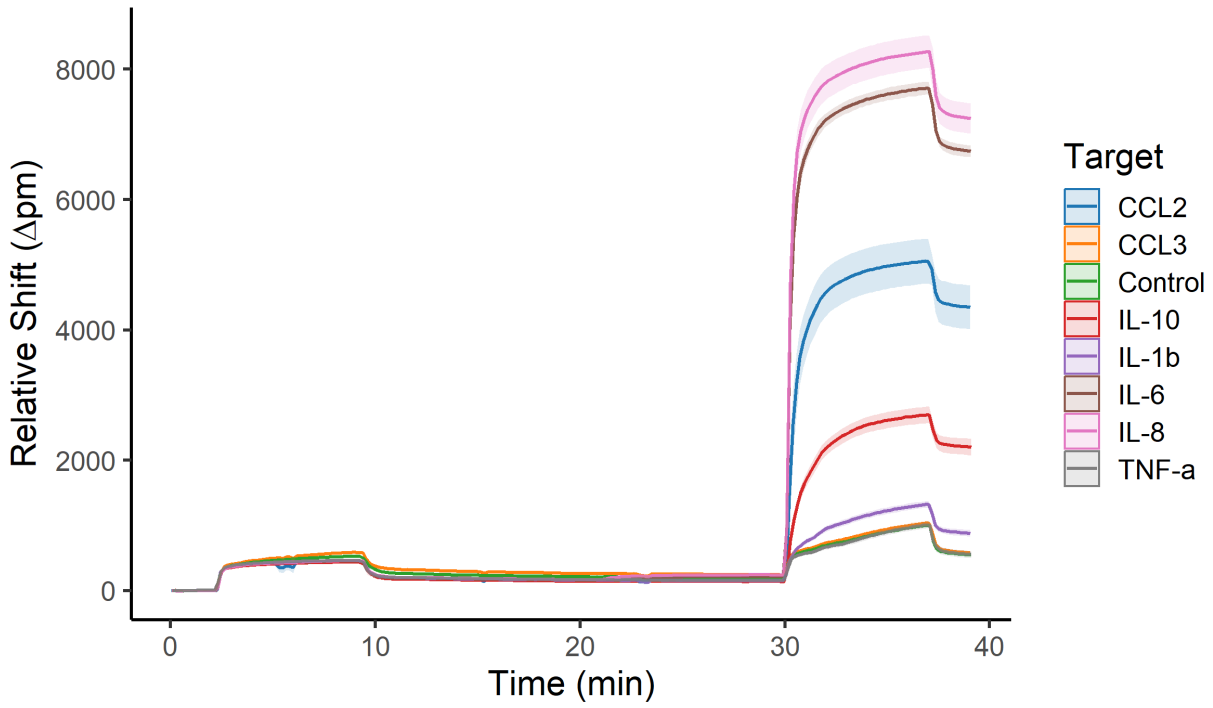

Figure 4-1. Example microring trace of a multiplexed immunoassay for neonatal residual serum. All flow steps are automated and sequential with running buffer rinses between reagents. Net shifts are calculated from subtracting the relative shift at t=29min from the relative shift at t=38min.

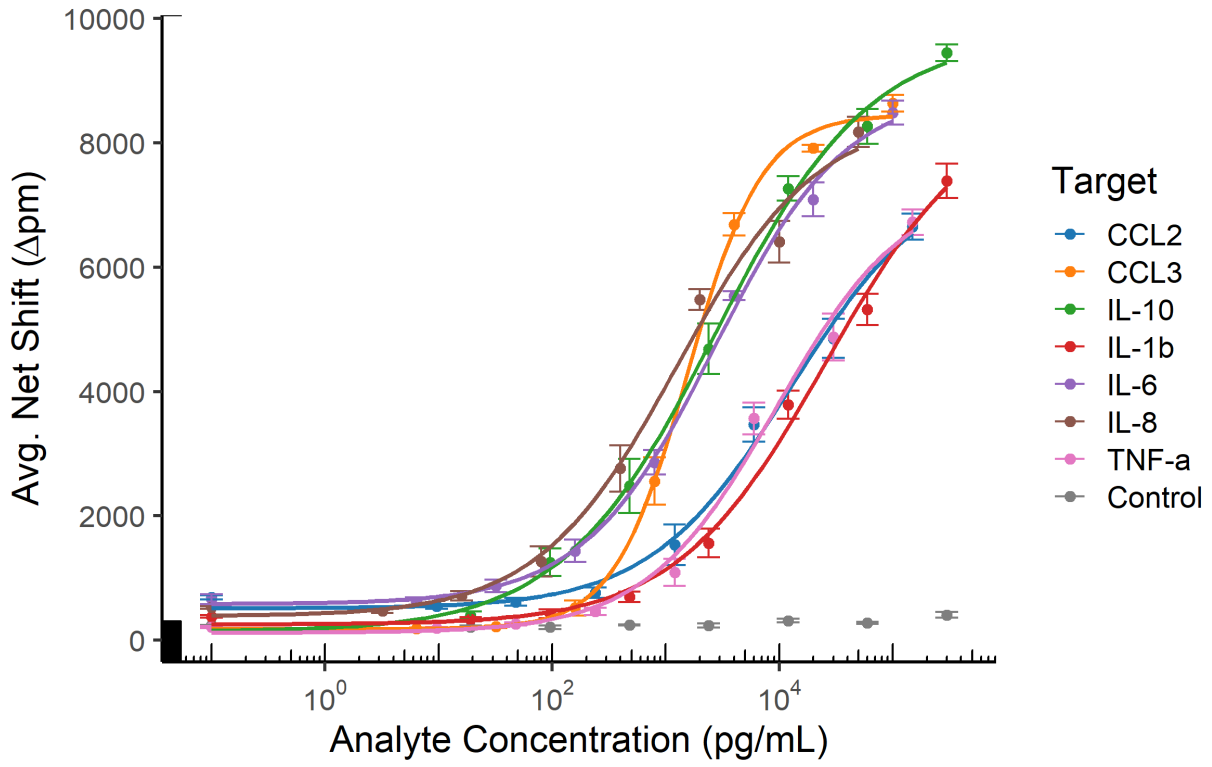

Figure 4-2. Multiplexed serum calibrations for 50% serum samples. Error bars represent standard deviation from n=4 calibrations, n=8 ring replicates per target.

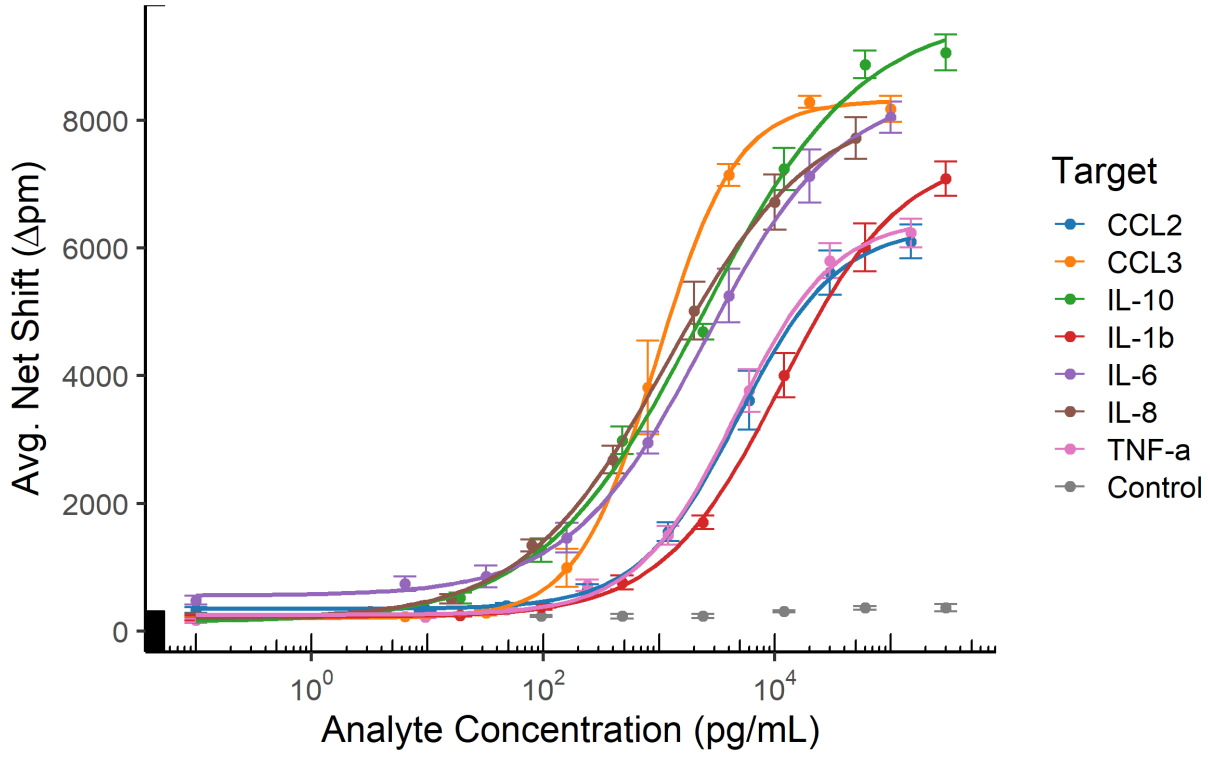

Figure 4-3. Simultaneous multiplexed calibrations on the Genalyte Matchbox platform for 10% serum samples. Error bars represent standard deviation and are from n=4 calibrations, n=8 rings per target.

Table 4-3. Limits of Detection (LOD) for 50% and 10% serum calibrations, calculated from the signal of the blank plus three times the standard deviation of the blank.

Target	50% Serum LODs	10% Serum LODs
CCL2	211.4 pg/mL	223.1 pg/mL
CCL3	64.5 pg/mL	41.8 pg/mL
IL-1β	124.0 pg/mL	185.4 pg/mL
IL-6	83.2 pg/mL	37.1 pg/mL
IL-8	10.4 pg/mL	8.5 pg/mL
IL-10	4.0 pg/mL	6.8 pg/mL
TNF-α	86.2 pg/mL	73.7 pg/mL

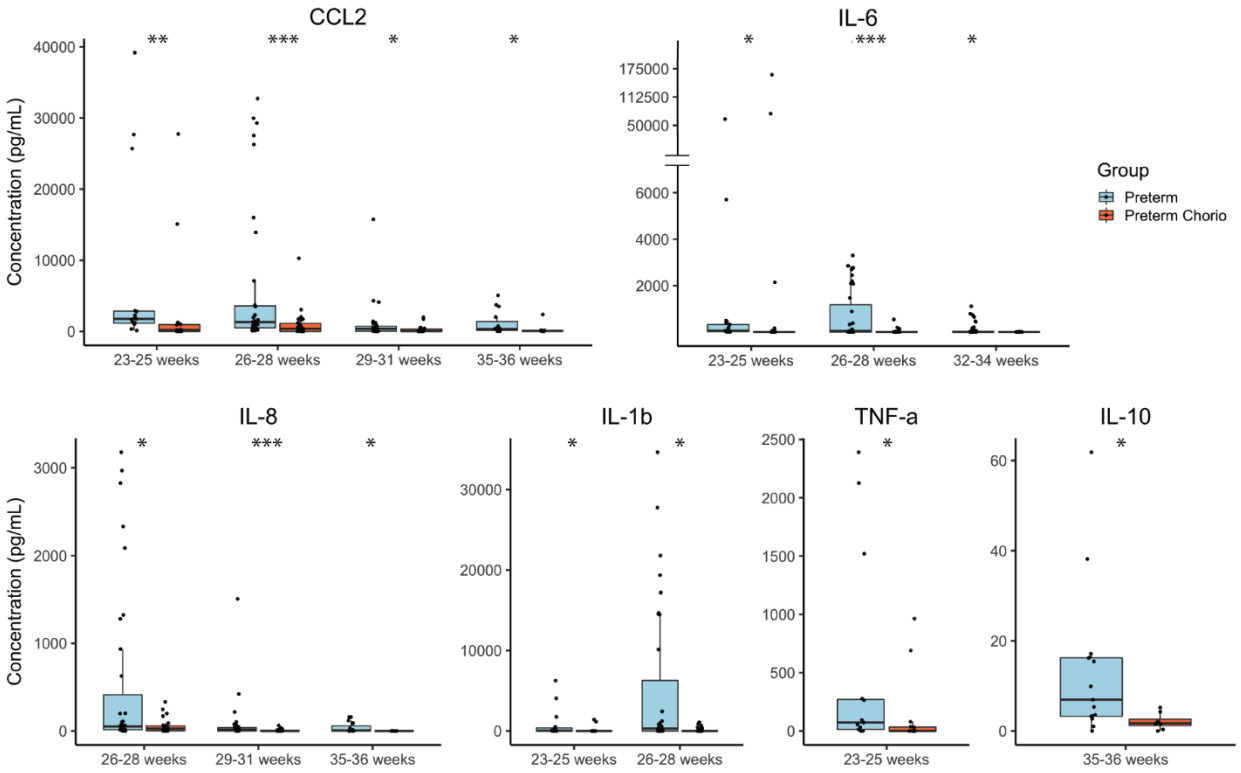

Figure 4-4. Significant Mann-Whitney analyses comparing healthy and chorio-infected preterm infants for all multiplexed cytokines. Box plots represent the 25th and 75th percentile, median, and mean. Subpopulations for each box plot range from 8-33 sample points. *p<0.05, **p<0.01, ***p<0.001

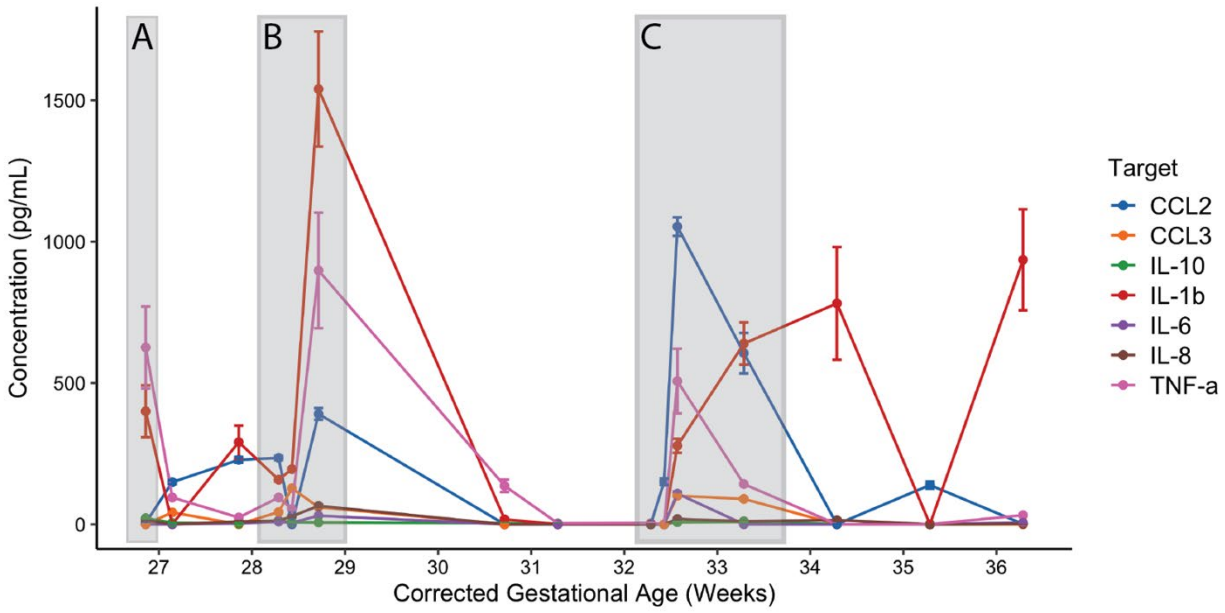

Figure 4-5. Longitudinal analyses of a neonatal subject. Grey areas are correlated to clinical events, including A) early onset neonatal sepsis, B) ventilator associated pneumonia, and C) urinary tract infection and treatment thereof. Error bars are from n=8 technical ring replicates.

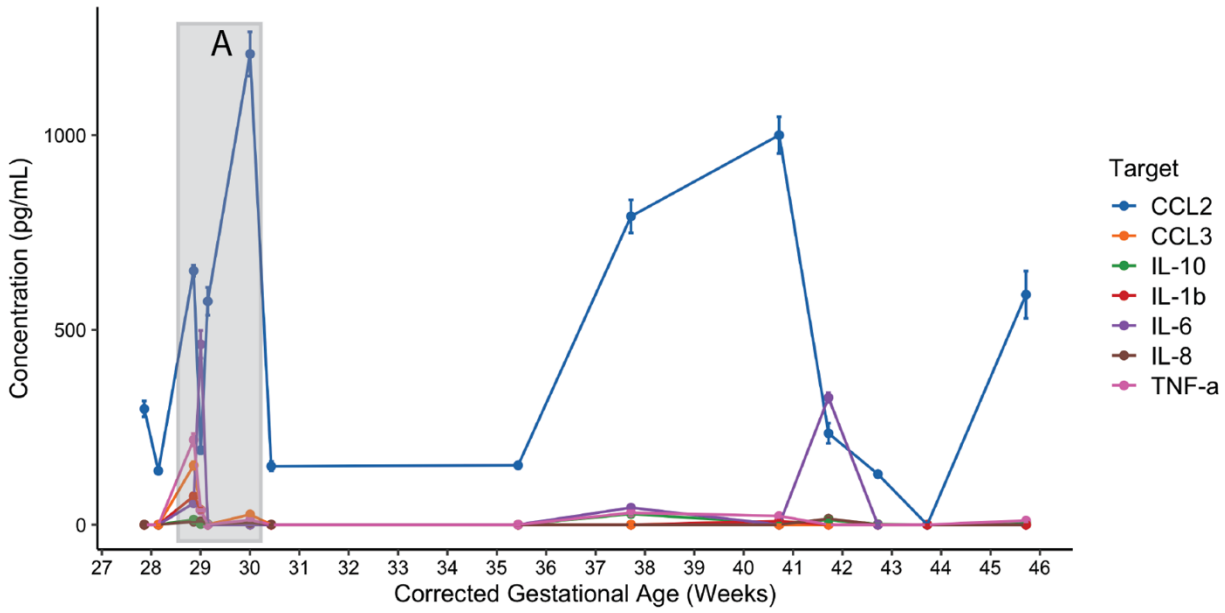

Figure 4-6. Example of longitudinal cytokine profiling with cytokine levels correlating to LONS treatment. Error bars are from n=8 technical ring replicates.

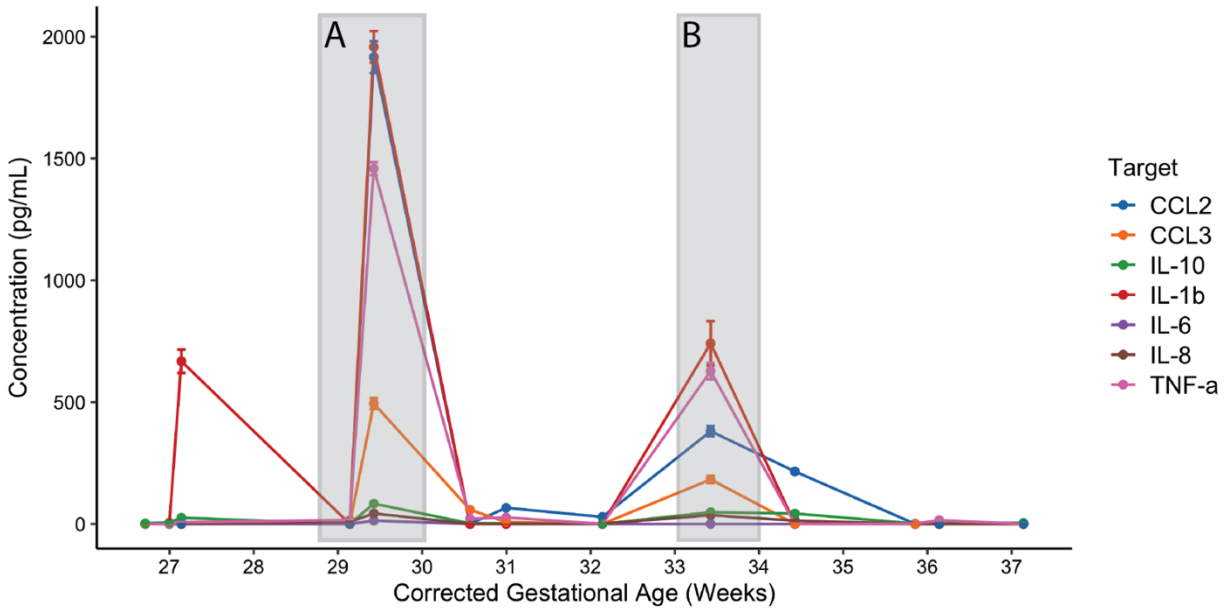

Figure 4-7. Example of longitudinal cytokine profiling with cytokine levels correlating to NEC treatments. Error bars are from n=8 technical ring replicates.

References

1. WHO | Survive and thrive: transforming care for every small and sick newborn (2020).

2. Simonsen K. A., Anderson-Berry A. L., Delair S. F., Davies H.D. Early-onset neonatal sepsis. *Clin Microbiol Rev*. **27,** 21-47 (2014).

3. Sharma A. A., *et al.* Impaired NLRP3 inflammasome activity during fetal development regulates IL-1β production in human monocytes. *Eur J Immunol*. **45**, 238-49 (2015).

4. Strunk T., *et al*. Responsiveness of human monocytes to the commensal bacterium Staphylococcus epidermidis develops late in gestation. *Pediatr Res*. **72,** 10-8 (2012).

5. Tatad A. M., *et al*. Cytokine expression in response to bacterial antigens in preterm and term infant cord blood monocytes. *Neonatology*. **94,** 8-15 (2008).

6. Salio M., *et al*. Modulation of human natural killer T cell ligands on TLR-mediated antigen-presenting cell activation. *Proc Natl Acad Sci*. **104,** 20490-5 (2007).

7. Blencowe H., *et al.* National, regional, and worldwide estimates of preterm birth rates in the year 2010 with time trends since 1990 for selected countries: a systematic analysis and implications. *Lancet* **379,** 2162–72 (2012).

8. Kim C. J., *et al.* Acute chorioamnionitis and funisitis: definition, pathologic features, and clinical significance. *Am J Obstet Gynecol* **213,** S29-52 (2015).

9. Tita A. T. N., Andrews W. W. Diagnosis and Management of Clinical Chorioamnionitis. *Clin Perinatol* **37,** 339–54 (2010).

10. Peng C-C., Chang J-H., Lin H-Y., Cheng P-J., Su B-H. Intrauterine inflammation, infection, or both (Triple I): A new concept for chorioamnionitis. *Pediatrics & Neonatology* **59,** 231–7 (2018).

11. Higgins R. D., *et al.* Evaluation and Management of Women and Newborns With a Maternal Diagnosis of Chorioamnionitis: Summary of a Workshop. *Obstet Gynecol* **127,** 426–36 (2016).

12. Romero R., *et al*. Clinical chorioamnionitis at term V: umbilical cord plasma cytokine profile in the context of a systemic maternal inflammatory response. *J Perinat Med*. **44,** 53-76 (2016).

13. de Jong E., *et al*. Exposure to chorioamnionitis alters the monocyte transcriptional response to the neonatal pathogen Staphylococcus epidermidis. *Immunol Cell Biol*. **96,** 792-804 (2018).

14. Bermick J., *et al*. Chorioamnionitis exposure remodels the unique histone modification landscape of neonatal monocytes and alters the expression of immune pathway genes. *FEBS J*. **286,** 82-109 (2019).

15. Schrag S. J., *et al*. Risk factors for invasive, early-onset Escherichia coli infections in the era of widespread intrapartum antibiotic use. *Pediatrics*. **118,** 570-6 (2006).

16. García-Muñoz Rodrigo F., Galán Henríquez G., Figueras Aloy J., García-Alix Pérez A. Outcomes of very-low-birth-weight infants exposed to maternal clinical chorioamnionitis: a multicentre study. *Neonatology*. **106,** 229-34 (2014).

17. Robison H. M., Bailey R. C. A Guide to Quantitative Biomarker Assay Development using Whispering Gallery Mode Biosensors. *Curr Protoc Chem Biol* **9,** 158–73 (2017).

18. Robison H. M., *et al.* Precision immunoprofiling to reveal diagnostic signatures for latent tuberculosis infection and reactivation risk stratification. *Int Bio (Cam)* **11,** 16–25 (2019).

19. Mudumba S., *et al.* Photonic ring resonance is a versatile platform for performing multiplex immunoassays in real time. *Journal of Immunological Methods* **448,** 34–43 (2017).

20. Redline R. W., *et al*. Amniotic infection syndrome: nosology and reproducibility of placental reaction patterns. *Pediatr Dev Pathol*. **6,** 435-48 (2003).

21. Ofman G., Vasco N., Cantey J. B. Risk of Early-Onset Sepsis following Preterm, Prolonged Rupture of Membranes with or without Chorioamnionitis. *Am J Perinatol*. **33,** 339-42 (2016).

22. Strunk T., *et al*. Histologic chorioamnionitis is associated with reduced risk of late-onset sepsis in preterm infants. *Pediatrics*. **129,** e134-41 (2012).

23. Puri K., *et al*. Association of Chorioamnionitis with Aberrant Neonatal Gut Colonization and Adverse Clinical Outcomes. *PLoS One*. **11,** e0162734 (2016).

24. Villamor-Martinez E., *et al*. Association of Histological and Clinical Chorioamnionitis With Neonatal Sepsis Among Preterm Infants: A Systematic Review, Meta-Analysis, and Meta-Regression. *Front Immunol*. **11,** 972 (2020).

25. Cantó E., Rodriguez-Sanchez J. L., Vidal S. Distinctive response of naïve lymphocytes from cord blood to primary activation via TCR. *J Leukoc Biol*. **74,** 998-1007 (2003).

26. Marodi L. Down-regulation of Th1 responses in human neonates. *Clin Exp Immunol*. **128,** 1-2 (2002).

27. Iroh Tam P-Y., Bendel C. M. Diagnostics for neonatal sepsis: current approaches and future directions. *Pediatric Research* **82,** 574–83 (2017).

28. Kinjo T., *et al.* Serum chemokine levels and developmental outcome in preterm infants. *Early Hum Dev* **87,** 439–43 (2011).

29. Franz A. R., Steinbach G., Kron M., Pohlandt F. Interleukin-8: a valuable tool to restrict antibiotic therapy in newborn infants. *Acta Paediatr* **90,** 1025–1032 (2001).

30. de Bont E. S., *et al.* Tumor necrosis factor-alpha, interleukin-1 beta, and interleukin-6 plasma levels in neonatal sepsis. *Pediatric Research* **33,** 380–3 (1993).

31. Dulay A.T., *et al.* Compartmentalization of acute phase reactants Interleukin-6, C-Reactive Protein and Procalcitonin as biomarkers of intra-amniotic infection and chorioamnionitis. *Cytokine* **76,** 236–43 (2015).

32. Chaemsaithong P., *et al.* A point of care test for interleukin-6 in amniotic fluid in preterm prelabor rupture of membranes: a step toward the early treatment of acute intra-amniotic inflammation/infection. *J Matern Fetal Neonatal Med* **29,** 360–7 (2016).

33. Ye Q., Du L., Shao W-X., Shang S. Utility of cytokines to predict neonatal sepsis. *Pediatric Research* **81,** 616–21 (2017).

34. Kumar R., *et al*. Prematurity, chorioamnionitis, and the development of recurrent wheezing: a prospective birth cohort study. *J Allergy Clin Immunol*. **121,** 878-84 (2008).

35. Jakobsson H. E., *et al*. Decreased gut microbiota diversity, delayed Bacteroidetes colonisation and reduced Th1 responses in infants delivered by caesarean section. *Gut*. **63,** 559-66 (2014).

CHAPTER 5

COVID-19 Cytokine Levels in Stimulated Patient Samples: A Multiplexed Assay For Immunoprofiling Disease Severity and Vaccine Efficacy

Acknowledgements

I would like to acknowledge Dr. Patricio Escalante, Dr. Tobias Peikert, and Courtney Erskine for clinical assistance, cell stimulations, and general guidance. I would also like to acknowledge Krista Meserve for her help in assay validation and sample processing.

Abstract

The COVID-19 pandemic is a global health emergency, with almost 70 million cases and 1.6 million deaths as of December 2020. Currently, disease severity has been linked to dysregulated and excessive immunity and the early pathophysiologic drivers of this immune dysregulation has yet to be further defined. Though early identification of patients with COVID-19 likely to develop critical illness is of enormous importance, reliable biomarkers to identify these patients are lacking. In the context of the ongoing COVID-19 pandemic, prediction of disease susceptibility, disease severity, re-infection risk, and protective long-term immunity are essential. We have developed a 15-plex cytokine panel on our microring resonator platform to analyze stimulated PBMC serum samples from COVID patients to define immunological parameters of disease severity and longitudinal immunity. These cytokines provide a broad immunoprofile, consisting of chemokines, pro- and anti-inflammatory cytokines, as well as immune growth factors, all with potential significance to COVID-19. From stimulation conditions for SARS-CoV-2 spike protein subunits and off-target responses, we interrogated PMBC cytokine levels using precision medicine approaches. Mann-Whitney analyses were utilized to distinguish biomarkers of importance for COVID+ individuals, which at this time include absolute and normalized levels of CCL3, GM-CSF, IFN-λ1, IL-1β, IL-2, and IL-7.

Introduction

The COVID-19 pandemic is a global health emergency of unparalleled proportions. With almost 70 million cases and 1.6 million deaths globally as of December 2020, the SARS-CoV-2 virus has crippled healthcare systems worldwide.[1-3] COVID-19 causes symptoms similar to that of the flu, but with more severe outcomes including respiratory failure, cytokine storms, septic shock, blood clots and pneumonia. Collectively, the clinical and scientific community has come together to focus on the pandemic, spanning diagnostic research to detected infections, understanding physiologically how the virus is spreading and affecting patients, finding optimal treatment strategies, and developing vaccines for implementation. As this research is progressing, SARS-CoV-2 continues to infect and mutate, and so there is an imperative to study quickly but robustly all aspects of the virus.

The first line of defense for this infection has been detection, and therefore diagnostics. Over the past year, diagnostic solutions have steadily become more sophisticated and quicker. A wide variety of options are available, from PCR and neutralizing antibody blood tests to nasal swab and saliva tests.[4] These diagnostics are at the stage where we are accurately and rapidly identifying sick individuals and attempting to mitigate spread. However, overall understanding of this infection and its outcomes and long-term effects are limited.[5-8] Therefore, we need to pivot our diagnostic focus towards sick individuals and investigate the host-pathogen response, so that proper care can be met.

While most infected individuals develop only mild disease, a subset of patients progress to develop severe COVID-19, which is associated with high morbidity and

mortality.[9-11] Currently, disease severity has been linked to dysregulated and excessive immunity in COVID-19 and the early pathophysiologic drivers of this immune dysregulation has yet to be further defined.[6,12-14] Unfortunately, though early identification of patients with COVID-19 likely to develop critical illness is of enormous importance, reliable biomarkers to identify these patients are lacking.[10,16,17] Furthermore, studies in SARS-CoV-1 and human studies in COVID-19 indicate that antibody responses can be potentially short-lived, while the presence of specific antigens could be associated with the establishment of long-term protection in SARS-CoV-1.[17-23] In the context of the ongoing COVID-19 pandemic, prediction of disease susceptibility, disease severity, re-infection risk, and protective long-term immunity are essential for individualized patient management, optimal allocation of health care resources, safe operation of the society, and for vaccine design, testing, and deployment.

From this prospective profile of COVID-19 from ongoing research and understanding of SARS-CoV-1, a focus on host immune response is vital. Cytokine analyses are a directed way to understand the immune response to infection, not only in the short-term clearance of pathogens, but also in revealing aspects of potential long-term conferred immunity.[24-30] Therefore, in collaboration with Mayo Clinic, we have developed a 15-plex cytokine panel consisting of TNF-α, IFN-λ1, IFN-γ, TGF-α, GM-CSF, IP-10, IL-10, IL-7, IL-6, IL-2, IL-1β, CCL7, CCL4, CCL3, and CCL2 on the Genalyte microring resonator platform to analyze stimulated PBMC serum samples from COVID patients. These cytokines provide a broad profile of immune system responses, consisting of chemokines, pro- and anti-inflammatory cytokines, as well as immune growth factors, al with potential significance to COVID-19.[9,16,31-44] From seven stimulation

conditions (Spike protein S1 and S2, SARS-CoV-1 spike protein, tetanus toxoid, myoglobin, anti-CD3 antibody, and cell media), we plan to interrogate PMBC cytokine levels from conditions both directly related to COVID-19 as well as off-target metrics. Previous research in our lab has shown the utility of this approach to understand absolute cytokine levels and basally normalized conditions. From these stimulation conditions and cytokines, we hope to identify biomarkers that indicate disease severity, potential clinical outcomes, and long-term vaccine efficacy.

Methods

Reagents and buffers

Dulbecco's phosphate buffered saline (PBS, catalog # D5573), bovine serum albumin (BSA, catalog # A2153), and (3-Aminopropyl)triethoxysilane (catalog # 440140) were bought from Millipore Sigma (3050 Spruce Street, St. Louis, MO 63103). Glycerol (catalog # BP229), bis(sulfosuccinimidyl)suberate (catalog # A39266), starting block blocking buffer (catalog # 37538), Pierce high sensitivity streptavidin-HRP (SA-HRP, catalog # 21130), and 4-chloronaphthol (4-CN, catalog # 34012) were bought from Thermo Fisher Scientific (168 Third Avenue, Waltham, MA USA 02451). Drycoat assay stabilizer (catalog # AG066) was bought from Virusys Corporation (PO Box 56, Taneytown, MD 21787). Vendors and catalog numbers for antibodies for all multiplexed assay components are summarized in Table 5-1. Running buffer for all assays was 0.5% BSA in 1X PBS, pH 7.4.

Cell Culture and Antigen Stimulations

Whole blood samples were collected from convalescent donors who had recovered from COVID infection. PBMCs were separated by from whole blood by Ficoll separation and the pellets frozen with 10% DMSO in liquid nitrogen. Thawed PBMC pellets were stimulated for 40 hours with either COVID-relevant or off-target antigens. Supernatants from stimulated PBMCs were stored at −80°C and shipped on dry ice for cytokine measurements using the 15-plex antigen immunoassay on the microring resonators. A total of 16 subjects were collected and stimulated, including 6 Healthy and 16 COVID+ individuals.

Multiplexed immunoassay instrumentation and assay design

Microring resonator immunoassays were validated and performed on the Maverick M1 and Matchbox systems (Genalyte, Inc., San Diego, CA), respectively, as previously described.[45-47] The Microring chips were functionalized through spotting to create a 15-plex cytokine capture array, with 4 sensors per target per channel. After introducing sample to the chip surface, a mixture of all tracer antibodies was flowed across the chip, followed by streptavidin-tagged enzymes for signal amplification. Assays were performed at a 30µl/min flow rate for all steps. There was an initial rinse of 5 minutes with the running buffer to ensure equilibration of the chip prior to sample analysis. The assay included steps as follows: 1) running buffer (2min); 2) sample (7min); 3) running buffer rinse (2min); 4) biotinylated tracer antibodies (7min); 5) running buffer rinse (2min); 6) SA-HRP (7min); 7) running buffer rinse (2min); 8) 4-CN (7min); 9) running buffer rinse (2min). The total assay time was 38 minutes (Figure 4-1).

Calibrations and Sample Analyses

The 15-plex immunoassay was simultaneously calibrated for all analytes in a multiplexed format.[45] Serial dilutions from a mixed saturating analyte sample for all multiplexed targets created eight-point calibrations correlating relative sensor shifts to standard concentrations. To quantify relative shifts, the signal during the buffer rinse before the assay enhancement step (t=29min) was subtracted from the final assay rinse step (t=38min).

Net resonance wavelength shifts (Δpm) were plotted as a function of standard concentration and fit to a four-parameter logistic function (Figure 5-2 and 5-3). Limits of detection (LOD) and quantification (LOQ) were defined as the blank signal plus 3 times and 10 times the standard deviation of the blank, respectively (Table 5-2). Each calibration was performed at least in triplicate for each sample dilution as measured with 4 sensors per technical replicate.

Results/Discussion

There are many unknowns currently in understanding the immune response to Sars-CoV-2 infection, particularly what responses are leading to the disease severity. One of the most severe symptoms is that of cytokine storms, a similar overreaction to infection as that of sepsis. And while diagnostic work towards detection of COVID infections has been diverse, plentiful, and successful in a clinical setting, more work is needed to identify which biomarkers are leading changes in symptom severity. Here we created a custom panel with guidance from Mayo clinicians to profile 15 cytokines across a variety of subfamilies to investigate immune responses based on relevant stimulation conditions to Sars-CoV-2.

The custom multiplexed panel was carefully validated target by target, to understand the representative calibrations in buffer before multiplexing or sample matrix effect introduction. All immunoassays were optimized for tracer concentrations, dynamic ranges, and necessary buffer conditions. Once individually calibrated, the captures were machine spotted by Genalyte for multiplexed analyses. Primary and secondary binding experiments were tested sequentially for each immunoassay to ensure distinct and cross-reactivity free signals per corresponding capture. Calibrations were created simultaneously for all assays in expected serum concentrations needed for analysis (Figure 5-2, 5-3). LOD/LOQ calculations indicated the feasibility of this 15-plex panel for sample quantitation (Table 5-2).

We have currently analyzed 22 subjects for our preliminary analysis, 6 healthy, and 16 COVID+ individuals. PBMCs were isolated from all convalescent samples and used for cell culture and subsequent 40-hour stimulation. There were seven stimulations (including a cell media control) used for the cytokine panel analyses. The two positive stimulation conditions were SS1 and SS2, which are recombinant subunits of the SARS-CoV-2 spike protein, which should elicit a strong response from PMBCs exposed to COVID infection. SARS-CoV-1 spike protein (SARS), tetanus toxoid (TET), myoglobin (MYO) and anti-CD3 (CD3) conditions were all utilized as controls for basal stimulation responses, and cell media (MED) was used as a negative control. From these stimulation conditions, we can interrogate both absolute cytokine levels, as well as normalized results specific to each subjects' basal immune responses. In brief, control conditions are subtracted per cytokine target from both positive stimulation conditions, creating a total of 150 potential normalized features (15 cytokines x 10 normalized conditions) in addition

to the 105 absolute features (15 cytokines x 7 stimulations). This precision normalization has been shown previously to account for variability in biological responses across subjects. With only 22 subjects total, some trends and preliminary results can be obtained. Mann-Whitney comparisons were made between healthy and COVID+ subjects, looking for significant population differences ($p<0.05$). From our 15-plex panel, 6 cytokines show preliminary promise across both absolute and normalized conditions with a total of 16 features.

CCL3 is the sole target to show only absolute cytokine level significance in the Mann-Whitney results, where we see significantly higher levels for COVID subjects in TET and CD3 stimulation conditions (Figure 5-4). These conditions could be interesting for understanding general immune response to COVID, since CD3 is a pan-stimulation that should indicate overall immune response health, and the tetanus toxoid could suggest the impact of foreign antigen presentation. With CCL3 activating an acute inflammatory response and fever most cases, this could be relevant in further evaluations of COVID response.[9] However, we do not see normalized results in this target, most likely due to large population heterogeneities in control conditions. This would lead to larger population distributions from normalization and more general overlap between COVID+ and healthy individuals. This would suggest that CCL3 might not be truly indicative of COVID infection or severity, since normalization, and therefore basal immune responses, reduces its significance.

In all other significant cytokines, we see both absolute and normalized significances. These targets include GM-CSF, IFN-λ1, IL-1β, IL-2, and IL-7. GM-CSF had significantly higher results in COVID+ compared to healthy subjects for SS2 (Figure 5-5)

and SS2_MED (Figure 5-6). SS2 is a positive, infection-specific stimulation, and to see it both in absolute and normalized conditions implies that GM-CSF response is related to the present of spike protein for viral infiltration. GM-CSF is important for macrophage proliferation, and so could be indicative of direct COVID infection mechanisms.[36] We also see IFN-λ1 show multiple significant conditions, including absolute values of SS2 and TET (Figure 5-7) and normalized values of SS2_MED, SS2_MYO, and SS2_SAR (Figure 5-8). In all instances, IFN-λ1 levels were lower in COVID subjects compared to the healthy cohort. IFN-λ1 is a type III interferon that is important for viral clearance, and regulation of this antigen might play a unique role in COVID infection clearance and potential severity.[32,33]

Multiple interleukins resulted in significant distinctions for COVID+ subjects. IL-1β proved significant in absolute levels for CD3 (Figure 5-9) and normalized levels for SS1_SAR and SS2_MED (Figure 5-10). These conditions are mixed with CD3 and SS2_MED showing lower cytokine levels in COVID, and higher levels in SS1_SAR. This could describe differences in the immune response to the different spike protein subunits. As a mediator of inflammation, IL-1β has a variety of uses in the immune response to infection, including cell differentiation and apoptosis, and would indicate the importance of its regulation.[41] IL-2 showed importance for SS2 (Figure 5-11) and SS2_MED (Figure 5-12) conditions. IL-2 regulates general activation of leukocytes, and provides a route for immunity, and seems to show diminished cytokine production post-COVID.[40] IL-7 also showed lower levels for SS2 (Figure 5-13) and SS2-TET in COVID subjects (Figure 5-14). Since IL-7 is important for T-cell development, a decrease in IL-7 levels could prove problematic for long term immunity.[39]

Conclusions/Future Directions

Our study is currently in preliminary stages. We are severely sample limited, and therefore our statistical power is low. The cytokines presented are the most responsive results so far from our small sample cohort. It is highly promising that we are seeing six of our fifteen cytokine markers showing distinct cytokine level differences in COVID+ subjects. We hope that with continuing sample enrollment and analysis we will continue to establish biomarker significance for COVID-19.

Future directions are numerous. With our method being quick, 15-plexed, and results produced from minimal sample input, we hope to interrogate not only markers of host response in general, but also response based on infection severity. Long-term adverse recovery events are a serious issue in COVID+ individuals and monitoring specific cytokine levels might produce clinically implementable results. We also hope to work in continuing collaboration with Mayo Clinic to understand immune profiling for those treated with neutralizing antibodies and those who are vaccinated in the future. It is imperative that we understand both recovery and long-term immunity metrics, and our multiplexed panel facilitates a path towards that goal.

Table 5-1. Antibodies and recombinant standard proteins used in the multiplexed immunoassay, as well as concentrations for tracers used.

Target	Role	Source	Catalog Number	Tracer (µg/mL)
CCL2	Capture	Thermo Fisher	14-7099	2
	Antigen	Thermo Fisher	14-8398	
	Tracer	Thermo Fisher	13-7096	
CCL3	Capture	R&D Systems	MAB670-100	1
	Antigen	R&D Systems	270-LD-010	
	Tracer	R&D Systems	MAB270-100	
CCL4	Capture	R&D Systems	MAB271-100	2
	Antigen	R&D Systems	271-BME-010	
	Tracer	R&D Systems	CUSTOI702-IGH021710A	
CCL7	Capture	R&D Systems	MAB282-100	1
	Antigen	R&D Systems	282-P3-010	
	Tracer	R&D Systems	BAF282	
IFN-γ	Capture	Mabtech	3420-3-250	1
	Antigen	Thermo Fisher	BMS303	
	Tracer	Mabtech	3420-6-250	
IFN-λ1	Capture	R&D Systems	MAB15981-100	1
	Antigen	R&D Systems	1598-IL-025	
	Tracer	R&D Systems	BAF1598	
IL-1β	Capture	Thermo Fisher	14-7018-85	2
	Antigen	Thermo Fisher	RIL1BI	
	Tracer	Thermo Fisher	13-7016-85	
IL-2	Capture	BD Biosciences	555051	2
	Antigen	Thermo Fisher	14-8029	
	Tracer	BD Biosciences	555040	
IL-6	Capture	Thermo Fisher	16-7069	2
	Antigen	Thermo Fisher	14-8069	
	Tracer	Thermo Fisher	13-7068	
IL-7	Capture	R&D Systems	MAB207-100	1
	Antigen	R&D Systems	207-IL-010	
	Tracer	R&D Systems	BAF207	
IL-10	Capture	Thermo Fisher	16-7108	2
	Antigen	Thermo Fisher	14-8109-80	
	Tracer	Thermo Fisher	13-7109	
IP-10	Capture	BD Biosciences	555046	0.5
	Antigen	BD Biosciences	551130	
	Tracer	R&D Systems	BAF266	
TNF-α	Capture	Biolegend	502802	2
	Antigen	Biolegend	570102	
	Tracer	Biolegend	502904	
TGF-α	Capture	R&D Systems	AF-239-100	1
	Antigen	R&D Systems	239-A-100	
	Tracer	R&D Systems	BAF239	
GM-CSF	Capture	R&D Systems	MAB615-100	1
	Antigen	R&D Systems	7954-GM-010/CF	
	Tracer	R&D Systems	BAM215	

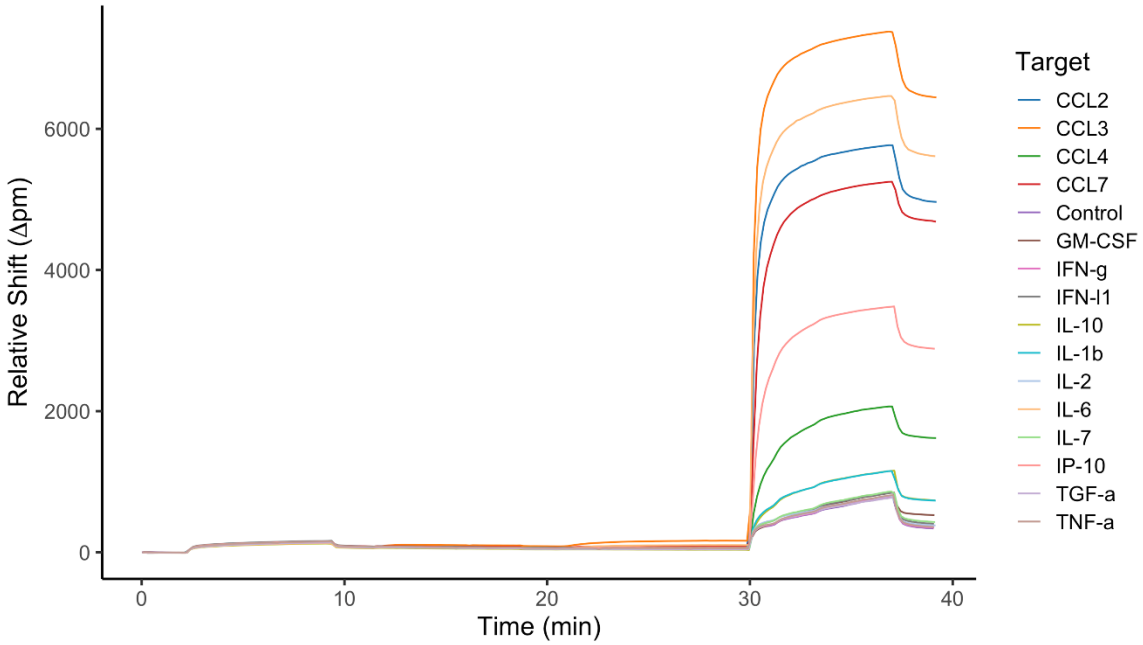

Figure 5-1. Example microring trace of a multiplexed immunoassay for neonatal waste serum. All flow steps are automated and sequential with running buffer rinses between reagents. Net shifts are calculated from subtracting the relative shift at t=29min from the relative shift at t=38min.

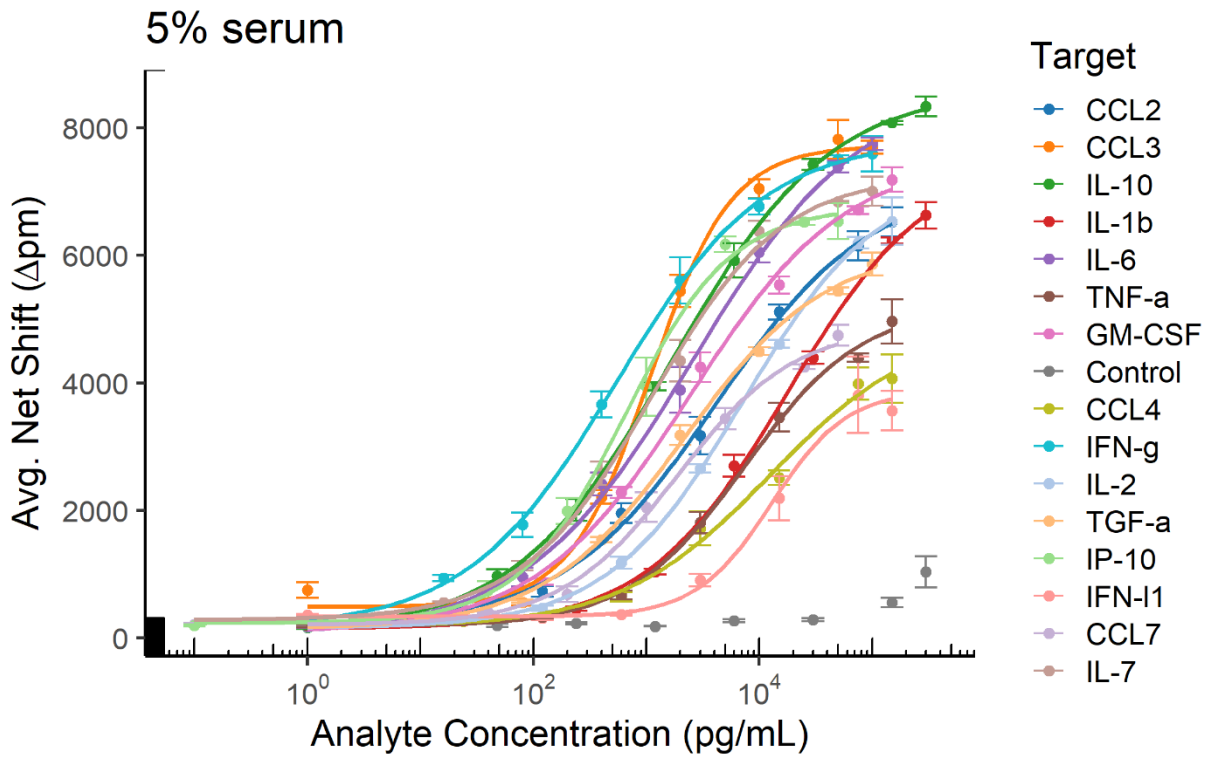

Figure 5-2. Multiplexed serum calibrations for 5% serum samples. Error bars represent standard deviation from n=3 calibrations, n=4 ring replicates per target.

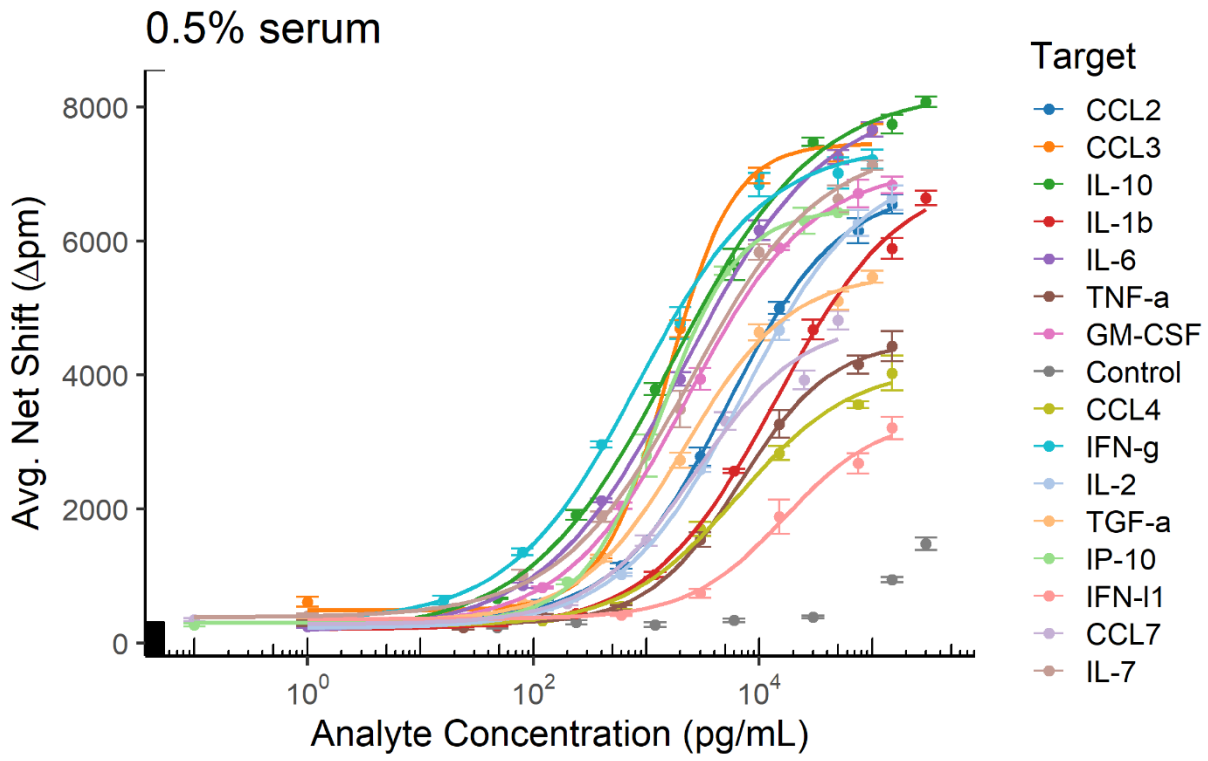

Figure 5-3. Multiplexed serum calibrations for 0.5% serum samples. Error bars represent standard deviation from n=3 calibrations, n=4 ring replicates per target.

Table 5-2. Limits of Detection (LOD) and Quantitation (LOQ) for 5% and 0.5% serum calibrations in pg/mL, calculated from the signal of the blank plus three times the standard deviation of the blank.

Target	5% Serum		0.5% Serum	
	LOD	LOQ	LOD	LOQ
CCL2	5.8	11.9	129.4	487.7
CCL3	238.5	707.7	295.4	656.5
CCL4	104.2	479.2	329.6	1202
CCL7	31.8	141.3	103.2	315.1
GM-CSF	14.2	47.8	46.0	185.8
IFN-γ	2.4	9.0	8.0	39.3
IFN-λ1	1004	2415	1588	5410
IL-10	4.9	23.1	11.8	44.1
IL-1β	92.8	419.9	146.9	477.2
IL-2	19.2	91.4	90.7	327.5
IL-6	7.1	28.2	16.9	70.1
IL-7	5.4	26.2	26.9	135.2
IP-10	5.5	28.0	48.4	155.7
TGF-α	21.8	83.5	43.0	164.3
TNF-α	102.9	466.2	538.7	1808

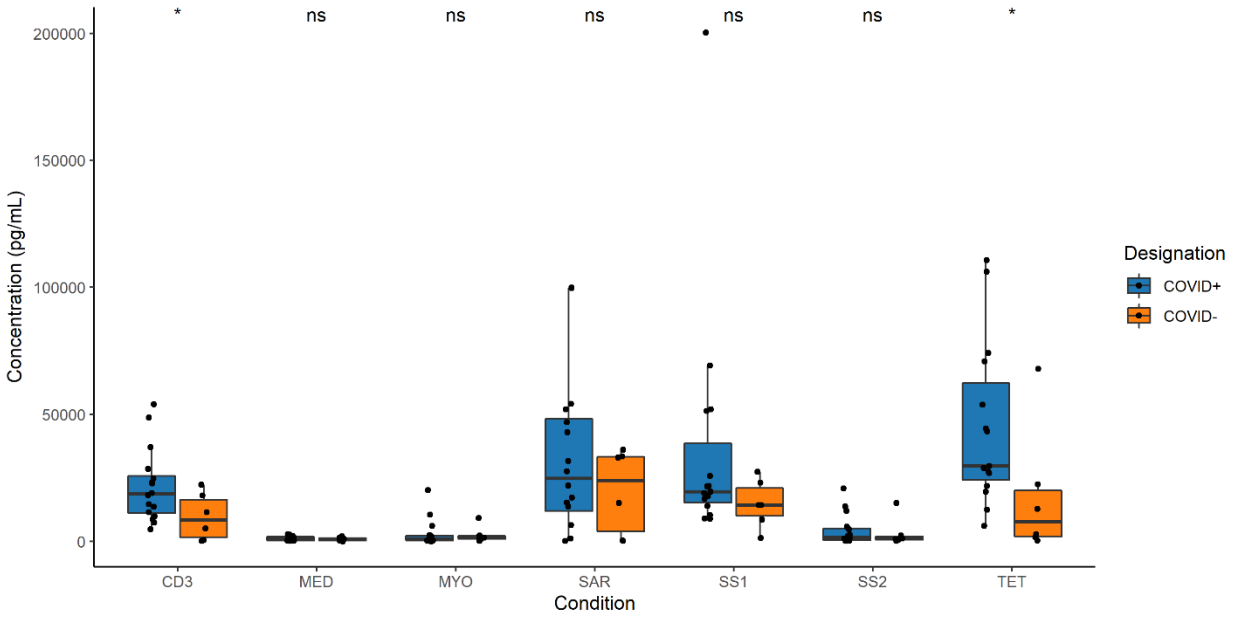

Figure 5-4. Mann-Whitney analyses for absolute CCL3 levels. Box plots represent the 25th and 75th percentile, median, and mean. *p<0.05

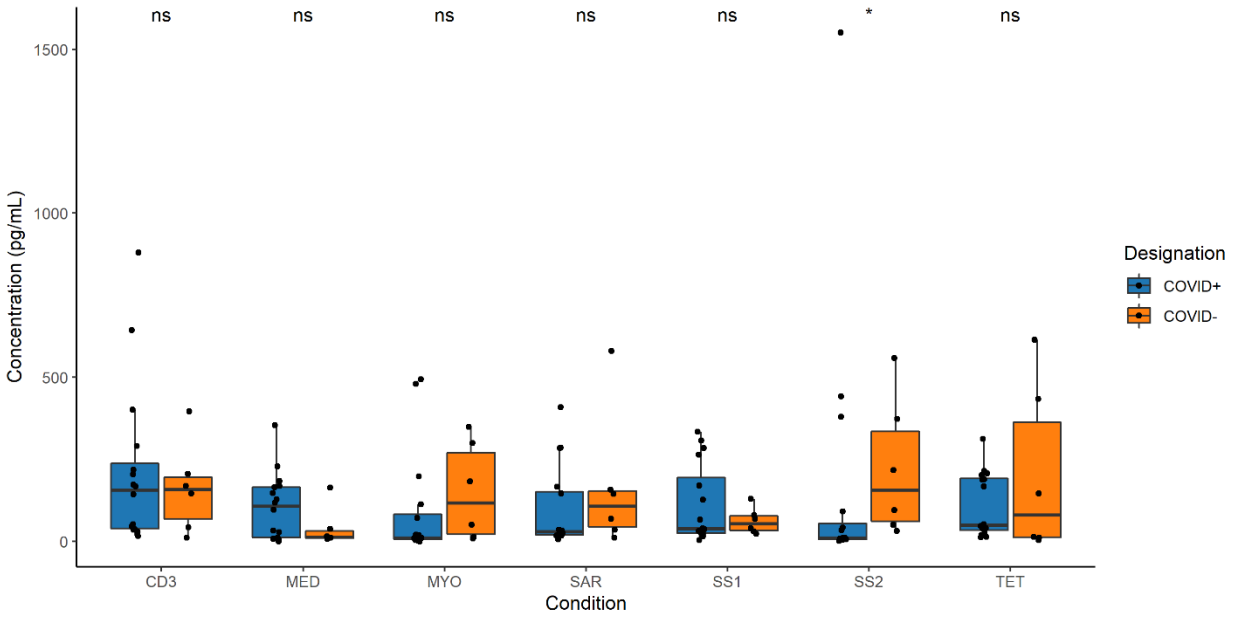

Figure 5-5. Mann-Whitney analyses for absolute GM-CSF levels. Box plots represent the 25th and 75th percentile, median, and mean. *p<0.05

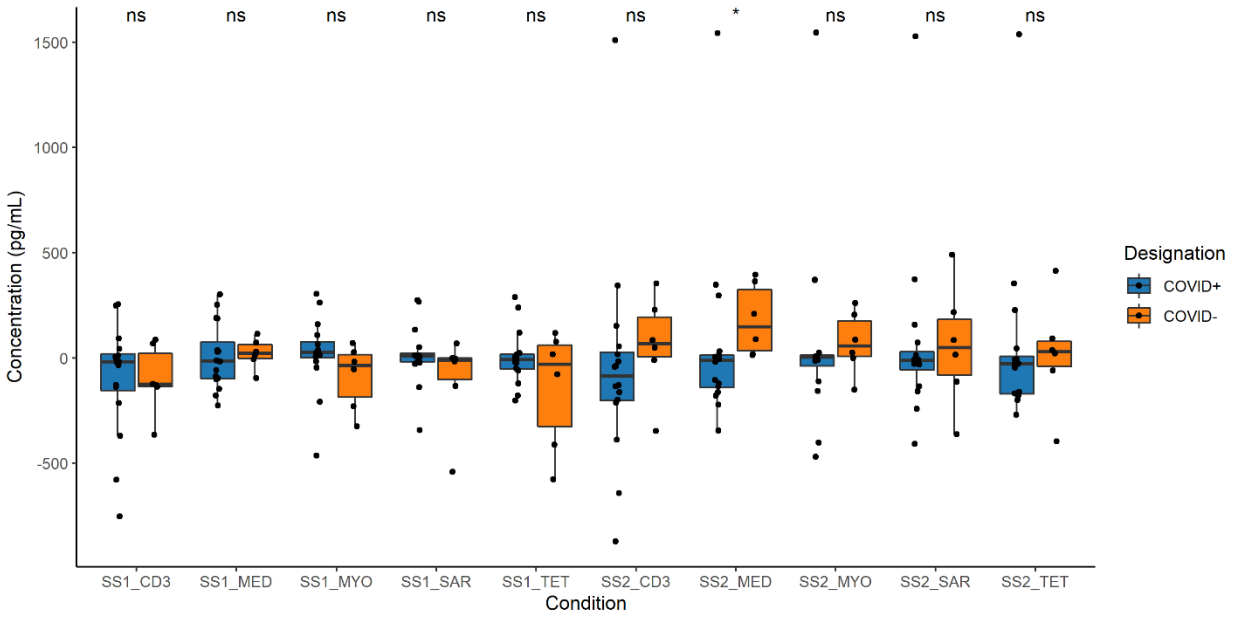

Figure 5-6. Mann-Whitney analyses for normalized GM-CSF levels. Box plots represent the 25th and 75th percentile, median, and mean. *p<0.05

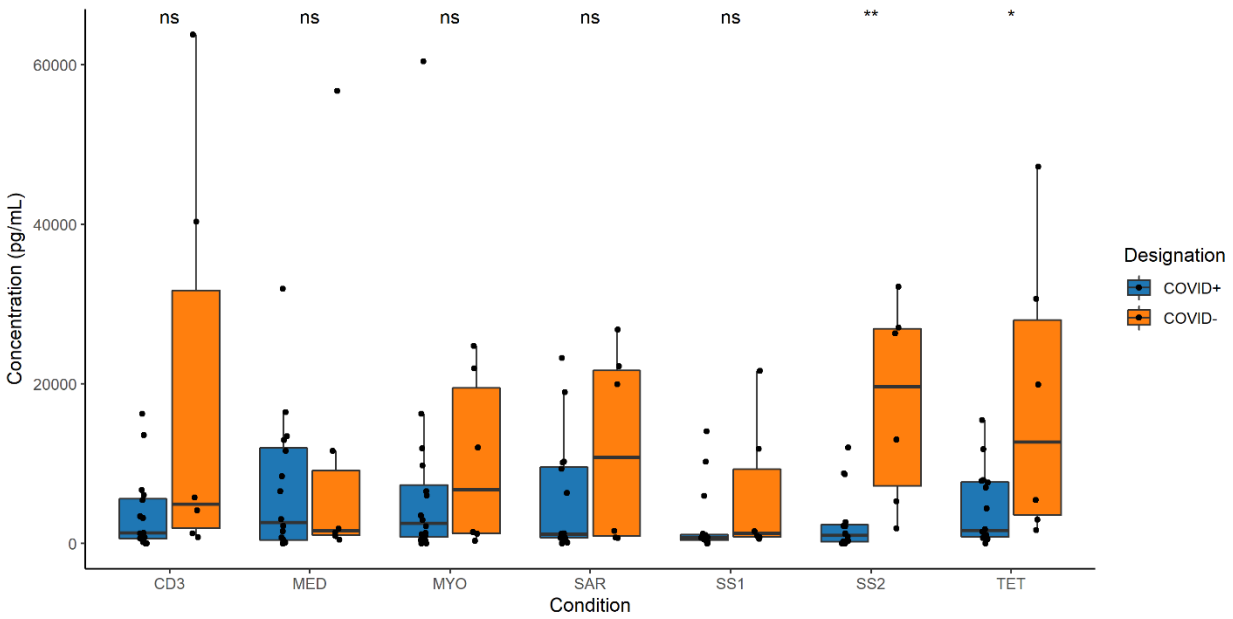

Figure 5-7. Mann-Whitney analyses for absolute IFN-λ1 levels. Box plots represent the 25th and 75th percentile, median, and mean. *p<0.05, **p<0.01

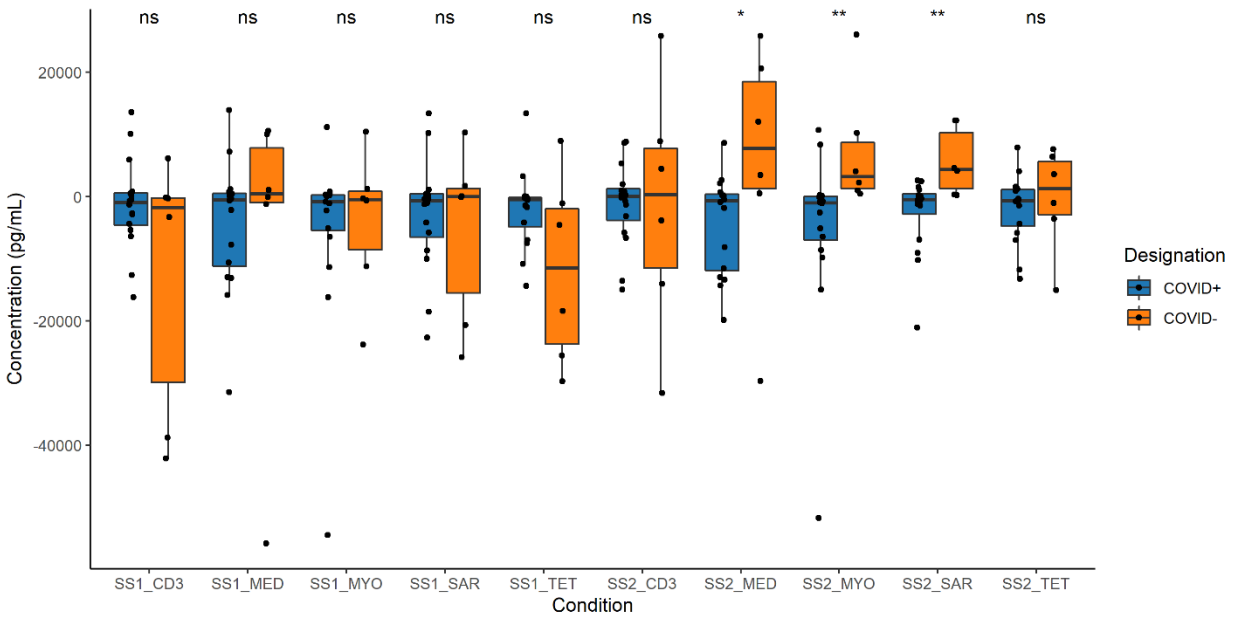

Figure 5-8. Mann-Whitney analyses for normalized IFN-λ1 levels. Box plots represent the 25th and 75th percentile, median, and mean. *p<0.05, **p<0.01

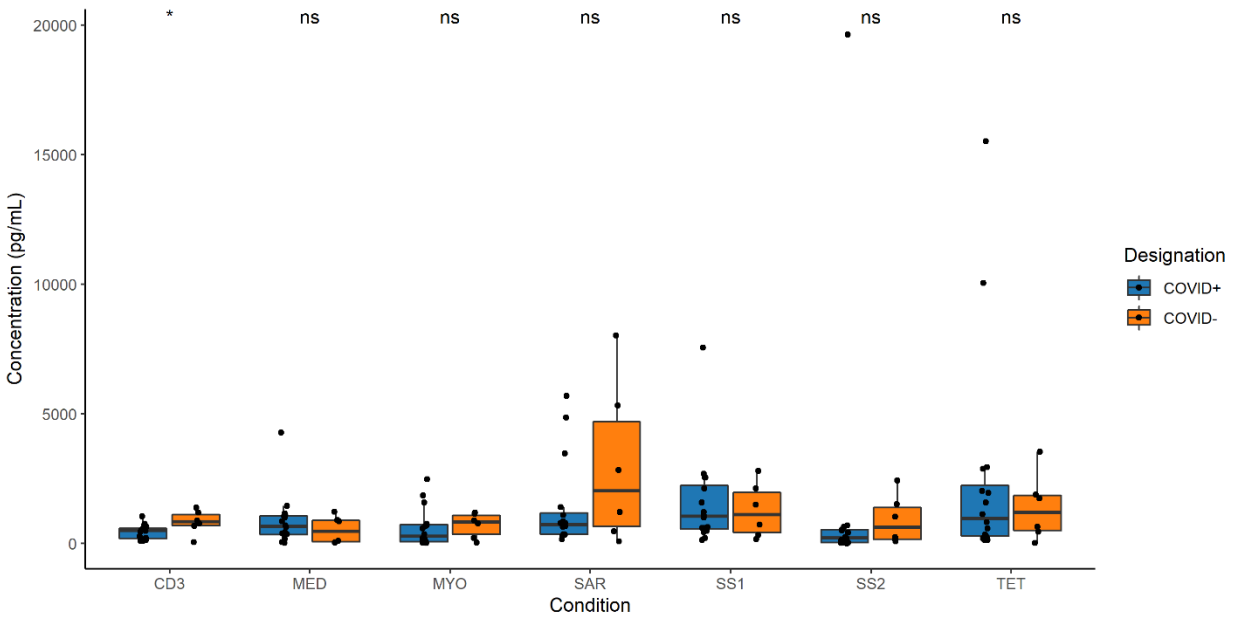

Figure 5-9. Mann-Whitney analyses for absolute IL-1β levels. Box plots represent the 25th and 75th percentile, median, and mean. *p<0.05

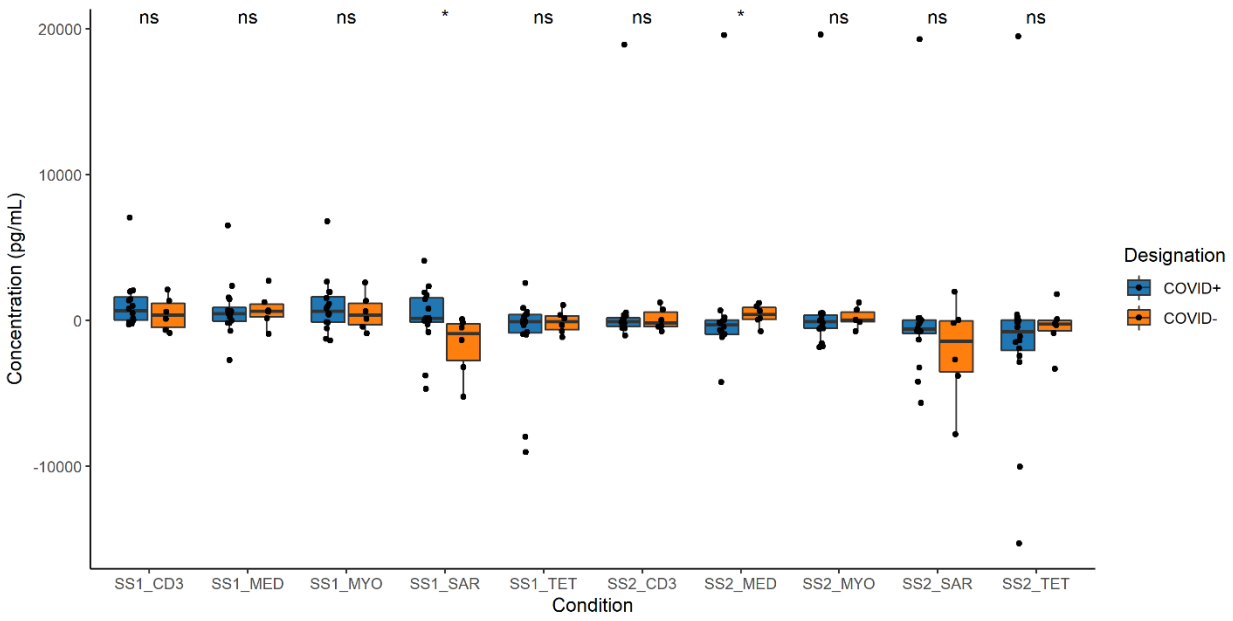

Figure 5-10. Mann-Whitney analyses for normalized IL-1β levels. Box plots represent the 25th and 75th percentile, median, and mean. *p<0.05

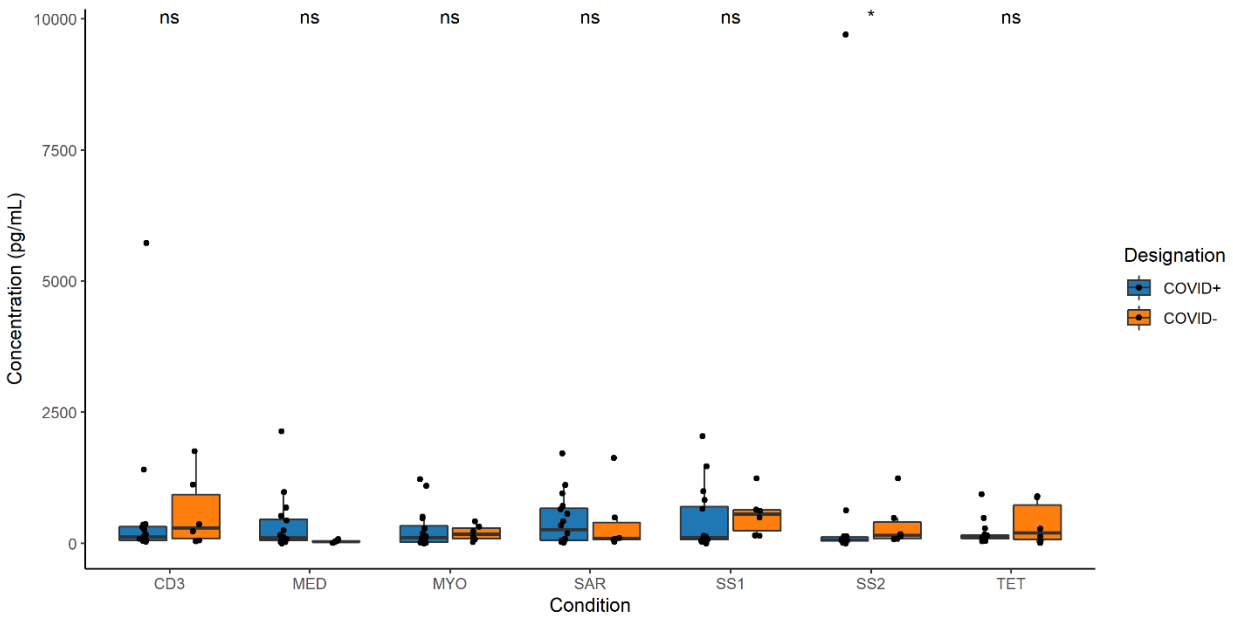

Figure 5-11. Mann-Whitney analyses for absolute IL-2 levels. Box plots represent the 25th and 75th percentile, median, and mean. *p<0.05

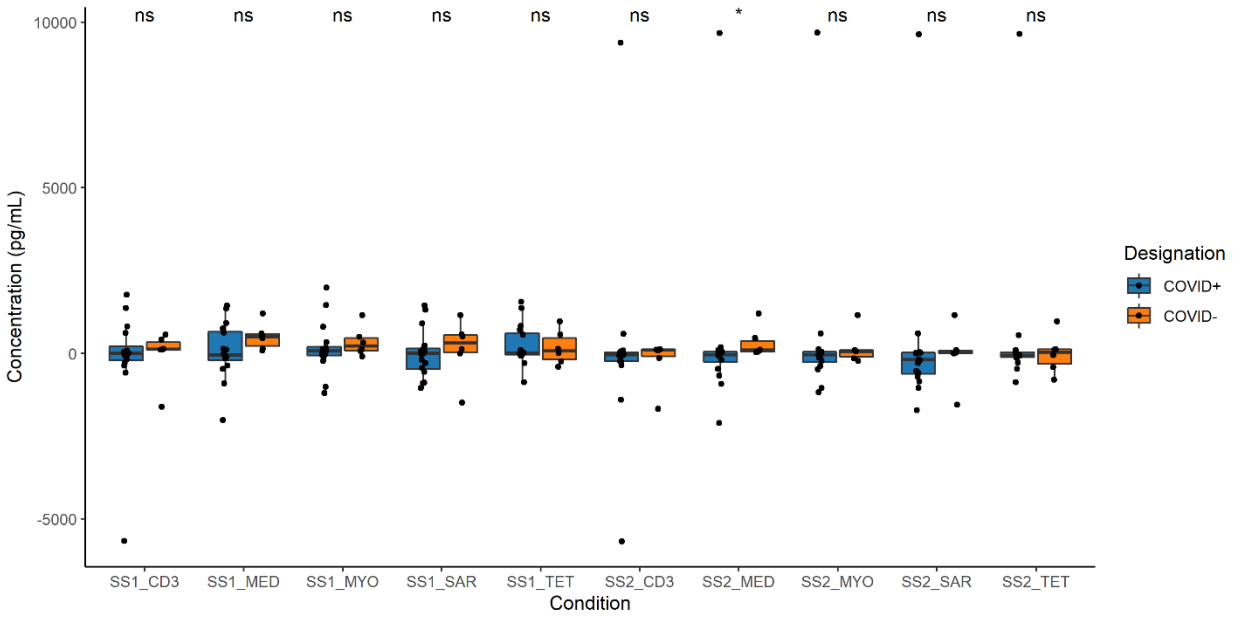

Figure 5-12. Mann-Whitney analyses for normalized IL-2 levels. Box plots represent the 25th and 75th percentile, median, and mean. *p<0.05

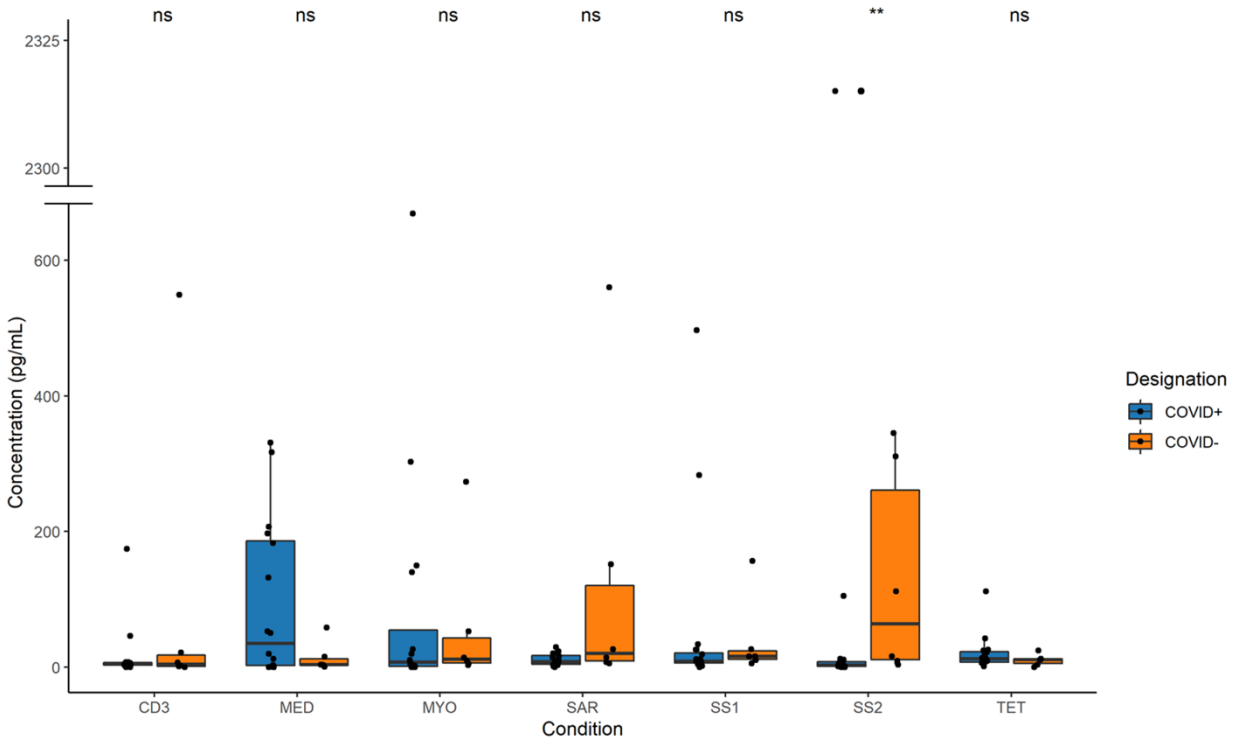

Figure 5-13. Mann-Whitney analyses for absolute IL-7 levels. Box plots represent the 25th and 75th percentile, median, and mean. *p<0.05

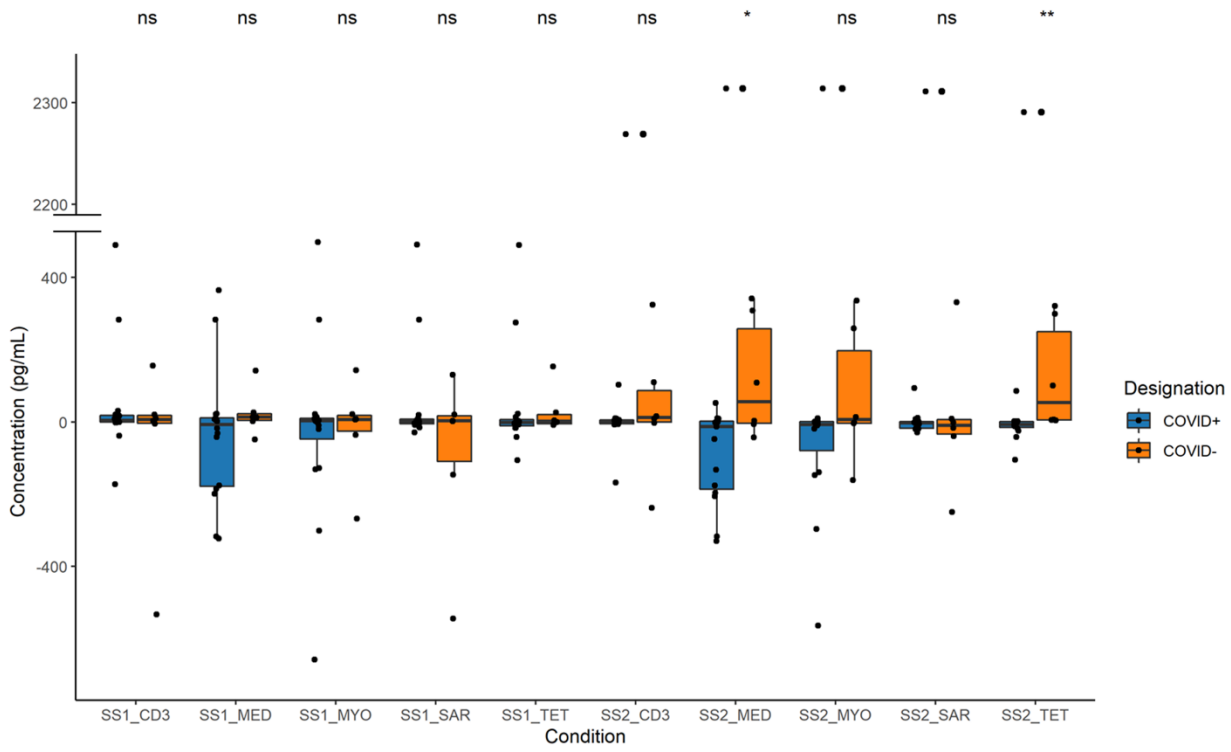

Figure 5-14. Mann-Whitney analyses for normalized IL-7 levels. Box plots represent the 25th and 75th percentile, median, and mean. **p<0.01

REFERENCES

1. CDC. Coronavirus disease 2019 (COVID-19): cases in U.S. US Department of Health and Human Services, CDC 2020.
1. 2.Dongarwar, D. & Salihu, H. M. COVID-19 Pandemic: Marked Global Disparities in Fatalities According to Geographic Location and Universal Health Care. *Int J MCH AIDS* **9**, 213–216 (2020).
2. Garg, S. Hospitalization Rates and Characteristics of Patients Hospitalized with Laboratory-Confirmed Coronavirus Disease 2019 — COVID-NET, 14 States, March 1–30, 2020. *MMWR Morb Mortal Wkly Rep* **69**, (2020).
3. Carter, L. J., *et al.* Assay Techniques and Test Development for COVID-19 Diagnosis. *ACS Cent. Sci.* **6**, 591–605 (2020).
4. Wu, F., *et al.* Neutralizing Antibody Responses to SARS-CoV-2 in a COVID-19 Recovered Patient Cohort and Their Implications. *medRxiv* 2020.03.30.20047365 (2020).
5. Cossarizza, A., *et al.* SARS-CoV-2, the Virus That Causes COVID-19: Cytometry and the New Challenge for Global Health. *Cytometry A* **97**, 340–343 (2020).
6. Kirkcaldy, R. D., King, B. A. & Brooks, J. T. COVID-19 and Postinfection Immunity: Limited Evidence, Many Remaining Questions. *JAMA* **323**, 2245 (2020).
7. Stephens, D. S. & McElrath, M. J. COVID-19 and the Path to Immunity. *JAMA* **324**, 1279 (2020).

8. Huang, C., *et al.* Clinical Features of Patients Infected with 2019 Novel Coronavirus in Wuhan, China. *The Lancet* **395**, 497–506 (2020).

9. Petrilli, C. M., *et al.* Factors Associated with Hospital Admission and Critical Illness among 5279 People with Coronavirus Disease 2019 in New York City: Prospective Cohort Study. *BMJ* **369**, m1966 (2020).

10. Richardson, S., *et al.* Presenting Characteristics, Comorbidities, and Outcomes Among 5700 Patients Hospitalized With COVID-19 in the New York City Area. *JAMA* **323**, 2052 (2020).

11. Channappanavar, R., *et al.* Dysregulated Type I Interferon and Inflammatory Monocyte-Macrophage Responses Cause Lethal Pneumonia in SARS-CoV-Infected Mice. *Cell Host Microbe* **19**, 181–193 (2016).

12. Li, X., Geng, M., Peng, Y., Meng, L. & Lu, S. Molecular Immune Pathogenesis and Diagnosis of COVID-19. *Journal of Pharmaceutical Analysis* **10**, 102–108 (2020).

13. Prompetchara, E., Ketloy, C. & Palaga, T. Immune Responses in COVID-19 and Potential Vaccines: Lessons Learned from SARS and MERS Epidemic. *Asian Pac J Allergy Immunol* **38**, 1–9 (2020).

14. Ji, D., *et al.* Prediction for Progression Risk in Patients With COVID-19 Pneumonia: The CALL Score. *Clinical Infectious Diseases* **71**, 1393–1399 (2020).

15. Yang, Y., *et al.* Plasma IP-10 and MCP-3 Levels Are Highly Associated with Disease Severity and Predict the Progression of COVID-19. *J Allergy Clin Immunol* **146**, 119-127 (2020).

16. Channappanavar, R., Fett, C., Zhao, J., Meyerholz, D. K. & Perlman, S. Virus-Specific Memory CD8 T Cells Provide Substantial Protection from Lethal Severe Acute Respiratory Syndrome Coronavirus Infection. *Journal of Virology* **88**, 11034–11044 (2014).

17. Chen, H., *et al.* Response of Memory CD8+ T Cells to Severe Acute Respiratory Syndrome (SARS) Coronavirus in Recovered SARS Patients and Healthy Individuals. *J Immunol* **175**, 591–598 (2005).

18. Li, C. K., *et al.* T Cell Responses to Whole SARS Coronavirus in Humans. *The Journal of Immunology* **181**, 5490–5500 (2008).

19. Liu, W., *et al.* Two-Year Prospective Study of the Humoral Immune Response of Patients with Severe Acute Respiratory Syndrome. *The Journal of Infectious Diseases* **193**, 792–795 (2006).

20. Liu, W. J., *et al.* T-Cell Immunity of SARS-CoV: Implications for Vaccine Development against MERS-CoV. *Antiviral Res* **137**, 82–92 (2017).

21. Tang, F., *et al.* Lack of Peripheral Memory B Cell Responses in Recovered Patients with Severe Acute Respiratory Syndrome: A Six-Year Follow-up Study. *J Immunol* **186**, 7264–7268 (2011).

22. Zhao, J., *et al.* Airway Memory CD4(+) T Cells Mediate Protective Immunity against Emerging Respiratory Coronaviruses. *Immunity* **44**, 1379–1391 (2016).

23. Braun, J., *et al.* SARS-CoV-2-Reactive T Cells in Healthy Donors and Patients with COVID-19. *Nature* **587**, 270–274 (2020).

24. Chen, G., *et al.* Clinical and Immunological Features of Severe and Moderate Coronavirus Disease 2019. *J Clin Invest* **130**, 2620–2629 (2020).

25. Deng, W., *et al.* Primary Exposure to SARS-CoV-2 Protects against Reinfection in Rhesus Macaques. *Science* **369**, 818–823 (2020).

26. Grifoni, A., *et al.* Targets of T Cell Responses to SARS-CoV-2 Coronavirus in Humans with COVID-19 Disease and Unexposed Individuals. *Cell* **181**, 1489-1501 (2020).

27. Le Bert, N., *et al.* SARS-CoV-2-Specific T Cell Immunity in Cases of COVID-19 and SARS, and Uninfected Controls. *Nature* **584**, 457–462 (2020).

28. Mateus, J., *et al.* Selective and Cross-Reactive SARS-CoV-2 T Cell Epitopes in Unexposed Humans. *Science* **370**, 89–94 (2020).

29. Weiskopf, D., *et al.* Phenotype and Kinetics of SARS-CoV-2–Specific T Cells in COVID-19 Patients with Acute Respiratory Distress Syndrome. *Science Immunology* **5**, 48 (2020).

30. Burrage, D. R., Koushesh, S. & Sofat, N. Immunomodulatory Drugs in the Management of SARS-CoV-2. *Front. Immunol.* **11** (2020).

31. Amodio, E., *et al.* SARS-CoV-2 Viral Load, IFNλ Polymorphisms and the Course of COVID-19: An Observational Study. *J Clin Med* **9**,10 (2020).

32. Prokunina-Olsson, L., *et al.* COVID-19 and Emerging Viral Infections: The Case for Interferon Lambda. *J Exp Med* **217**, 5 (2020).

33. Montalvo Villalba, M. C., *et al.* Interferon Gamma, TGF-B1 and RANTES Expression in Upper Airway Samples from SARS-CoV-2 Infected Patients. *Clinical Immunology* **220**, 108576 (2020).

34. Mogi, M., *et al.* Interleukin-1β, Interleukin-6, Epidermal Growth Factor and Transforming Growth Factor-α Are Elevated in the Brain from Parkinsonian Patients. *Neuroscience Letters* **180**, 147–150 (1994).

35. Bonaventura, A., *et al.* Targeting GM-CSF in COVID-19 Pneumonia: Rationale and Strategies. *Front Immunol* **11** (2020).

36. Chen, Y., *et al.* IP-10 and MCP-1 as Biomarkers Associated with Disease Severity of COVID-19. *Mol Med* **26**, 97 (2020).

37. Han, H., *et al.* Profiling Serum Cytokines in COVID-19 Patients Reveals IL-6 and IL-10 Are Disease Severity Predictors. *Emerg Microbes Infect* **9**, 1123–1130 (2020).

38. Costela-Ruiz, V. J., Illescas-Montes, R., Puerta-Puerta, J. M., Ruiz, C. & Melguizo-Rodríguez, L. SARS-CoV-2 Infection: The Role of Cytokines in COVID-19 Disease. *Cytokine & Growth Factor Reviews* **54**, 62–75 (2020).

39. Sattler, A., *et al.* SARS–CoV-2–Specific T Cell Responses and Correlations with COVID-19 Patient Predisposition. *J Clin Invest* **130**, 6477–6489 (2020).

40. Ma, Q., *et al.* Liu Shen Capsule Shows Antiviral and Anti-Inflammatory Abilities against Novel Coronavirus SARS-CoV-2 via Suppression of NF-KB Signaling Pathway. *Pharmacological Research* **158**, 104850 (2020).

41. Tang, Y., Liu, J., Zhang, D., Xu, Z., Ji, J. & Wen, C. Cytokine Storm in COVID-19: The Current Evidence and Treatment Strategies. *Front. Immunol.* **11** (2020).

42. Azar, M. M., Shin, J. J., Kang, I. & Landry, M. Diagnosis of SARS-CoV-2 Infection in the Setting of the Cytokine Release Syndrome. *Expert Review of Molecular Diagnostics* **20**, 1087–1097 (2020).

43. Francesco T., *et al.* Platelets Promote Thromboinflammation in SARS-CoV-2 Pneumonia. *Arteriosclerosis, Thrombosis, and Vascular Biology* **40**, 2975–2989 (2020).

44. Robison, H. M. & Bailey, R. C. A Guide to Quantitative Biomarker Assay Development Using Whispering Gallery Mode Biosensors. *Curr Protoc Chem Biol* **9**, 158–173 (2017).

45. Robison, H. M., *et al.* Precision Immunoprofiling to Reveal Diagnostic Signatures for Latent Tuberculosis Infection and Reactivation Risk Stratification. *Integr Biol (Camb)* **11**, 16–25 (2019).

46. Mudumba, S., *et al.* Photonic Ring Resonance Is a Versatile Platform for Performing Multiplex Immunoassays in Real Time. *J Immunol Methods* **448**, 34–43 (2017).

CHAPTER 6

Conclusions and Future Directions

Acknowledgements

I would like to acknowledge Dr. Patricio Escalante for his continued efforts to further both LTBI and COVID diagnostic research collaborations, along with the team at Mayo Clinic for support. I also acknowledge Dr. Jennifer Bermick and Dr. Gretchen Stepanovich for continued endeavors in neonatal clinical evaluations. Finally, I would like to acknowledge Krista Meserve for her contributions in developing and validating the next generation of custom multiplexed immunoassay panels for many diagnostic applications.

Dissertation Summary

This work summarized multiple clinically relevant projects, all stemming from an analytical challenge: what considerations are necessary to create a robust and applicable multiplexed immunoassay of blood analytes, particularly for clinical deployment? Chapter 1 discussed analytical factors vital to this process, including targets of interest, sample processing, viable assay formats, sensitivity, selectivity, and general usability. Compounding these analytical considerations are clinical factors, such as sample types, sample correlation to disease, matrix effects, cross-reactivity from off-target species, expected analyte concentrations, and clinical feasibility. Furthermore, multiplexing adds new concerns including background signal from assay reagents, assay-to-assay cross-reactivities, and potential number of analytes measured. Commercialized systems, such as Quanterix[1], Luminex[2], and Genalyte[3] were discussed as potential platforms for multiplexed clinical analyses.

Chapter 2 and 3 described innovations in analytical development and bioinformatics implementation to investigate cytokine profiling for latent tuberculosis infection (LTBI) and reactivation risk. Chapter 2 was a successor to previous work in the lab[4], where we have expanded our analyses to 13 cytokines, seven stimulation conditions in cell supernatant, and turned to Random Forest informatics to determine relevant cytokine signatures. We utilized ROC curves to present clinical predictive accuracies greater than 80% for both LTBI and reactivation risk. Chapter 3 focused on progressing this immunoassay panel into a clinical pipeline, where we used plasma from QFT analyses for cytokine detection in plasma. From the 3 stimulation conditions available, we were able to distinguish LTBI and risk of reactivation at similar or better levels compared

to our supernatant study. Overall, the direction of the LTBI project is promising for further work within the clinical workflow, where instrumentation and assays could be adapted to replace and enhance cytokine profiling.

Chapter 4 described a more fundamental application of clinical immunoassays in the form of neonatal immune response evaluation. Analyses for both basal immune responses in unstimulated, healthy preterm infants were compared to those infected with chorioamnionitis, a common cause of preterm birth. The 7-plex panel showed significances for multiple targets across 23-36 weeks of gestational age, indicating the importance of temporal measurements to understand changes in clinical status. Additionally, the time to result for the multiplexed assay (38 minutes) provided a potential for direct clinical use, as rapid assay results would change treatment options and outcomes.

Finally, Chapter 5 showed the preliminary results of translating the LTBI workflow towards urgent profiling needs in SARS-CoV-2 infection and recovery. Stimulated samples for COVID-specific and off-target conditions were used to create normalized features that could be compared between healthy and COVID+ subjects. While sample limited, significances were found for multiple targets from the custom 15-plex immunoassay panel we validated and developed. Furthermore, these preliminary results showed promise for continued analysis for disease severity and vaccine efficacy through immune correlates.

Future Directions

We now have almost 20 available cytokines that are validated and calibrated, and most are cross-validated for multiplexed cytokine immunoassay detection schemes. Additional targets can easily be validated as needed for clinical problems, and available multiplexed assay panels are currently in use for clinical samples in a variety of matrices. There are potential avenues for further work in LTBI, COVID, and neonatal analyses, with planned directions already underway.

LTBI diagnostics will continue using the current workflow. The next phase of clinical analysis will include samples in collaboration with Mayo Clinic, focusing on temporal studies of health care workers (HCW) from Tijuana, Mexico. The rate of TB prevalence in Tijuana far exceeds that of the US population, and therefore creating a viable and easily trackable population to understand dynamic immunoprofile changes over time is vital. Mayo Clinic will enroll 300 HCWs for which samples will be collected approximately every six months for analysis from our multiplexed panel. With longitudinal sampling, we hope to evaluate changes in risk of reactivation, and potentially predict when someone might reactivate. Using the previous studies from Chapter 2 and 3 as training sets, new samples can be compared in both supernatant and plasma samples for clinical designations. We believe that from this new cohort, we will create a more complete cytokine profile for LTBI and reactivation risk within the clinical workflow for true diagnostic use.

Beyond continued studies within the current pipeline, we can also consider refocusing our efforts into addressing clinical limitations. Unfortunately, it is not necessarily accurate to describe LTBI as a binary classifier. Since LTBI is directly related to a dynamic host-pathogen equilibrium, it more closely resembles a spectrum of changes

that correlate to reactivation risk. Therefore, we need to realize new strategies for stratifying risk within the LTBI population. Concurrently, we want to move towards more actionable results from our bioinformatics approaches that could produce tangible clinical directives. To this end, supervised learning methods may provide additional information, at the potential loss of some accuracy. For example, linear discriminant analyses (LDA) have been used in clinical analyses for cytokine profiling, and specifically for understanding complex feature comparisons.[5,6] LDA produces linear combinatorial outputs of relevant features, generally from a reduced selection of most important targets, that in clinical applications can be directly related to biomarker concentrations. Through this analysis, we could conceivably create interpretable equations that could differentiate these LTBI spectrum differences. For example, a linear combination of biomarkers such as IP-10, CCL2, and IL-6, along with a statistical equation, could create a profile where dynamic changes in cytokine levels (i.e. IP-10 and IL-6 being high, and CCL2 being low) directly correlate to risk. While this method creates a linear combination, which is commonly less accurate as the number of features increases, we could utilize that ambiguity to “stratify” the binary discrimination into multiple categories. In this instance, the variation of binary classifications for LDA could be used to identify patients that land within a moderate risk category. And as we accumulate temporal samples, we could watch the classifier drift towards one group or the other, indicating change is risk of reactivation. If a patient were to consistently track towards higher risk, we would implement treatment strategies to mitigate the potential for active infection. This method is outlined in Figure 6-1 and is a possible avenue to create applicable stratification that

could be easily implemented in the clinic through direct concentration measurements and risk stratification.

Similarly, COVID cytokine evaluations will focus on increasing sample cohort size and planning for longitudinal work. The COVID panel has been rigorously validated and tested, but cohort size limits its effectiveness presently. More subjects would help evaluate what cytokines are necessary for further studies. Additionally, analyses in COVID severity and vaccine efficacy will improve current understanding of host-pathogen interactions, disease progression, and necessary conditions for clearance, immunity, and survival.[5-7] Furthermore, we can continue to refine our method as clinical strategies adapt over time. For example, it may be pertinent for us to analyze Bronchoalveolar Lavage (BAL) or nasal swab samples, as these could be more directly related to the localized cytokine responses we expect from COVID. And as with the LTBI workflow, we could consider building quick and applicable discriminatory analyses to stratify disease severity. Work will be continued with Mayo Clinic to enroll subjects and establish an analytical-clinical workflow for proper analysis and useable output metrics.

Finally, neonatal work will most likely pivot to focus on understanding co-infections within the preterm neonatal population. Continuing work with Dr. Jennifer Bermick, who is now at the University of Iowa, we expect to expand out 7-plex panel into other markers of interest and bin subpopulations by their gestational age and co-infection designations. While current work within this thesis showed the importance of basal immune responses and understanding (dys)regulation temporally, we had a substantial number of samples that were necessary to exclude from analysis due to their co-infection statuses. These conditions included early onset neonatal sepsis (EONS), late onset neonatal sepsis

(LONS), necrotizing enterocolitis (NEC), pneumonia, and urinary tract infections (UTI). Understanding how these conditions complicate and are complicated by chorioamnionitis, and how in combination they affect neonatal immunes responses will be vital for positive clinical outcomes, and therefore need to be studied in earnest.[8] Finally, longitudinal profiling will need to extend beyond the NICU for true clinical utility. Understanding outcomes and basal levels as neonates reach term and move into pediatric care will be important for both healthy and chorio-exposed individuals, as chronic disorders and immunosuppression are of primary concern.

Concluding Remarks

In summary, this work has contributed to the field of multiplexed diagnostics, focusing on clinical utility within disease evaluation. By integrating common immunoassay formats with silicon photonics and a multi-sensor commercialized system, we were able to establish cytokine panels for projects spanning preliminary studies, longitudinal evaluations, and clinical designations. All these clinical results, from simple population comparisons to extensive bioinformatics, are impossible without a fundamentally analytical approach, which provides robust and valuable clinical insight. Future implementation and translation of this sensor-based work will continue to improve immunodiagnostic capacity and clinical usability, potentially to a level of routine point-of-care evaluations.

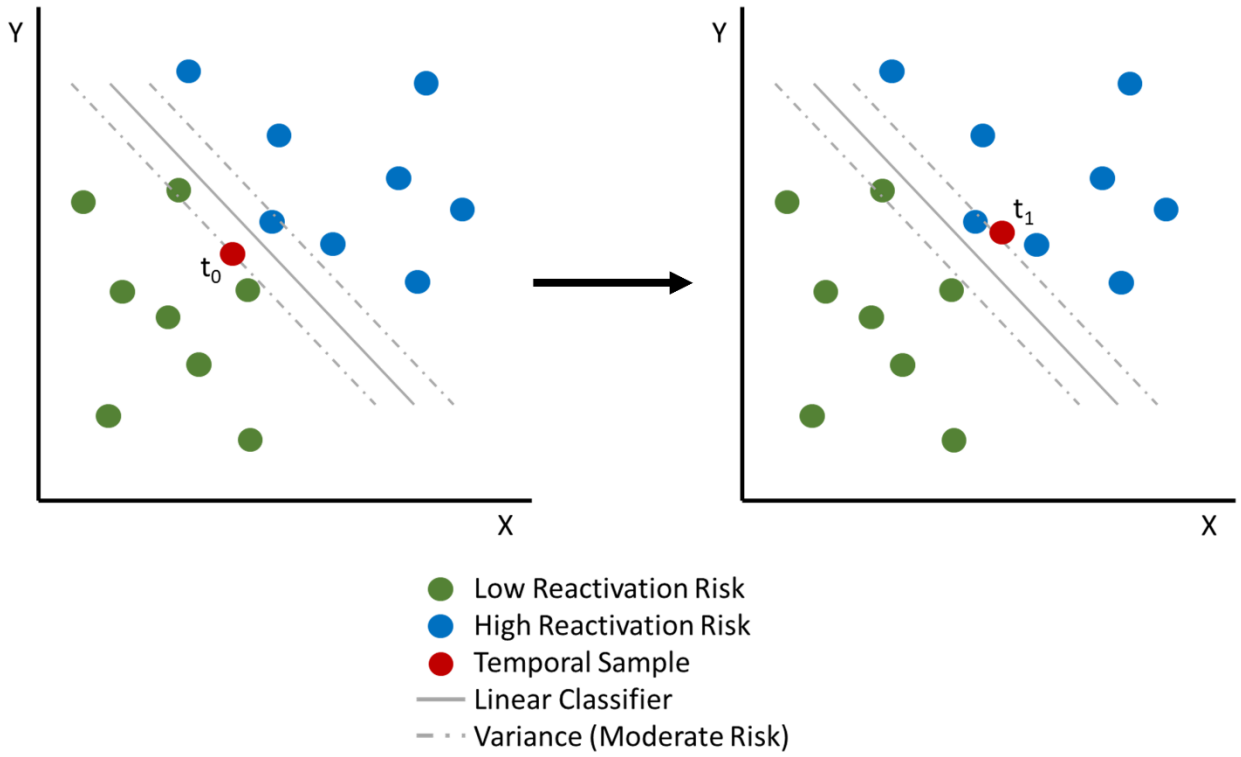

Figure 6-1. An example of Linear Discriminant Analysis (LDA) within the LTBI reactivation risk assessment workflow. Through a linear classifier system that accounts for variance, temporal dynamics of reactivation risk could be directly mapped from biomarker measurements.

References

1. Wu, C., Maley, A. M. & Walt, D. R. Single-molecule measurements in microwells for clinical applications. *Critical Reviews in Clinical Laboratory Sciences* **57**, 270–290 (2020).
2. Reslova, N., Michna, V., Kasny, M., Mikel, P. & Kralik, P. xMAP Technology: Applications in Detection of Pathogens. *Front. Microbiol.* **8**, (2017).
3. Washburn, A. L. & Bailey, R. C. Photonics-on-a-chip: recent advances in integrated waveguides as enabling detection elements for real-world, lab-on-a-chip biosensing applications. *Analyst* **136**, 227–236 (2010).
4. Robison, H. M. *et al.* Precision immunoprofiling to reveal diagnostic signatures for latent tuberculosis infection and reactivation risk stratification. *Integrative Biology* **11**, 16–25 (2019).
5. Yang, M., Meng, F., Gao, M. *et al.* Cytokine signatures associate with disease severity in children with *Mycoplasma pneumoniae* pneumonia. *Scientific Reports* **9,** 17853 (2019).
6. Obraztsov, I. V. *et al.* Multiple Cytokine Profiling: A New Model to Predict Response to Tumor Necrosis Factor Antagonists in Ulcerative Colitis Patients. *Inflammatory Bowel Diseases* **25**, 524–531 (2018).
7. Yang, Y., *et al.* Plasma IP-10 and MCP-3 Levels Are Highly Associated with Disease Severity and Predict the Progression of COVID-19. *J Allergy Clin Immunol* **146**, 119-127 (2020).

8. Kirkcaldy, R. D., King, B. A. & Brooks, J. T. COVID-19 and Postinfection Immunity: Limited Evidence, Many Remaining Questions. *JAMA* **323**, 2245 (2020).

9. Prompetchara, E., Ketloy, C. & Palaga, T. Immune Responses in COVID-19 and Potential Vaccines: Lessons Learned from SARS and MERS Epidemic. *Asian Pac J Allergy Immunol* **38**, 1–9 (2020).

10. Wolfs TGAM, *et al.* Inflammation-induced immune suppression of the fetus: a potential link between chorioamnionitis and postnatal early onset sepsis. *J Matern Fetal Neonatal Med* **25**, 8–11 (2012).